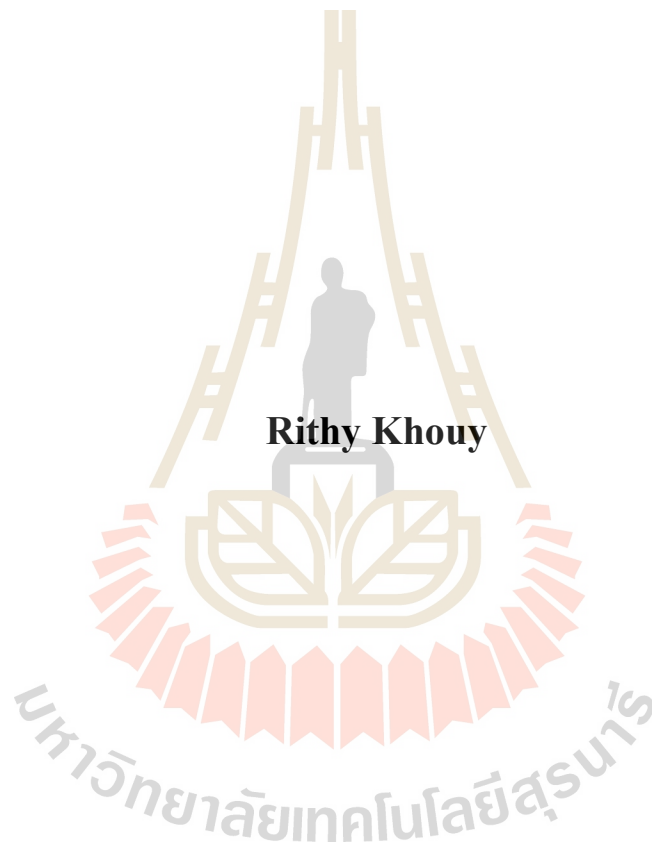
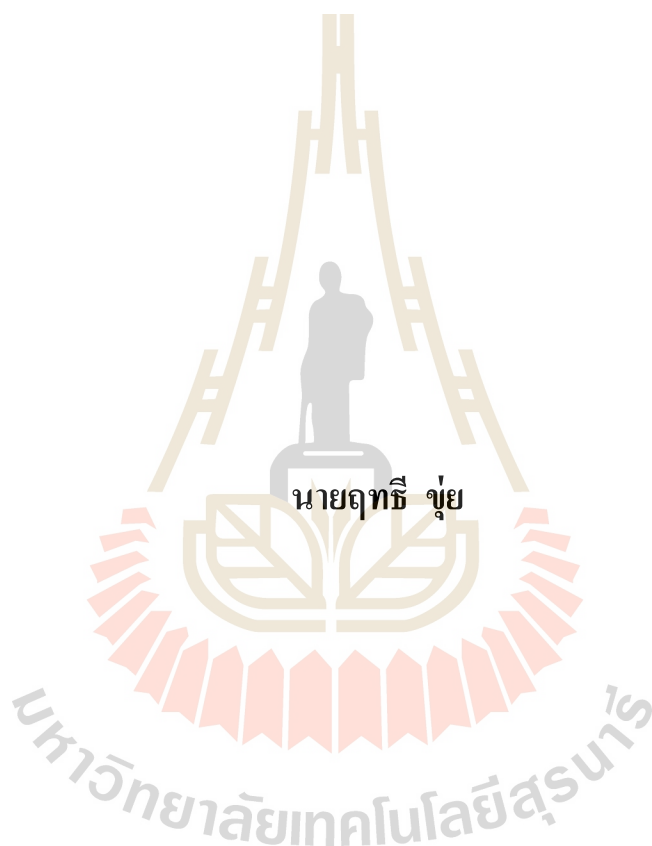


**PERFORMANCE-BASED SEISMIC DESIGN OF THE  
EXISTING RC BUILDING USING BRACED STEEL  
FRAME**



**A Thesis Submitted in Partial Fulfillment of the Requirements for the  
Degree of Master of Engineering in Civil, Transportation  
and Geo-resources Engineering  
Suranaree University of Technology  
Academic Year 2019**

การออกแบบแผ่นดินไหวเชิงสมรรถนะของอาคารคอนกรีตเสริมเหล็กที่มีอยู่  
เดิมโดยใช้โครงเหล็กค้ำยัน



วิทยานิพนธ์นี้เป็นส่วนหนึ่งของการศึกษาตามหลักสูตรปริญญาวิศวกรรมศาสตรมหาบัณฑิต  
สาขาวิชาวิศวกรรมโยธา ขนส่ง และทรัพยากรธรณี  
มหาวิทยาลัยเทคโนโลยีสุรนารี  
ปีการศึกษา 2562

# PERFORMANCE-BASED SEISMIC DESIGN OF THE EXISTING RC BUILDING USING BRACED STEEL FRAME

Suranaree University of Technology has approved this thesis submitted in partial fulfillment of the requirements for a Master's Degree.

Thesis Examining Committee



(Asst. Prof. Dr. Jaksada Thumrongvut)

Chairperson



(Asst. Prof. Dr. Mongkol Jiravacharadet)

Member (Thesis Advisor)



(Assoc. Prof. Dr. Chatchai Jothityangkoon)

Member



(Prof. Dr. Santi Maensiri)

Vice Rector for Academic Affairs  
and Internationalization



(Assoc. Prof. Ft. Lt. Dr. Kontorn Chamniprasart)

Dean of Institute of Engineering

มหาวิทยาลัยเทคโนโลยีสุรนารี

ฤทธิ์ ขุ่ม : การออกแบบแผ่นดินไหวเชิงสมรรถนะของอาคารคอนกรีตเสริมเหล็กที่มีอยู่เดิมโดยใช้โครงเหล็กค้ำยัน (PERFORMANCE-BASED SEISMIC DESIGN OF THE EXISTING RC BUILDING USING BRACED STEEL FRAME) อาจารย์ที่ปรึกษา : ผู้ช่วยศาสตราจารย์ ดร.มงคล จิรวัชรเดช, 193 หน้า.

แผ่นดินไหวเป็นภัยธรรมชาติที่ทำลายโครงสร้างในช่วงทศวรรษนี้ซึ่งเกิดขึ้นในภาคเหนือของประเทศไทย จากเหตุการณ์เหล่านี้วิทยานิพนธ์ฉบับนี้มีวัตถุประสงค์เพื่อประเมินระดับสมรรถนะของอาคารคอนกรีตเสริมเหล็กที่มีอยู่ วิเคราะห์อาคารสามชั้นหกชั้นและเก้าชั้นโดยใช้ SAP2000 และ Nonlinear Static Procedure เลือกวิธีการประเมินที่แตกต่างกันสี่วิธีสำหรับการศึกษา วิธีแรกคือวิธีการแทนที่ค่าสัมประสิทธิ์ที่แสดงใน ASCE / SEI 41-13 และ FEMA 440 วิธีนี้ใช้ในการคำนวณเป้าหมายการเคลื่อนตัวด้านข้าง (Target Displacement) เพื่อชี้ให้เห็น สมรรถนะของอาคารคอนกรีตเสริมเหล็กที่มีอยู่ วิธีที่สองคือวิธีสเปกตรัมตอบสนอง (Capacity Spectrum) ที่ตีพิมพ์ใน ACT 40 ใช้เพื่อระบุขีด จำกัด การเสียรูปเพื่อเปรียบเทียบกับอัตราส่วนการเคลื่อนตัวด้านข้างของหลังคาทั้งหมด ( $\Delta_{Rooftop} / H$ ) ที่จุดการเคลื่อนตัวด้านข้างสูงสุดเพื่อจำแนกระดับสมรรถนะต่างๆ วิธีที่สามคือการเคลื่อนตัวสัมพัทธ์ระหว่างชั้น (Inter-story drift) ใน ASE41-06 ซึ่งพิจารณาจากความแตกต่างระหว่างการเคลื่อนตัวของสองชั้นที่อยู่ติดกันซึ่งสามารถแสดงเป็นเปอร์เซ็นต์ของความสูง วิธีสุดท้าย ASCE / SEI 41-13 ใช้เกณฑ์การ จำกัด ค่ามอดูลเพื่อเปรียบเทียบกับค่ามอดูลพลาสติกสูงสุดสำหรับการประเมินสมรรถนะของอาคารคอนกรีตเสริมเหล็กที่มีอยู่ จากผลลัพธ์ของอาคารคอนกรีตเสริมเหล็กที่มีอยู่ กับอาคารสามชั้นวิธีที่หนึ่ง สอง และสามได้พบกับระดับความปลอดภัยต่อชีวิต (Life Safety, LS) ที่จำเป็นระดับการใช้งานได้ทันที (Immediate Occupancy, IO) และระดับความปลอดภัยต่อชีวิต (LS) ตามลำดับ ผลลัพธ์จากวิธีที่สี่ของวิทยานิพนธ์นี้ถูกแยกออกเป็นระดับสมรรถนะของคานและเสาซึ่งทั้งคู่ได้พบกับระดับประสิทธิภาพของระดับ (LS) สำหรับอาคารหกชั้นวิธีแรก วิธีที่สอง และสามตรงระดับความปลอดภัยต่อชีวิต (LS) ที่ระดับการใช้งานได้ทันที (IO) และระดับความปลอดภัยต่อชีวิต (LS) ตามลำดับ ผลลัพธ์จากวิธีที่สี่ของวิทยานิพนธ์นี้ถูกแยกออกเป็นระดับสมรรถนะของคานและเสาซึ่งทั้งคู่ได้พบกับระดับความปลอดภัยต่อชีวิต (LS) สำหรับอาคารเก้าชั้นวิธีแรกวิธีที่สองและสามตรงตามระดับความปลอดภัยของชีวิต (LS) ที่ต้องการระดับการเข้าพักทันที (IO) และระดับสมรรถนะโครงสร้างแบบป้องกันแบบพังทลาย (Collapse Prevention, CP) ตามลำดับ ผลลัพธ์จากวิธีที่สี่ของวิทยานิพนธ์นี้ถูกแยกออกเป็นระดับสมรรถนะของคานและเสาซึ่งทั้งคู่ได้พบกับระดับความปลอดภัยต่อชีวิต (LS) จากการทดลองแสดงให้เห็นว่าหากผู้เขียนใช้โครงเหล็กค้ำยันเพื่อเสริมกำลังโครงสร้างมันจะอยู่ในระดับการใช้งานได้ทันที (IO) สำหรับวิธีการทั้งหมด ผู้เขียนมีการลองคิดลอง

ถูกในการค้นหาคุณสมบัติเหล็กที่เหมาะสมเพื่อให้อาคารคอนกรีตเสริมเหล็กที่มีอยู่ ในระดับการใช้งานได้ทันที (IO) นอกจากนี้งานก่อสร้างของโครงเหล็กด้านนอกจะไม่หยุดการใช้งานของอาคาร ส่วนใหญ่จะช่วยลดค่าใช้จ่ายและลดการเคลื่อนตัวด้านข้างของอาคาร



สาขาวิชาวิศวกรรมโยธา  
ปี การศึกษา 2562

ลายมือชื่อนักศึกษา \_\_\_\_\_  
ลายมือชื่ออาจารย์ที่ปรึกษา \_\_\_\_\_

RITHY KHOUY : PERFORMANE-BASED SEISMIC DESIGN OF THE  
EXISTING RC BUILDING USING BRACED STEEL FRAMES. THESIS  
ADVISOR : ASST. PROF. MONGKOL JIRAVACHARADET, Ph.D.,  
193 PP.

NONLINEAR STATIC PROCEDURE/DISPLACEMENT COEFFICIENT  
METHOD/CAPACITY SPECTRUM METHOD/INTER-STORY DRIFT/  
SAP2000.

Earthquake is a natural disaster that destroyed the large properties and two deaths with many injuries during this decade, occurring at the north of Thailand. From these incidents, this paper aims to evaluate the performance level of existing reinforced concrete building and braced steel frames. A three-story building was analyzed using SAP2000 and the Nonlinear Static Procedure. Four different evaluation methods were chosen for this study. The first method is the Displacement Coefficient Method presented in ASCE/SEI 41-13 and FEMA 440. This is used to calculate target displacement to point out building performance levels. The second method, Capacity Spectrum Method published in ACT 40, is used to identify deformation limits to compare with total roof displacement ratio ( $\Delta_{\text{rooftop}} / H$ ) at the performance point to classify various performance levels. The third method is the Inter-story drift ratio in ASE41-06 is determined as the difference between the deflections of two adjacent floors which can be expressed as a percentage of the story height. The last method, ASCE/SEI 41-13 uses hinge rotation limit criteria to compare with maximum plastic hinge rotation for member evaluation of the RC frames. According to the result before retrofitting, the first, second and third methods meet the required Life Safety (LS)

level, Immediate Occupancy (IO) levels and Life Safety (LS) level, respectively. The results from the fourth method of this paper are separated into column and beam performance levels, where both met the performance levels of LS levels. From the experiment, it showed that if we use the concentrically braced steel frames to retrofit the structure, it will lie in Immediate Occupancy (IO) level for all of the methods. Furthermore, the construction works of outer steel frames do not stop the function of the buildings. Mainly, it reduces the cost and the displacement of the building.



School of Civil Engineering

Academic Year 2019

Student's Signature \_\_\_\_\_

Advisor's Signature \_\_\_\_\_

## ACKNOWLEDGEMENTS

The research work presented in this thesis entitled Performance-Based Seismic Design of the Existing RC Building using Braced Steel Frame was conducted at the School of Civil Engineering of Suranaree University of Technology, Thailand.

The author wishes to acknowledge the financial support provided by Office of the Higher Education Commission (OHEC) and Suranaree University of Technology, Thailand.

The author wishes to express his sincere gratitude to his supervisor, Dr. Mongkol Jiravacharadet, for his professional guidance, invaluable advice, and continuous encouragement. It is a great benefit and honor under him.

The author would like to thank Dr. Mongkol Jiravacharadet, Dr. Sittichai Seangatith, Dr. Pornpot Tanseng, Dr. Akawut Siriruk for their lectures, and providing engineering background knowledge, advice, discussion, and encouragement in order to obtain his master degree successfully.

The author would like to thank the CIA office, all the staffs, and the faculty members in School of Civil Engineering, Suranaree University of Technology, for their supports in academic, informing the updated information to student scholar, administration, and technical work during his study in Thailand.

The author sincerely appreciates his friends for their helping, discussion, giving ideas, etc.



Last but not least, the author would like to express his love and gratitude to his parents and relatives for their encouragement, supporting, and understanding throughout his life.

Rithy Khouy



# TABLE OF CONTENTS

	<b>Page</b>
ABSTRACT (THAI) .....	I
ABSTRACT (ENGLISH) .....	III
ACKNOWLEDGEMENTS .....	V
TABLE OF CONTENTS .....	VII
LIST OF TABLES.....	XVI
LIST OF FIGURES.....	XX
<b>CHAPTER</b>	
<b>I INTRODUCTION.....</b>	<b>1</b>
1.1 Background.....	1
1.2 Research Objective .....	2
1.3 Scope of research .....	2
1.4 Research Procedure.....	3
<b>II THEORITICAL BACKWGROUND AND</b>	
<b>LITERATURE REVIEW.....</b>	<b>5</b>
2.1 Introduction.....	5
2.2 Displacement Coefficient Method .....	6
2.3 Capacity Spectrum Method .....	17
2.4 Inter-story Drift Method .....	33
2.5 Acceptance Criteria.....	34
2.6 Braced Steel Frame.....	40

## TABLE OF CONTENTS (Continued)

	<b>Page</b>
<b>III METHOD AND METHODOLOGY.....</b>	<b>43</b>
3.1 Structural Modeling .....	43
3.1.1 Three-story building modeling .....	43
3.1.2 Six-story building modeling .....	45
3.1.3 Nine-story building modeling .....	46
3.2 Structural Modeling of retrofitted building .....	47
3.2.1 Three-story retrofitted building modeling .....	47
3.2.2 Six-story retrofitted building modeling .....	48
3.2.3 Nine-story retrofitted building modeling .....	49
3.3 Performance Evaluation of Existing Building .....	50
3.3.1 Displacement Coefficient Method of the three-story building .....	50
3.3.2 Displacement Coefficient Method of the six-story building .....	52
3.3.3 Displacement Coefficient Method of the nine-story building .....	53
3.3.4 Capacity Spectrum Method of the three- story building .....	54
3.3.5 Capacity Spectrum Method of the six- story building .....	56

## TABLE OF CONTENTS (Continued)

	<b>Page</b>
3.3.6 Capacity Spectrum Method of the nine-story building .....	57
3.3.7 Inter-story Drift Method of the three-story building .....	58
3.3.8 Inter-story Drift Method of the six-story building .....	61
3.3.9 Inter-story Drift Method of the nine-story building .....	63
3.3.10 Acceptance Criteria of the three-story building .....	64
3.3.10.1 Conditions of the Column .....	64
3.3.10.2 Conditions of the Beam .....	65
3.3.11 Acceptance Criteria of the six-story Building .....	66
3.3.11.1 Conditions of the Column .....	66
3.3.11.2 Conditions of the Beam .....	67
3.3.12 Acceptance Criteria of the nine-story building .....	69
3.3.12.1 Conditions of the Column .....	69
3.3.12.2 Conditions of the Beam .....	70
3.3.13 Stiffness Calculation Beam-Column Joints .....	71
3.4 Performance Evaluation of Retrofitted Building .....	73

## TABLE OF CONTENTS (Continued)

	<b>Page</b>
3.4.1 Displacement Coefficient Method of the three-story building.....	73
3.4.2 Displacement Coefficient Method of the six-story building .....	74
3.4.3 Displacement Coefficient Method of the nine-story building.....	75
3.4.4 Capacity Spectrum Method of the three- story building .....	76
3.4.5 Capacity Spectrum Method of the six- story building.....	77
3.4.6 Capacity Spectrum Method of the nine- story building .....	77
3.4.7 Inter-story Drift Method of the three- story building .....	78
3.4.8 Inter-story Drift Method of the six- story building .....	80
3.4.9 Inter-story Drift Method of the nine- story building .....	81
3.4.10 Acceptance Criteria of the three-story building.....	83

## TABLE OF CONTENTS (Continued)

	Page
3.4.10.1 Performance Evaluation of the Column.....	83
3.4.10.2 Performance Evaluation of the Beam .....	84
3.4.11 Acceptance Criteria of the six-story building .....	85
3.4.11.1 Performance Evaluation of the Column.....	85
3.4.11.2 Performance Evaluation of the Beam .....	87
3.4.12 Acceptance criteria of the nine-story building.....	88
3.4.12.1 Performance Evaluation of the Column.....	88
3.4.12.2 Performance Evaluation of the Beam .....	89
<b>IV RESULT AND COMPARISON .....</b>	<b>91</b>
4.1 Introduction.....	91
4.2 Performance Evaluation of Existing Building.....	92
4.2.1 Displacement Coefficient Method of the three-story building .....	92
4.2.2 Displacement Coefficient Method of the six-story building .....	93
4.2.3 Displacement Coefficient Method of the six-story building .....	94
4.2.4 Capacity Spectrum Method of the three- building.....	96
4.2.5 Capacity Spectrum Method of the six-story building .....	97

## TABLE OF CONTENTS (Continued)

	Page
4.2.6 Capacity Spectrum Method of the nine-story building.....	97
4.2.7 Inter-story Drift Method of the three-story building.....	97
4.2.8 Inter-story Drift Method of the six-story building.....	98
4.2.9 Inter-story Drift Method of the nine-story building.....	99
4.2.10 Member-Level Performance Method of the three-story building.....	101
3.4.10.1 Performance Level of the Column.....	101
3.4.10.2 Performance Level of the Beam.....	102
4.2.11 Member-Level Performance Method of the six-story building.....	104
3.4.11.1 Performance Level of the Column.....	104
3.4.11.2 Performance Level of the Beam.....	105
4.2.12 Member-Level Performance Method of the nine-story building.....	107
3.4.12.1 Performance Level of the Column.....	107
3.4.12.2 Performance Level of the Beam.....	108

## TABLE OF CONTENTS (Continued)

	<b>Page</b>
4.3 Performance Evaluation of Strengthening Building .....	110
4.3.1 Displacement Coefficient Method of the three-story building .....	110
4.3.2 Displacement Coefficient Method of the six-story building .....	113
4.3.3 Displacement Coefficient Method of the nine-story building .....	114
4.3.4 Capacity Spectrum Method of the three-story building .....	114
4.3.5 Capacity Spectrum Method of the six-story building .....	115
4.3.6 Capacity Spectrum Method of the nine-story building .....	115
4.3.7 Inter-story Drift Method of the three-story building .....	116
4.3.8 Inter-story Drift Method of the six-story building .....	116
4.3.9 Inter-story Drift Method of the nine-story building .....	117
4.3.10 Member-Level Performance Method of the three-story building .....	119



## TABLE OF CONTENTS (Continued)

	<b>Page</b>
3.4.10.1 Performance Level of the Column.....	119
3.4.10.2 Performance Level of the Beam .....	120
4.3.11 Member-Level Performance Method of the six-story building .....	122
3.4.11.1 Performance Level of the Column.....	122
3.4.11.2 Performance Level of the Beam .....	123
4.3.11.3 Braced steel frames of six-story building .....	123
4.3.12 Member-Level Performance Method of the Column.....	126
3.4.12.1 Performance Level of the Column.....	126
3.4.12.2 Performance Level of the Beam .....	127
4.3.12.3 Braced steel frames of nine-story building .....	128
4.4 Comparison of the result .....	130
4.4.1 Existing and strengthening of the three-story building.....	130
4.4.2 Existing and strengthening of the six-story building .....	131
4.4.3 Existing and strengthening of the nine-story building.....	131

## TABLE OF CONTENTS (Continued)

	<b>Page</b>
<b>V CONCLUSION</b> .....	132
5.1 Conclusion .....	132
5.2 Recommendation.....	133
REFERENCES.....	134
<b>APPENDICES</b>	
APPENDIX A. SIX-STORY BUILDING.....	137
APPENDIX B. NINE-STORY BUILDING.....	142
APPENDIX C. DISPLACEMENT COEFFICIENT METHOD .....	147
APPENDIX D. CAPACITY SPECTRUM METHOD.....	150
APPENDIX E. DESIGN METHOD .....	154
APPENDIX F. PUBLICATION .....	178
BIOGRAPHY .....	193

## LIST OF TABLES

<b>Table</b>		<b>Page</b>
2.1	Values for Modification Factor $C_0$ .....	9
2.2	Values for Modification Factor $C_0^1$ .....	14
2.3	Values for Modification Factor $C_2$ .....	15
2.4	Values for Damping Modification Factor, $\kappa$ .....	26
2.5	Minimum Allowable SRA and SRV values <sup>1</sup> .....	27
2.6	Structural Behavior Types.....	27
2.7	Modeling Parameters and Numerical Acceptance Criteria for Nonlinear Procedures-Reinforced Concrete Beam .....	37
2.8	Modeling Parameters and Numerical Acceptance Criteria for Nonlinear Procedures-Reinforced Concrete Column.....	38
3.1	Parameter and target displacement ( $\delta_t$ ) of three-story building .....	52
3.2	Parameter and target displacement ( $\delta_t$ ) of six-story building.....	53
3.3	Parameter and target displacement ( $\delta_t$ ) of nine-story building.....	54
3.4	Deformation limits .....	55
3.5	Conditions of the columns of the three-story building.....	65
3.6	Condition of the beams of the three-story building.....	66
3.7	Conditions of the columns of the six-story building.....	67
3.8	Condition of the beams of the six-story building.....	68
3.9	Conditions of the columns of the nine-story building.....	69
3.10	Condition of the beams of the nine-story building.....	71

## LIST OF TABLES (Continued)

<b>Table</b>		<b>Page</b>
3.11	Joint stiffness of the interior columns.....	72
3.12	Parameter and target displacement ( $\delta_t$ ) of three-story building.....	73
3.13	Parameter and target displacement ( $\delta_t$ ) of six-story building.....	74
3.14	Parameter and target displacement ( $\delta_t$ ) of nine-story building.....	75
3.15	Conditions of the columns of the three-story building.....	84
3.16	Conditions of the beam of the three-story building.....	85
3.17	Conditions of the columns of the three-story building.....	86
3.18	Conditions of the beam of the three-story building.....	87
3.19	Conditions of the columns of the three-story building.....	88
3.20	Conditions of the beam of the three-story building.....	90
4.1	Pushover steps of the three-story building.....	92
4.2	Pushover steps of the six-story building.....	94
4.3	Pushover steps of the nine-story building.....	95
4.4	Inter-story drift ratio (IDR).....	98
4.5	Inter-story drift ratio (IDR).....	99
4.6	Inter-story drift ratio (IDR).....	99
4.7	Structural Performance Levels and Damage <sub>1,2,3</sub> -Vertical Elements.....	100
4.8	Numerical acceptance criteria for plastic hinge rotation of the beams of the three-story building.....	102

## LIST OF TABLES (Continued)

<b>Table</b>	<b>Page</b>
4.9 Numerical acceptance criteria for plastic hinge rotation of the beams of the three-story building .....	103
4.10 Numerical acceptance criteria for plastic hinge rotation of the Columns of the six-story building .....	105
4.11 Numerical acceptance criteria for plastic hinge rotation of the beams of the six-story building.....	106
4.12 Numerical acceptance criteria for plastic hinge rotation of the columns of the nine-story building.....	108
4.13 Numerical acceptance criteria for plastic hinge rotation of the beams of the nine-story building.....	109
4.14 Pushover steps of the three-story building.....	111
4.15 Pushover steps of the six-story building.....	113
4.16 Pushover steps of the nine-story building.....	114
4.17 Inter-story drift ratio (IDR).....	116
4.18 Inter-story drift ratio (IDR).....	117
4.19 Inter-story drift ratio (IDR).....	118
4.20 Numerical acceptance criteria for plastic hinge rotation of the columns of the three-story building.....	119
4.21 Numerical acceptance criteria for plastic hinge rotation of the beams of the three-story building .....	121

## LIST OF TABLES (Continued)

Table	Page
4.22	Numerical acceptance criteria for plastic hinge rotation of the Columns of the six-story building ..... 122
4.23	Numerical acceptance criteria for plastic hinge rotation of the beams of the six-story building ..... 124
4.24	Numerical acceptance criteria for plastic hinge rotation of the columns of the nine-story building ..... 126
4.25	Numerical acceptance criteria for plastic hinge rotation of the beams of the nine-story building ..... 128
C.1	Spectral response acceleration $S_S$ and $S_1$ ..... 148
D.1	Seismic zone factor $Z$ ..... 153
D.2	Seismic Coefficient, $C_A$ ..... 153
D.3	Seismic Coefficient, $C_V$ ..... 153
E.1	Transverse Reinforcement Details: Condition to Be Used for Columns in Table E.2 ..... 168
E.2	Modeling Parameters and Numerical Acceptance Criteria for Nonlinear Procedures-Reinforced Concrete Columns ..... 169
E.3	Modeling Parameters and Numerical Acceptance Criteria for Nonlinear Procedures-Reinforced Concrete Beams ..... 176

## LIFE OF FIGURES

Figure	Page
1.1	Scope of research ..... 4
2.1	Displacement Coefficient. ( ATC 40)..... 7
2.2	Idealized Force–Displacement Curves. (ASEC41-13) ..... 10
2.3	Capacity Spectrum Method. (ATC 40)..... 19
2.4	Response spectra in Traditional and ADRS formats. (ATC 40)..... 22
2.5	Derivation of Damping For Spectral Reduction. (ATC 40) ..... 23
2.6	Derivation of Energy Dissipated..... 24
2.7	Derivation of Energy ..... 24
2.8	Reduced Response Spectrum. (ATC 40) ..... 25
2.9	Capacity spectra Procedure “B” after step 2. (ATC 40) ..... 28
2.10	Capacity spectra Procedure “B” after step 3. (ATC 40) ..... 29
2.11	Capacity spectrum procedure “B” after step 4. (ATC 40)..... 30
2.12	Capacity spectrum procedure “B” after step 6. (ATC 40) ..... 32
2.13	Capacity spectrum procedure “B” after step 6. (ATC 40)..... 33
2.14	Capacity spectrum procedure “B” after step 6. (ATC 40)..... 34
2.15	Generalized component force-deformation relations. (ASCE 41-13) ..... 35
3.1	3D view of three-story building. (SAP2000)..... 44
3.2	3D view of six-story building. (SAP2000) ..... 45
3.3	3D view of nine-story building. (SAP2000)..... 46
3.4	3D view of the three-story braced steel frame. (SAP2000)..... 47

## LIST OF FIGURES (Continued)

<b>Figure</b>	<b>Page</b>
3.5 3D view of the six-story braced steel frame. (SAP2000) .....	49
3.6 3D view of the nine-story braced steel frame. (SAP2000) .....	40
3.7 Multi-Degree-Of-Freedom.....	51
3.8 Single-Degree-Of-Freedom .....	51
3.9 Capacity spectrum curve of the three-story building. (SAP2000).....	55
3.10 Capacity spectrum curve of the six-story building. (SAP2000) .....	56
3.11 Capacity spectrum curve of the nine-story building. (SAP2000).....	57
3.12 Story deflections (cm).....	59
3.13 Inter-story drift (%).....	60
3.14 Inter-Story Drift Determination. (ASCE 41-13).....	60
3.15 Story deflections (cm).....	61
3.16 Inter-story drift (%).....	62
3.17 Story deflections (cm).....	63
3.18 Inter-story drift (%).....	64
3.19 Beam–Column joint stiffness modeling. (ASCE 41-13) .....	72
3.20 Capacity spectrum curve of three-story building. (SAP2000).....	76
3.21 Capacity spectrum curve of six-story building. (SAP2000) .....	77
3.22 Capacity spectrum curve of nine-story building. (SAP2000).....	78
3.23 Story deflections (cm).....	79
3.24 Inter-story drift (%).....	79
3.25 Story deflections (cm).....	80



## LIST OF FIGURES (Continued)

<b>Figure</b>	<b>Page</b>
3.26 Inter-story drift (%).....	81
3.27 Story deflections (cm).....	82
3.28 Inter-story drift (%).....	83
4.1 Performance levels of the three-story building.....	104
4.2 Performance levels of the six-story building .....	107
4.3 Performance levels of the nine-story building.....	110
4.4 Performance levels of the three-story building.....	123
4.5 Performance levels of the six-story building .....	125
4.6 Plastic hinges of the braced steel frame.....	125
4.7 Performance levels of the nine-story building.....	129
4.8 Plastic hinges of the braced steel frame.....	130
A.1 Beam section property .....	138
A.2 Reinforcement property .....	139
A.3 Column section property.....	140
A.4 Reinforcement property .....	141
B.1 Beam section property .....	143
B.2 Reinforcement property .....	144
B.3 Column section property.....	145
B.4 Reinforcement property .....	146
C.1 Spectral response acceleration $S_s$ and $S_1$ of the Chiang Rai city.....	149
D.1 Seismic zone factor $Z$ .....	152

## LIST OF FIGURES (Continued)

Figure	Page
D.2	Seismic coefficient $C_v$ and $C_a$ ..... 154
E.1	Dead load case shear force of the column as shown in the rectangular box ..... 156
E.2	Live load case shear force of the column as shown in the rectangular box ..... 156
E.3	Super impose dead load case shear force of the column as shown in the rectangular box ..... 157
E.4	Lateral load case shear force of the column as shown in the rectangular box ..... 157
E.5	Dead load case axial force of the column as shown in the rectangular box ..... 158
E.6	Live load case axial force of the column as shown in the rectangular box ..... 158
E.7	Super impose dead load case axial force of the column as shown in the rectangular box ..... 159
E.8	Lateral load case axial force of the column as shown in the rectangular box ..... 159
E.9	Dead load case bending moment of the column as shown in the rectangular box ..... 160
E.10	Live load case bending moment of the column as shown in the rectangular box ..... 160

## LIST OF FIGURES (Continued)

Figure	Page
E.11 Super impose dead case bending moment of the column as shown in the rectangular box .....	161
E.12 Lateral load case bending moment of the column as shown in the rectangular box .....	161
E.13 Column Section of the first floor .....	164
E.14 Bottom flexural capacity of the column.....	166
E.15 Top flexural capacity of the column .....	167
E.16 Design shears for beams and columns. (ACI 318-14).....	168
E.17 Dead load case shear force of the column as shown in the rectangular box .....	170
E.18 Dead load case shear force of the column as shown in the rectangular box .....	171
E.19 Dead load case shear force of the column as shown in the rectangular box .....	171
E.20 Dead load case shear force of the column as shown in the rectangular box .....	172
E.21 Beam section of the first floor .....	173

# CHAPTER I

## INTRODUCTION

### 1.1 Background

Many existing reinforced concrete have designed to use conventional code that never considers earthquakes to combine with gravity and another load because they believe that Thailand does not require seismic load for analyzing the building in the past, but everything has changed after the earthquakes have occurred in the north part of Thailand. By the way, many structures have collapsed and damaged that need to redesign and to strengthen for the whole or element of the building. The new standard, DPT.1303-57, is to assess and retrofit of the building structure in the area of the earthquake zones, This standard referred from ASCE/SEI 41-06 that updated to ASCE/SEI 41-13. Therefore, this paper has selected some standards, ASCE/SEI 41-13, FEMA 440, ATC 40 and ASCE/SEI 41-06 to assess building performance levels. After that, the nonlinear static analysis is one of the methods that use to evaluate the structural performances. There are plenty of technologies that build up the structure to resist the lateral load such as steel plate shear wall, damping, steel bracing, shear wall and so on. Moreover, braced steel frames were chosen to research the reaction of the building that opposed to the dynamic load. The evidence has seen clearly about the characteristics of the structural behaviors before and after retrofitting braced steel frames that to upgrade the strength, to increase the structural stiffness, to reduce structural deformation, to reduce construction time and to construct outside the building that does not affect building service. This paper is a case study that utilizes

many standards, separating into four different procedures like the Displacement Coefficient Method, the Capacity Spectrum Method, Inter-story Drift Method, and member-level performance Method to assess the building performance levels. Additionally, these varied approaches obtained similar results before retrofitting and the same results after retrofitting the building.

## **1.2 Research Objective**

1.2.1 To calculate the value, evaluate, and compare the performance level of the Displacement Coefficient Method, Capacity Spectrum Method, Inter-story Drift Method, and Member-Level Performance Method for existing RC building.

1.2.2 To calculate the value, evaluate, and compare the performance level of the Displacement Coefficient Method, Capacity Spectrum Method, Inter-story Drift Method, and Member-Level Performance Method for strengthening RC structure.

## **1.3 Scope of research**

Three-story, six-story, and nine-story building that locate in Chiang Rai city, Chiang Rai province, assume an existing building for studying the structural performance levels, is an ordinary reinforced concrete moment frame. The pushover Analysis was used to analyze the building and used four methods to evaluate the performance level of the existing building such as the Displacement Coefficient Method, Capacity Spectrum Method, Inter-story Drift Method and Member-Level Performance Method. The author selected the braced steel frames to strengthen the existing RC building and used the same method as the existing RC building to assess the performance level of the building.

## 1.4 Research Procedure

1.4.1 Study the previous research and related standards.

1.4.2 Using Department of Public Works and Town & Country Planning (DPT) 1302-52 for calculating the lateral force.

1.4.3 3D Modeling of the existing RC building by using SAP2000.

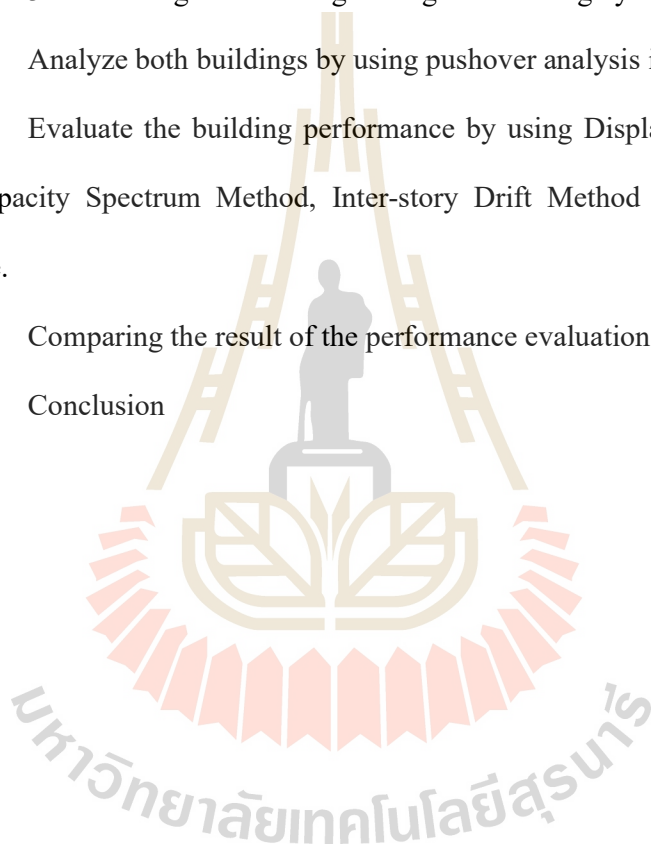
1.4.4 3D Modeling of the strengthening RC building by using SAP2000.

1.4.5 Analyze both buildings by using pushover analysis in SAP2000.

1.4.6 Evaluate the building performance by using Displacement Coefficient Method, Capacity Spectrum Method, Inter-story Drift Method and Member-Level Performance.

1.4.7 Comparing the result of the performance evaluation of the structure.

1.4.8 Conclusion



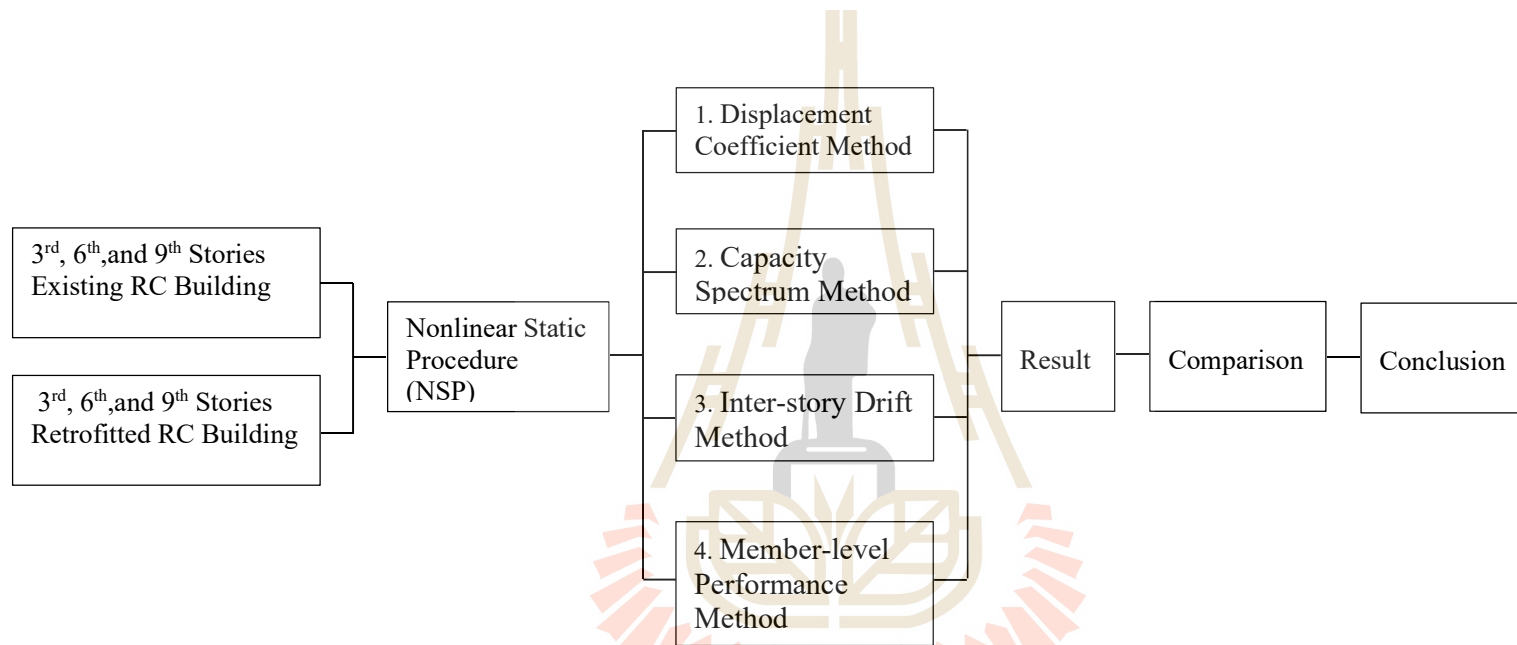


Figure 1.1 Scope of research

# **CHAPTER II**

## **THEORITICAL BACKWGROUND AND LITERATURE REVIEW**

### **2.1 Introduction**

Many methods can evaluate the building performance like Linear Static Procedure (LSP), Linear Dynamic Procedure (LDP), Nonlinear Static Procedure (NSP), and Nonlinear Dynamic Procedure (NDP). This paper was used Nonlinear Static Procedure (NSP) for evaluating the building performance. This method has many different ways to evaluate the building performance level such as Displacement Coefficient Method, Capacity Spectrum Method, Member-Level Performance, Inter-story Drift, Energy Based Analysis and so on. This paper was chosen Displacement Coefficient Method, Capacity Spectrum Method, Inter-story Drift Method, and Member-Level Performance Method for studying the performance level of the building. The nonlinear pushover analysis is carried out the analytical building model that consists of gravity and lateral load pattern. Before running the lateral load, the gravity load that considered as linear static is applied to the analyzed model in a step-by-step following ASCE/SEI 41-13 equation 7.3. At the end of the analytical gravity load, the lateral force continues to apply monotonically increasing in a stepwise till the building reached a target displacement or collapsed condition.

The lateral load pattern is performed on the structure with two different types the first mode shape of the analysis in the direction under consideration or the load pattern defined by the user. The moment-curvature analyses are performed base on the



section properties and the reinforcement at the plastic hinges in all members. The moment-rotation that to be instead of moment-curvature is used to performance elevation levels all the members. The relationship between base shear and lateral displacement of the control node is plotted to establish for control node displacements multiple by 1.5 of the target displacement. The control node displacement increases monotonically at every step of the analysis to reach the equilibrium between the external and the internal force of the structural deformation at this step. When the analysis reaches the equilibrium, then the analysis starts to the next step. During the proceeded analysis, the analysis will be terminated when the analysis meets the termination condition such as the target displacement, the maximum deformation of element and component.

Therefore, deformation-controlled and force-controlled action compared to the corresponding acceptance criteria to determine performance evaluations.

## 2.2 Displacement Coefficient Method

Displacement coefficient method was used to calculate the target displacement of the control node on the roof . The building that used to evaluate the performance levels is the symmetry configuration, needed only one direction for qualified its performance. The Displacement Coefficient method modifies  $\delta_{\text{elastic}}$  with coefficients to calculate a target displacement,  $\delta_t$ . The target displacement for ASCE 41-13,  $\delta_t$ , at each floor level shall be calculated in accordance with Eq. (2.1).

$$\delta_t = C_0 C_1 C_2 S_a \left( \frac{T_c}{2\pi} \right)^2 g \quad (2.1)$$

where: Period Determination for NSP The effective fundamental period in the direction under consideration shall be based on the idealized force–displacement curve defined in Fig. 2.2. The effective fundamental period,  $T_e$ , shall be calculated in accordance with Eq. (2.2):

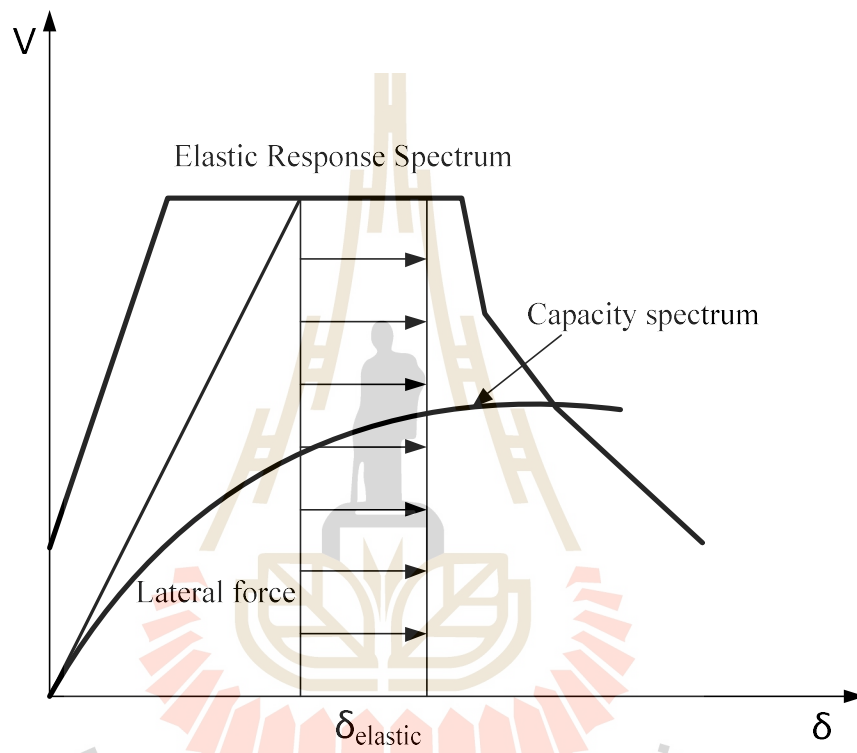


**Figure 2.1** Displacement Coefficient. (ATC 40)

$$T_e = T_i \sqrt{\frac{K_i}{K_e}} \quad (2.2)$$

where  $g$  : acceleration of gravity.

$T_i$  : Elastic foundation period (second) in the direction under consideration calculated by elastic dynamic analysis.

- $K_i$  : Elastic lateral stiffness of the building in the direction under consideration calculated using the modeling requirements in Fig 2.2.
- $K_e$  : Effective lateral stiffness of the building in the direction under consideration.
- $S_a$  : Response spectrum acceleration at the effective fundamental period and damping ratio of the building in the direction under consideration.
- $C_0$  : Modification factor to relate spectral displacement of an equivalent single-degree-of-freedom (SDOF) system to the roof displacement of the building multi-degree-of-freedom (MDOF) system calculated using one of the following procedures: The first mode mass participation factor multiplied by the ordinate of the first mode shape at the control node;  
The mass participation factor calculated using a shape vector corresponding to the deflected shape of the building at the target displacement multiplied by ordinate of the shape vector at the control node; or The appropriate value from Table 7-5;

**Table 2.1** Values for Modification Factor  $C_0$ 

Number of Stories	Shear Buildings <sup>a</sup>		Other Buildings
	Triangular Load Pattern (1.1, 1.2, 1.3)	Uniform Load Pattern (2.1)	Any Load Pattern
1	1.0	1.0	1.0
2	1.2	1.15	1.2
3	1.2	1.2	1.3
5	1.3	1.2	1.4
+10	1.3	1.2	1.5

NOTE: Linear interpolation shall be used to calculate intermediate values.

<sup>a</sup>Buildings in which, for all stories, story drift decreases with increasing height.

**Idealized Force–Displacement Curve for NSP** The idealized force–displacement curve is developed using an iterative graphical procedure to balance the areas below the actual and idealized curves up to  $\Delta_d$  such that the idealized curve has the properties defined in this section. The definition of the idealized force–displacement curve was modified from the definition in FEMA 356 (2000) based on the recommendations of FEMA 440 (2005).

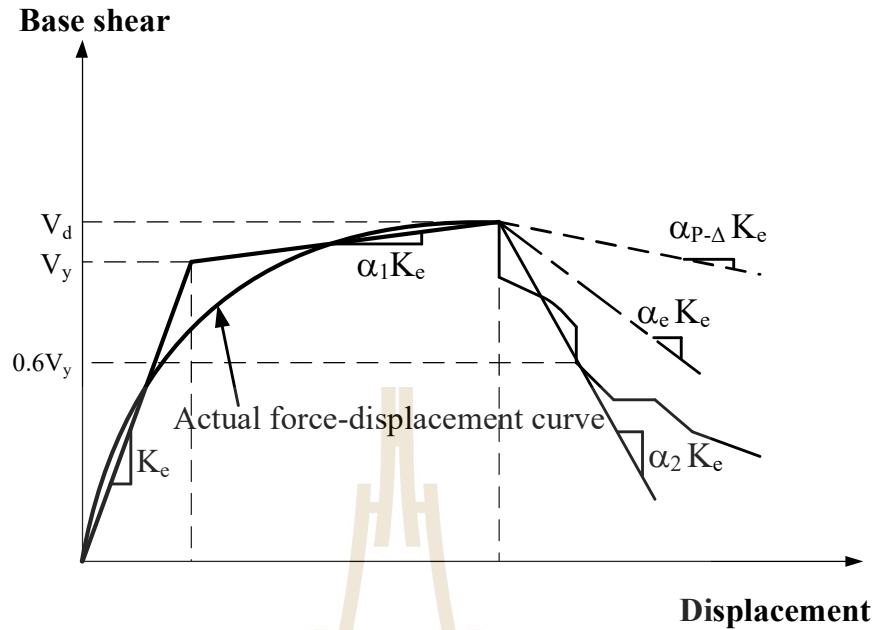


**Figure 2.2** Idealized Force–Displacement Curves. (ASEC41-13)

Other way to calculate the  $C_0$  coefficient accounts for the difference between the roof displacement of a multi-degree-of-freedom (MDOF) building and the displacement of the equivalent single-degree-of-freedom (SDOF) system. Using only the first mode shape ( $\phi_1$ ) and elastic behavior, coefficient  $C_0$  is equal to

$$C_0 = \Phi_{1,r} \frac{\{\Phi_1\}^T [M] \{1\}}{\{\Phi_1\}^T [M] \{\Phi_1\}} \quad (2.3)$$

$$= \Phi_{1,r} \Gamma_1$$

where  $\Phi_{1,r}$  : The ordinate of mode shape 1 at the roof (control node);

$[M]$  : A diagonal mass matrix; and

$\Gamma_1$  : The first modal mass participation factor.

Because the mass matrix is diagonal, Eq. 2.3 can be rewritten as

$$C_0 = \Phi_{1,r} \frac{\sum_1^N m_i \Phi_{i,n}}{\sum_1^N m_i \Phi_{i,n}^2}$$

where  $m_i$  : The mass at level  $i$  and

$\Phi_{i,n}$  : The ordinate of mode shape  $i$  at level  $n$ .

$C_1$  : Modification factor to relate expected maximum inelastic displacements to displacements calculated for linear elastic response.

For periods less than 0.2 s,  $C_1$  need not be taken greater than the value at  $T = 0.2$  s. For periods greater than 1.0 s,  $C_1 = 1.0$ .

$$C_1 = 1 + \frac{\mu_{\text{strength}} - 1}{a T_e^2} \quad (2.4)$$

where  $a$  : Site class factor:

: 130 Site Class A or B;

: 90 Site Class C;

: 60 Site Class D, E, or F;

$T_e$  : Effective fundamental period of the building in the direction under consideration, in seconds;

$T_s$  : Characteristic period of the response spectrum, defined as the period associated with the transition from the constant acceleration segment of the spectrum to the constant velocity segment of the spectrum.

$\mu_{\text{strength}}$  : Ratio of elastic strength demand to yield strength coefficient calculated in accordance with Eq. (2.6). Use of the NSP is not permitted where  $\mu_{\text{strength}}$  exceeds  $\mu_{\text{max}}$ .

$C_2$  : Modification factor to represent the effect of pinched hysteresis shape, cyclic stiffness degradation, and strength deterioration on the maximum displacement response.

For periods greater than 0.7 s,  $C_2 = 1.0$ ;

$$C_2 = 1 + \frac{1}{1800} \left( \frac{\mu_{\text{strength}} - 1}{T_c} \right)^2 \quad (2.5)$$

The strength ratio  $\mu_{\text{strength}}$  shall be calculated in accordance with Eq. (2.5):

$$\mu_{\text{strength}} = \frac{S_a}{V_y/W} C_m \quad (2.6)$$

where  $S_a$  : is defined above and

$V_y$  : Yield strength of the building in the direction under consideration calculated using results of the NSP for the idealized nonlinear force–displacement curve developed for the building.

$W$  : Effective seismic weight.

$C_m$  : Effective mass factor. Alternatively,  $C_m$ , taken as the effective modal mass participation factor calculated for the fundamental mode using an eigenvalue analysis, shall be permitted.  $C_m$  shall be taken as 1.0 if the fundamental period,  $T$ , is greater than 1.0s.

For buildings with negative post-yield stiffness, the maximum strength ratio,  $\mu_{\text{max}}$ , shall be calculated in accordance with Eq. (2.7) .

$$\mu_{\max} = \frac{\Delta_d}{\Delta_y} + \frac{|\alpha_e|^{-h}}{4} \quad (2.7)$$

where  $\alpha_e$  : Effective negative post-yield slope ratio.

$\Delta_d$  : Lesser of the target displacement,  $\delta_t$ , or displacement corresponding to the Maximum base shear defined in Fig. 2.2;

$\Delta_y$  : Displacement at effective yield strength defined in Fig. 2.2;

$H$  :  $1 + 0.15 \ln T_e$ ; and

$\alpha_e$  : Effective negative post-yield slope ratio.

The effective negative post-yield slope ratio,  $\alpha_e$ , shall be calculated in accordance with Eq. (2.8):

$$\alpha_e = \alpha_{p-\Delta} + \lambda(\alpha_2 - \alpha_{p-\Delta}) \quad (2.8)$$

where  $\alpha_2$  : Negative post-yield slope ratio defined in Fig. 2.2. This ratio includes

$P-\Delta$  : effects, in-cycle degradation, and cyclic degradation.

$\alpha_{p-\Delta}$  : Negative slope ratio caused by  $P-\Delta$  effects; and

$\lambda$  : Near-field effect factor:

: 0.8 if  $SX1 \geq 0.6$  for BSE-2N;

: 0.2 if  $SX1 \leq 0.6$  for BSE-2N.

The target displacement for FEMA 440,  $\delta_t$ , which corresponds to the displacement at roof level, can be estimated as Eq. (2.9).

$$\delta_t = C_0 C_1 C_2 C_3 S_a \left( \frac{T_e}{2\pi} \right)^2 g \quad (2.9)$$



where  $g$  : Gravitational acceleration.

$C_0$  : Modification factor to relate spectral displacement of an equivalent SDOF system to the roof displacement of the building MDOF system.

It can be calculated from

1. the first modal participation factor,
2. the appropriate value from Table 2.2 in FEMA 356.

**Table 2.2** Values for Modification Factor  $C_0$ <sup>1</sup>

Number of Stories	Shear Buildings <sup>2</sup>		Other Buildings
	Triangular Load Pattern (1.1, 1.2, 1.3)	Uniform Load Pattern (2.1)	Any Load Pattern
1	1.0	1.0	1.0
2	1.2	1.15	1.2
3	1.2	1.2	1.3
5	1.3	1.2	1.4
+10	1.3	1.2	1.5

1. Linear interpolation shall be used to calculate intermediate values.
2. Buildings in which, for all stories, inter-story drift decreases with increasing height.

$C_1$  : Modification factor to relate the expected maximum displacements of an inelastic SDOF oscillator with EPP hysteretic properties to displacements calculated for the linear elastic response.

$$C_1 = \begin{cases} 1.0 & \text{for } T_e \geq T_s \\ 1.0 + \frac{(R-1)T_s}{T_E} & \text{for } T_s < T_e \\ \frac{1.0}{R} & \end{cases} \quad (2.10)$$

but not greater than the values given in (Linear Static Procedure, LSP section) nor less than 1.

Values of  $C_1$  are

$$C_1 = \begin{cases} 1.5 & \text{for } T_e < 0.1 \text{ s} \\ 1.0 & \text{for } T_s \geq T_e \end{cases} \quad (2.11)$$

With linear interpolation used to calculate  $C_1$  for the intermediate values of  $T_e$ .

$C_2$ : Modification factor to represent the effect of pinched hysteretic shape, stiffness degradation, and strength deterioration on the maximum displacement response. Values of  $C_2$  for different framing systems and structural performance levels (i.e., immediate occupancy, life safety, and collapse prevention) are obtained from Table 2.3 of the FEMA 356 document. Alternatively,  $C_2$  can take the value of one in nonlinear procedures.

**Table 2.3** Values for Modification Factor  $C_2$

Structural Performance Level	$T \leq 0.1 \text{ second}^3$		$T \geq T_s \text{ second}^3$	
	Framing Type 1 <sup>1</sup>	Framing Type 2 <sup>2</sup>	Framing Type 1 <sup>1</sup>	Framing Type 2 <sup>2</sup>
Immediate Occupancy	1.0	1.0	1.0	1.0
Life Safety	1.3	1.0	1.1	1.0
Collapse Prevention	1.5	1.0	1.2	1.0

1. Structures in which more than 30% of the story shear at any level is resisted by any combination of the following components, elements, or frames: ordinary moment-resisting frames, concentrically-braced frames, frames with partially-restrained connections, tension-only braces, unreinforced masonry walls, shear-critical, piers, and spandrels of reinforced concrete or masonry.
2. All frames not assigned to Framing Type 1.
3. Linear interpolation shall be used for intermediate values of T.

$C_3$  : Modification factor to represent increased displacements due to dynamic P- $\Delta$  effects. For buildings with positive post-yield stiffness,  $C_3$  is set equal to 1. For buildings with negative post-yield stiffness, values of  $C_3$  are calculated using the following expression:

$$C_3 = 1.0 + \frac{|\alpha|(R-1)^{\frac{3}{2}}}{T_e} \quad (2.12)$$

where: R : Ratio of elastic strength demand to calculated strength capacity.

$T_e$  : Effective fundamental period of the building computed in accordance with Eq. (2.2):

$T_s$  : Characteristic period of the response spectrum, defined as the period associated with the transition from the constant-acceleration segment of the spectrum to the constant-velocity segment of the spectrum.

$S_a$  : Response spectrum acceleration, at the effective fundamental period and damping ratio of the building.

### 2.3 Capacity Spectrum Method

Two key elements of a performance-based design procedure are demand and capacity. Demand is a representation of the earthquake ground motion. Capacity is a representation of the structure's ability to resist the seismic demand. The performance is dependent on the manner that the capacity is able to handle the demand. In other words, the structure must have the capacity to resist the demands of the earthquake such that the performance of the structure is compatible with the objectives of the design.

Simplified nonlinear analysis procedures using pushover methods, such as the capacity spectrum method, require determination of three primary elements: capacity, demand (displacement) and performance. Each of these elements is briefly discussed below.

**Capacity:** The overall capacity of a structure depends on the strength and deformation capacities of the individual components of the structure. In order to determine capacities beyond the elastic limits, some form of nonlinear analysis, such as the pushover procedure, is required. This procedure uses a series of sequential elastic analyses, superimposed to approximate a force-displacement capacity diagram of the overall structure. The mathematical model of the structure is modified to account for reduced resistance of yielding components. A lateral force distribution is again applied until additional components yield. This process is continued until the structure becomes unstable or until a predetermined limit is reached. For two dimensional models, computer programs are available that directly model nonlinear behavior and can create a pushover curve directly. The pushover capacity curve approximates how structures behave after exceeding their elastic limit.

**Demand (displacement):** Ground motions during an earthquake produce complex horizontal displacement patterns in structures that may vary with time. Tracking this motion at every time-step to determine structural design requirements is judged impractical. Traditional linear analysis methods use lateral forces to represent a design condition. For nonlinear methods it is easier and more direct to use a set of lateral displacements as a design condition. For a given structure and ground motion, the displacement demand is an estimate of the maximum expected response of the building during the ground motion.

**Performance:** Once a capacity curve and demand displacement are defined, a performance check can be done. A performance check verifies that structural and nonstructural components are not damaged beyond the acceptable limits of the performance objective for the forces and displacements implied by the displacement demand.

The nonlinear static analysis procedure has also included the capacity spectrum method (CSM) that uses the intersection of the capacity-demand spectrum curve to estimate maximum roof displacement at the performance point as shown in figure. 2.3.

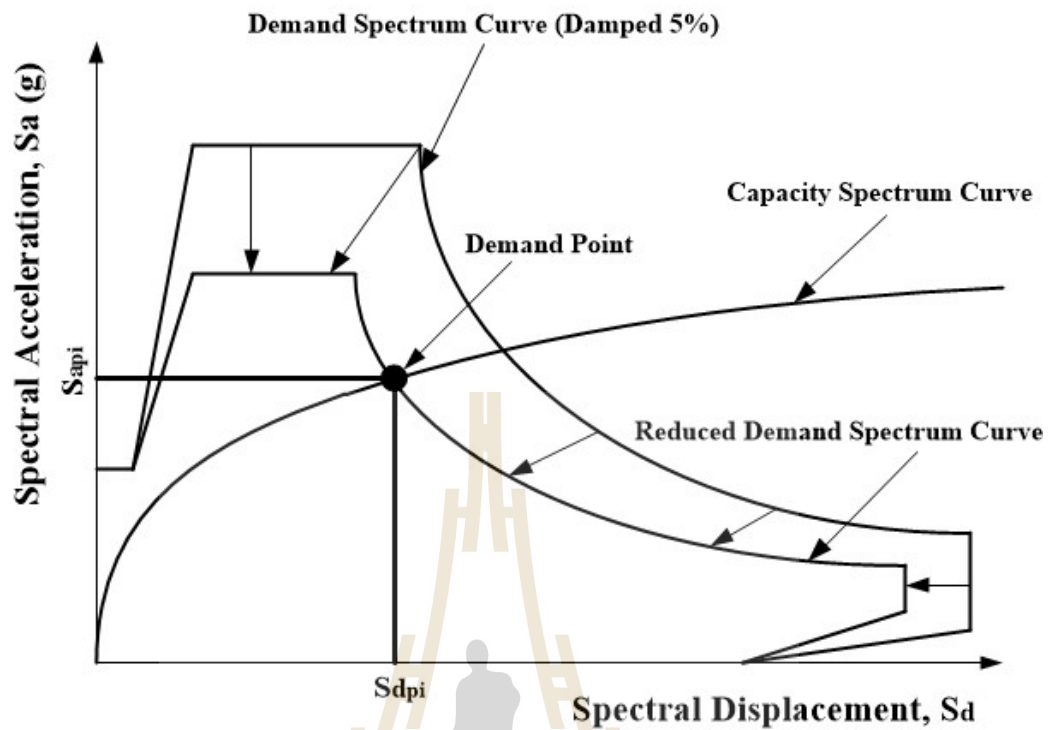


Figure 2.3 Capacity Spectrum Method. (ATC 40)

#### Conceptual Development of the Capacity Spectrum Method

To use the capacity spectrum method it is necessary to convert the capacity curve, which is in terms of base shear and roof displacement to what is called a capacity spectrum, which is a representation of the capacity curve in Acceleration-Displacement Response Spectra (ADRS) format (i.e.,  $S_a$  versus  $S_d$ ). The required equations to make the transformation are:

$$\Gamma_1 = \frac{\sum_{i=1}^N m_i \Phi_{i1}}{\sum_{i=1}^N m_i \Phi_{i1}^2} \quad (2.13)$$

$$\alpha_1 = \frac{\left( \sum_{i=1}^N m_i \Phi_{i1} \right)^2}{\left( \sum_{i=1}^N m_i \right) \left( \sum_{i=1}^N m_i \Phi_{i1}^2 \right)} \quad (2.14)$$

$$S_a = \frac{V_b}{W \alpha_1} \quad (2.15)$$

$$S_d = \frac{\delta_{\text{roof}}}{\Gamma_1 \Phi_{\text{roof}, 1}} \quad (2.16)$$

where  $\Gamma_1$  : modal participation factor for the first natural mode.

$\alpha_1$  : modal mass coefficient for the first natural mode.

$m_i$  : mass assigned to level  $i$ .

$\Phi_{i1}$  : amplitude of mode 1 at level  $i$ .

$N$  : level  $N$ , the level which is the uppermost in the main portion of the Structure.

$V$  : base shear.

$W$  : building dead weight plus likely live loads.

$\Delta_{\text{roof}}$ : roof displacement ( $V$  and the associated  $\Delta_{\text{roof}}$  make up points on the capacity curve).

$S_a$  : spectral acceleration.

$S_d$  : spectral displacement ( $S_a$  and the associated  $S_d$  make up points on the capacity spectrum).

### Response Spectrum Conversion

Application of the Capacity-Spectrum technique requires that both the demand response spectra and structural capacity (or pushover) curves be plotted. in the

spectral acceleration vs spectral displacement domain. Spectra plotted in this format are known as Acceleration-Displacement Response Spectra (ADRS). Every point on a response spectrum curve has associated with it a unique spectral acceleration,  $S_a$ , spectral velocity,  $S_v$ , spectral displacement,  $S_d$  and period,  $T$ . To convert a spectrum from the standard  $S_a$  vs  $T$  format found in the building code to ADRS format, it is necessary to determine the value of  $S_{di}$  for each point on the curve,  $S_{ai}$ ,  $T_i$  as shown in Figure 2.4. This can be done with the equation:

$$S_{d_i} = \frac{T_i^2}{4\pi^2} S_{a_i} g \quad (2.17)$$

Standard demand response spectra contain a range of constant spectral acceleration and a second range of constant spectral velocity. Spectral acceleration and displacement at period  $T_i$ , are given by:

$$S_{a_i} g = \frac{2\pi}{T_i} S_v \quad (2.18)$$

$$S_{d_i} = \frac{T_i}{2\pi} S_v \quad (2.19)$$

### Equivalent Viscous Damping

The damping that occurs when earthquake ground motion drives a structure into the inelastic range can be viewed as a combination of viscous damping that is inherent in the structure and hysteretic damping. Hysteretic damping is related to the area inside the loops that are formed when the earthquake force (base shear) is plotted against the structure displacement. Hysteretic damping can be represented as equivalent viscous damping using equations that are available in the literature.



The equivalent viscous damping,  $\beta_{eq}$ , associated with a maximum displacement of  $d_{pi}$ , can be estimated from the following equation:

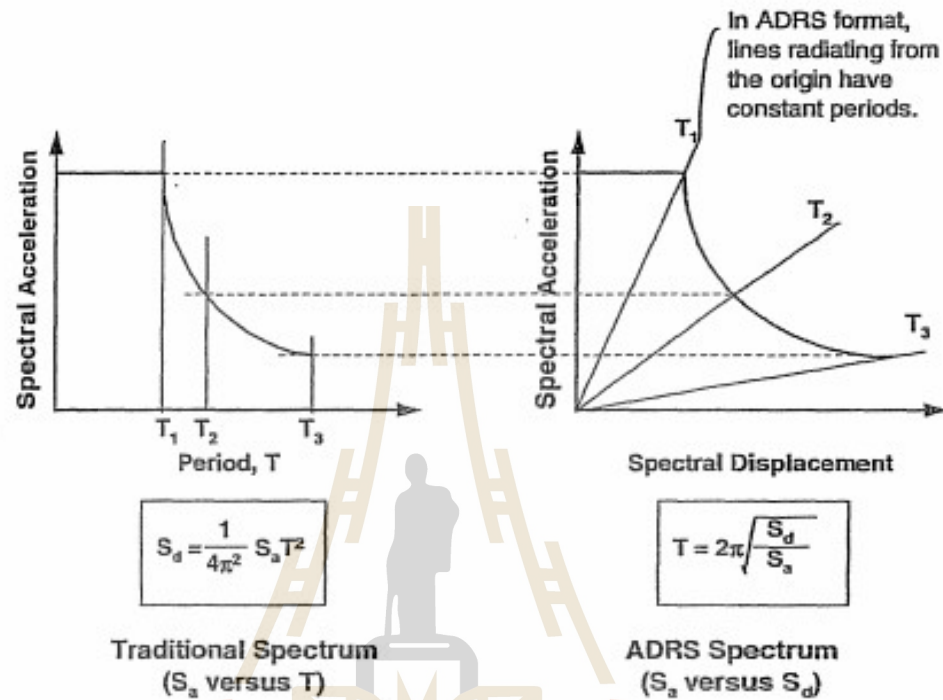


**Figure 2.4** Response spectra in Traditional and ADRS formats. (ATC 40)

$$\beta_{eq} = \beta_0 + 0.05 \quad (2.20)$$

where  $\beta_0$  : hysteretic damping represented as equivalent viscous damping

0.05 : 5% viscous damping inherent in the structure (assumed to be constant)

The term  $\beta_0$  can be calculated as (Chopra 1995):

$$\beta_0 = \frac{1}{4\pi} \frac{E_D}{E_{S_0}} \quad (2.21)$$

where  $E_D$  : energy dissipated by damping

$E_{S_0}$  : maximum strain energy

The physical significance of the terms  $E_D$  and  $E_{S_0}$  in equation 2.21 is illustrated in Figure 2.5.

$E_D$  = Energy dissipated by damping

= Area enclosed by hysteresis loop

= Area of parallelogram

$E_{S_0}$  = Maximum strain energy

= Area of hatched triangle

=  $a_{pi}d_{pi} / 2$

$\beta_0$  = Equivalent viscous damping associated with full hysteresis loop area

$$\beta_0 = \frac{1}{4\pi} \frac{E_D}{E_{S_0}}$$

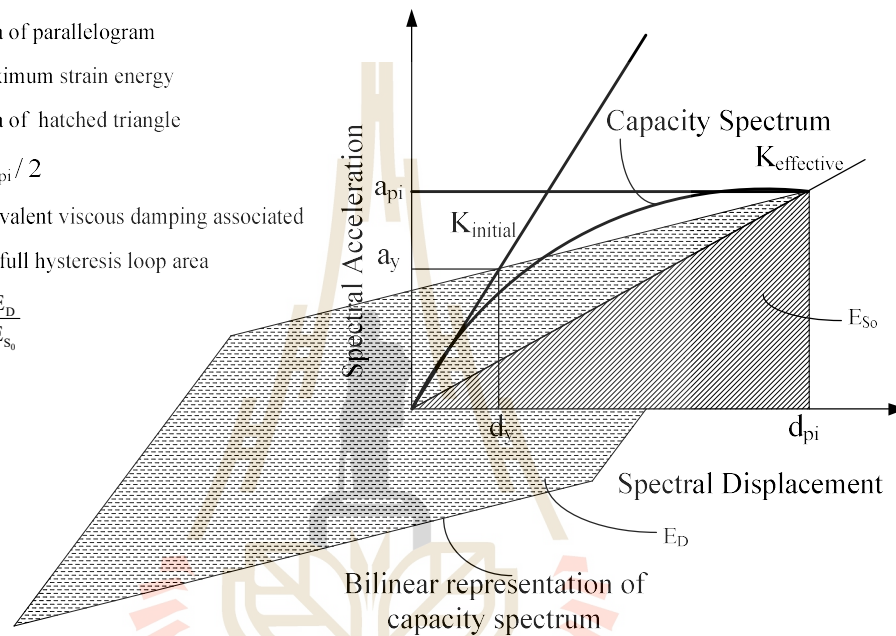


**Figure 2.5** Derivation of Damping For Spectral Reduction. (ATC 40)

$E_D$  is the energy dissipated by the structure in a single cycle of motion, that is, the area enclosed by a single hysteresis loop.  $E_{S_0}$  is the maximum strain energy associated with that cycle of motion, that is, the area of the hatched triangle.

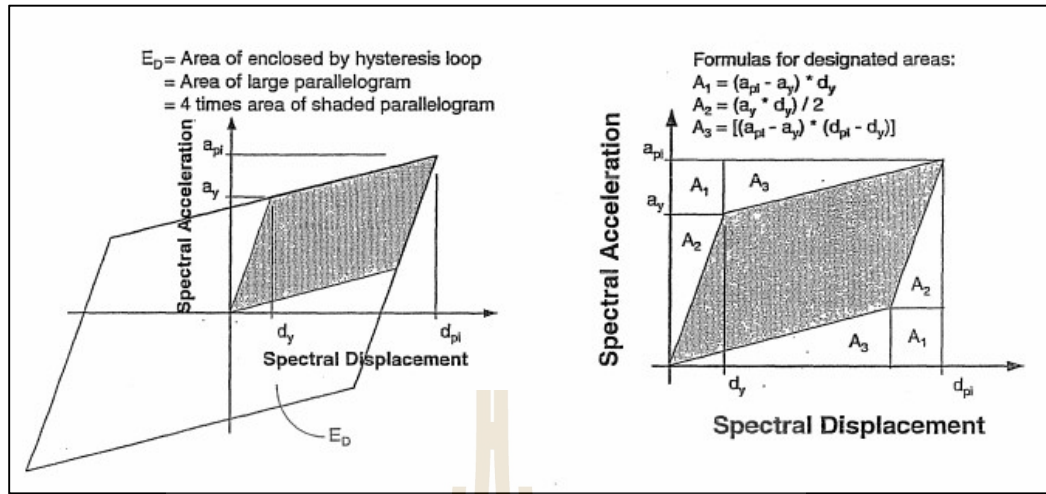


**Figure 2.6** Derivation of Energy Dissipated

**Figure 2.7** Derivation of Energy

dissipated by Damping, ED. (ATC 40)

by Damping, ED. (ATC 40)

Referring to Figures 2.5, 2.6 and 2.7, the term ED can be derived as

$$E_D = 4(a_y d_{pi} - d_y a_{pi}) \tag{2.22}$$

Referring to Figure 2.5, the term E<sub>so</sub> can be derived as

$$E_{so} = \frac{a_{pi} d_{pi}}{2} \tag{2.23}$$

### Effective Viscous Damping

In ATC 40, in order to be consistent with these previously developed damping coefficients, as well as to enable simulation of imperfect hysteresis loops (loops reduced in area), the concept of effective viscous damping using a damping modification factor, K, has been introduced. Effective viscous damping, β<sub>eff</sub>, is defined by:

$$\beta_{\text{eff}} = \kappa \beta_0 + 5 = \frac{63.7 \kappa (a_y d_{pi} - d_y a_{pi})}{a_{pi} d_{pi}} + 5 \quad (2.24)$$

where  $\beta_{\text{eff}}$  : Effective Viscous Damping

$\kappa$  : damping modification factor as shown in table 2.4.

### Reduced Response spectrum

Reduced Response Spectrum curve can be plotted from the Response Spectrum curve by using spectrum reduction factor to change elastic response

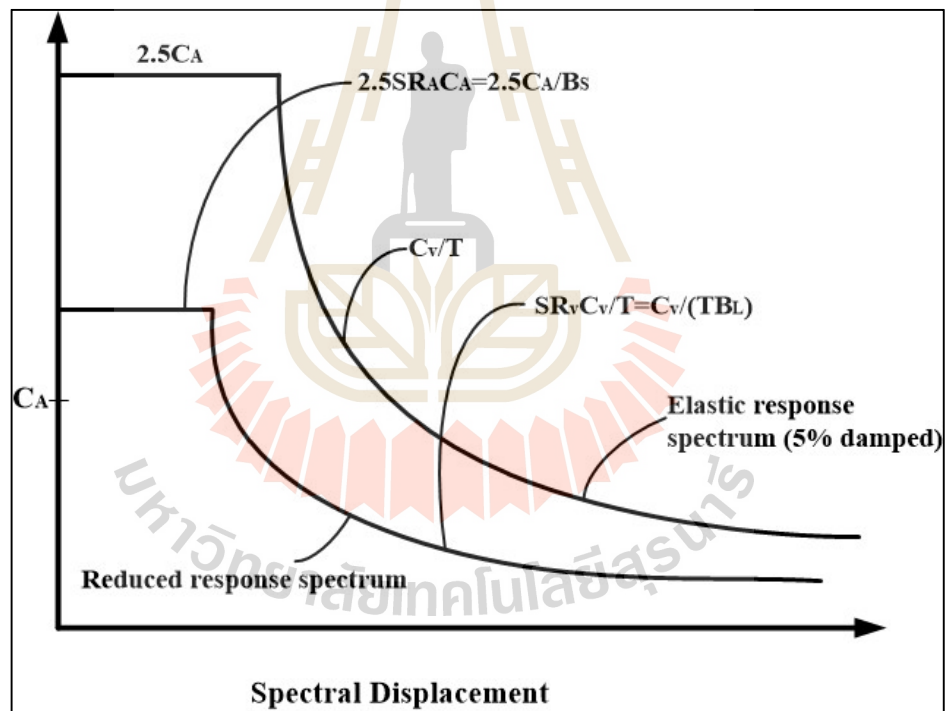


**Figure 2.8** Reduced Response Spectrum. (ATC 40)

spectrum to equivalent inelastic response spectrum as shown in figure 2.8. the spectrum reduction factors were shown in equation 2.25 and 2.26.

$$SR_A = \frac{3.21 - 0.68 \ln(\beta_{eff})}{2.12} \quad (2.25)$$

$$SR_V = \frac{2.31 - 0.41 \ln(\beta_{eff})}{1.62} \quad (2.26)$$

where  $SR_A$  : spectral reduction value in constant acceleration range of spectrum as shown in table 2.5.

$SR_V$  : spectral reduction value in constant velocity range of spectrum as shown in table 2.5.

$\beta_{eff}$  : Effective Viscous Damping.

**Table 2.4** Values for Damping Modification Factor,  $\kappa$

Structural behavior type <sup>1</sup>	$\beta_0$ (percent)	K
Type A <sup>2</sup>	$\leq 16.25$	1.0
	$> 16.25$	$1.13 - \frac{0.51(a_y d_{pi} - d_y a_{pi})}{a_{pi} d_{pi}}$
Type B	$\leq 25$	0.67
	$> 25$	$0.845 - \frac{0.446(a_y d_{pi} - d_y a_{pi})}{a_{pi} d_{pi}}$
Type C	Any value	0.33

1. See Table 2.6 for structural behavior types.
2. The formulas are derived from Tables of spectrum reduction factors, B (or BI), specified for the design of base isolated buildings in the 1991 UBC, 1994 UBC and 1994 NEHRP Provisions. The formulas created for this document give the same results as are in the Tables in the other documents.

**Table 2.5** Minimum Allowable  $SR_A$  and  $SR_V$  values<sup>1</sup>

Structural behavior type <sup>2</sup>	$SR_A$	$SR_V$
Type A <sup>2</sup>	0.33	0.50
Type B	0.44	0.56
Type C	0.56	0.67

1. Values for  $SR_A$  and  $SR_V$  shall not be less than those shown in this Table.
2. See Table 2.6 for structural behavior types.

**Table 2.6** Structural Behavior Types

Shaking Duration	Essentially New Building	Average Existing Building	Poor Existing Building
Short	Type A	Type B	Type C
Long	Type B	Type C	Type C

### Conceptual Development of the Method

ATC 40 uses three procedures to find the performance point, but this research use the Procedure B. This procedure makes a simplifying assumption that is not made in the other two procedures. It assumes that not only the initial slope of the bilinear representation of the capacity curve remains constant, but also the point  $a_y$ ,  $d_y$ , and the post-yield slope remains constant. This simplifying assumption allows a direct solution without drawing multiple curves because it forces the effective damping,  $\beta_{eff}$ , to depend only on  $d_{pi}$ . The following steps are involved:

1. Develop the 5 percent damped response spectrum appropriate for the site.
2. Draw the 5 percent damped response spectrum and draw a family of reduced spectra on the same chart. It is convenient if the spectra plotted correspond to effective damping values ( $\beta_{\text{eff}}$ ) ranging from 5 percent to the maximum value allowed for the building's structural behavior type. The maximum  $\beta_{\text{eff}}$  for Type A construction is 40 percent, Type B construction is 29 percent and Type C construction is 20 percent. Figure 2-9 shows an example family of demand spectra.

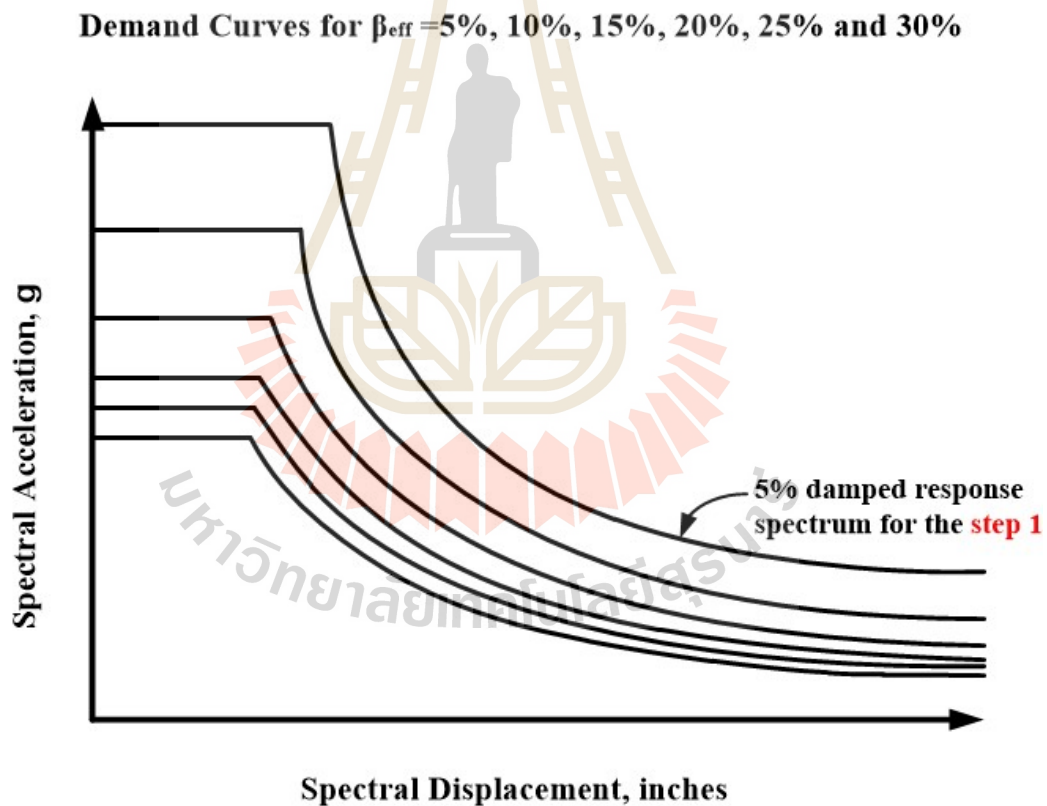


**Figure 2.9** Capacity spectra Procedure “B” after step 2. (ATC 40)

3. Transform the capacity curve into a capacity spectrum. using equations 2.13, 2.14, 2.15 and 2.16, and plot it on the same chart as the family of demand spectra, as illustrated in Figure 2-10.

### Demand Curves for $\beta_{\text{eff}}=5\%$ , 10%, 15%, 20%, 25% and 30%

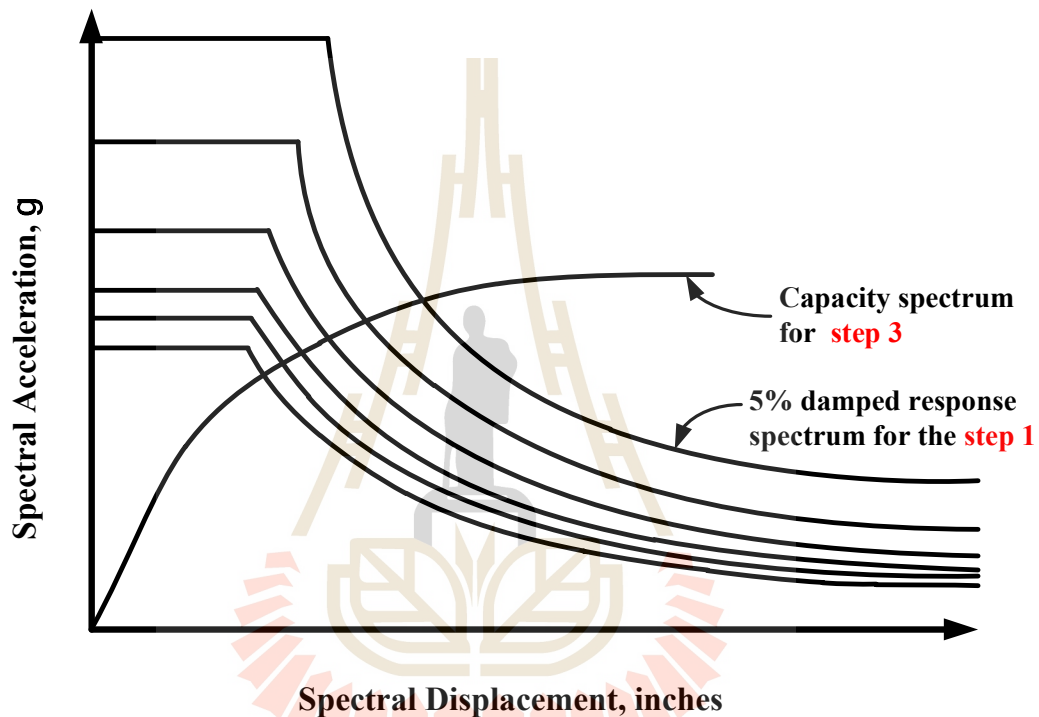


**Figure 2.10** capacity spectra Procedure “B” after step 3. (ATC 40)

1. Develop a bilinear representation of the capacity spectrum as illustrated in Figure 2.11. The initial slope of the bilinear curve is equal to the initial stiffness of the building. The post-yield segment of the bilinear representation should be run through the capacity spectrum at a displacement equal to the spectral displacement of the 5 percent damped spectrum at the initial pre-yield stiffness (equal displacement rule) point  $a^*$ ,  $d^*$ . The post-yield segment should then be rotated about this point to balance the areas  $A_1$  and  $A_2$ .



### Demand Curves for $\beta_{\text{eff}} = 5\%, 10\%, 15\%, 20\%, 25\%$ and $30\%$

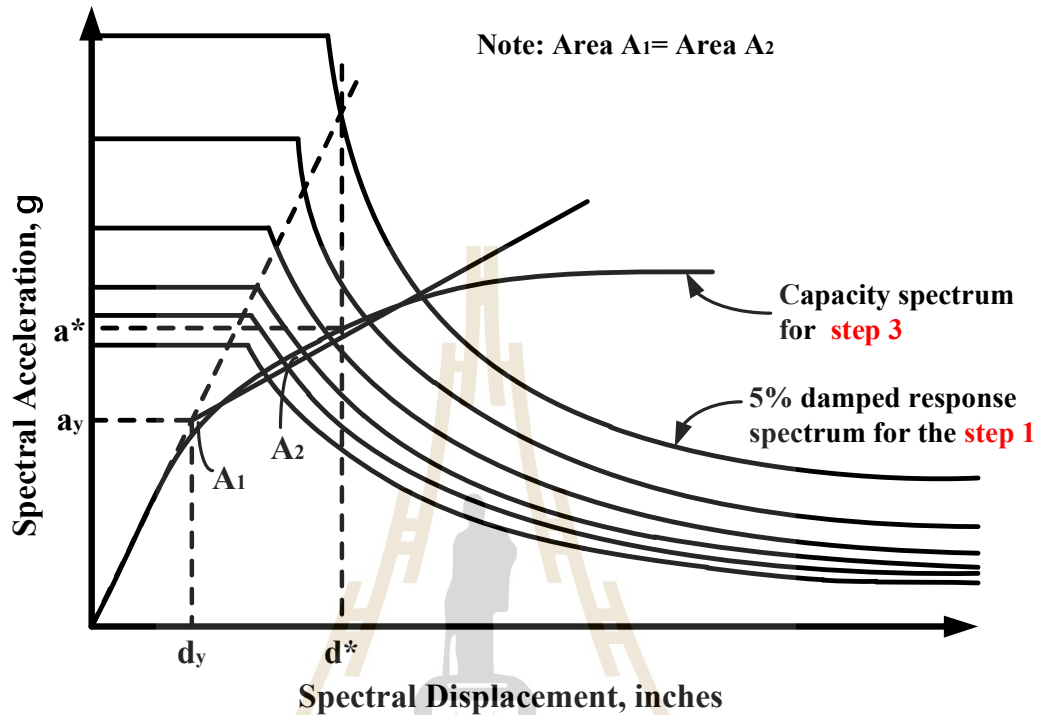


Figure 2.11 capacity spectrum procedure “B” after step 4. (ATC 40)

1. Calculate the effective damping for various displacements near the point  $a^*$ ,  $d^*$ . The slope of the post-yield segment of the bilinear representation of the capacity spectrum is given by:

$$\text{post yield slope} = \frac{a^* - a_y}{d^* - d_y} \quad (2.27)$$

For any point  $a_{pi}$ ,  $d_{pi}$ , on the post-yield segment of the bilinear representation, the slope is given by:

$$\text{post yield slope} = \frac{a_{pi} - a_y}{d_{pi} - d_y} \quad (2.28)$$

Since the slope is constant, equations 2.27 and 2.28 can be equated:

$$\frac{a_{pi} - a_y}{d_{pi} - d_y} = \frac{a^* - a_y}{d^* - d_y} \quad (2.29)$$

Solve equation 2.29 for  $a_{pi}$  in terms of  $d_{pi}$ . Call  $a_{pi}$  solved for in these terms  $a_{pi}'$ .

$$a_{pi}' = \frac{(a^* - a_y)(d_{pi} - d_y)}{d^* - d_y} + a_y \quad (2.30)$$

This value can be substituted for  $a_{pi}$  into equation 2.24 to obtain an expression for  $\beta_{eff}$  that is in terms of only one unknown,  $d_{pi}$ .

$$\beta_{eff} = \frac{63.7k(a_y d_{pi} - d_y a_{pi}')}{a_{pi}' d_{pi}} + 5 \quad (2.31)$$

2. For each  $d_{pi}$  value considered in step 5, plot the resulting  $d_{pi}$ ;  $\beta_{eff}$  point on the game chart as the family of demand spectra and the capacity spectrum. Figure 2.12 shows five of these points.

Demand Curves for  $\beta_{\text{eff}} = 5\%, 10\%, 15\%, 20\%, 25\%$  and  $30\%$

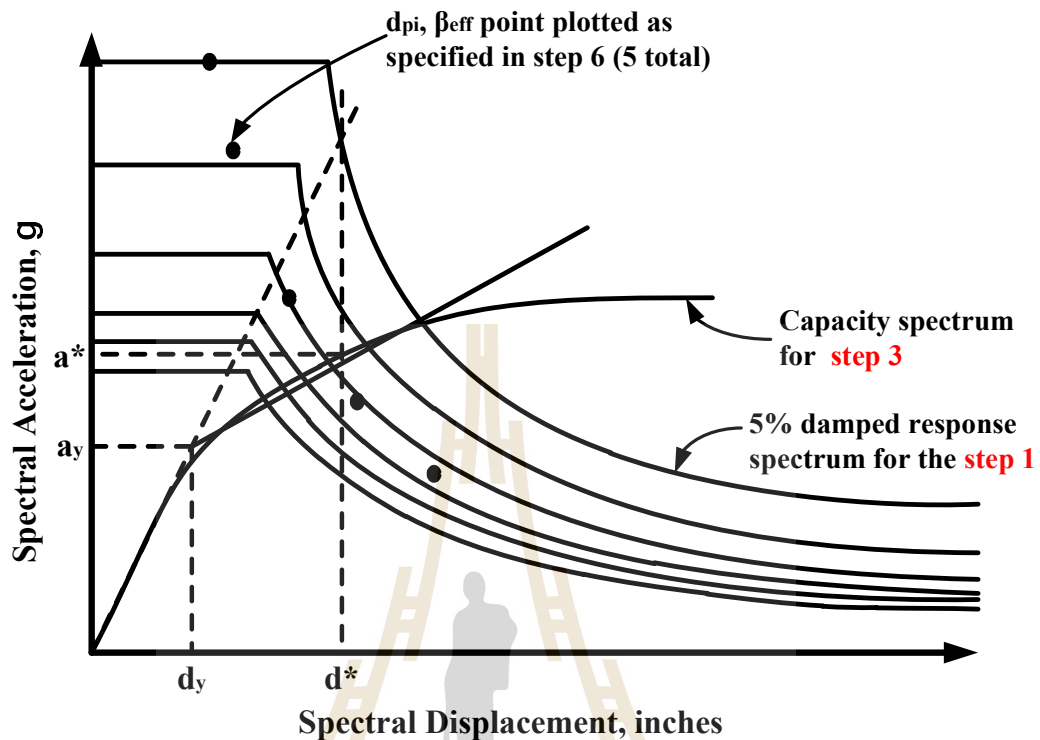


Figure 2.12 Capacity spectrum procedure “B” after step 6. (ATC 40)

- As illustrated in Figure 2.13, connect the points created in step 6, to form a line. The intersection of this line with the capacity spectrum defines the performance point. This procedure provides the same results as the other procedures if the performance point is at point  $a^*, d^*$ . The results will differ slightly from the other procedures if the performance point is not at point  $a^*, d^*$ . If the performance point is found to be distant from point  $a^*, d^*$ , then the engineer may want to verify the results using procedure A or C.

Demand Curves for  $\beta_{\text{eff}} = 5\%, 10\%, 15\%, 20\%, 25\%$  and  $30\%$

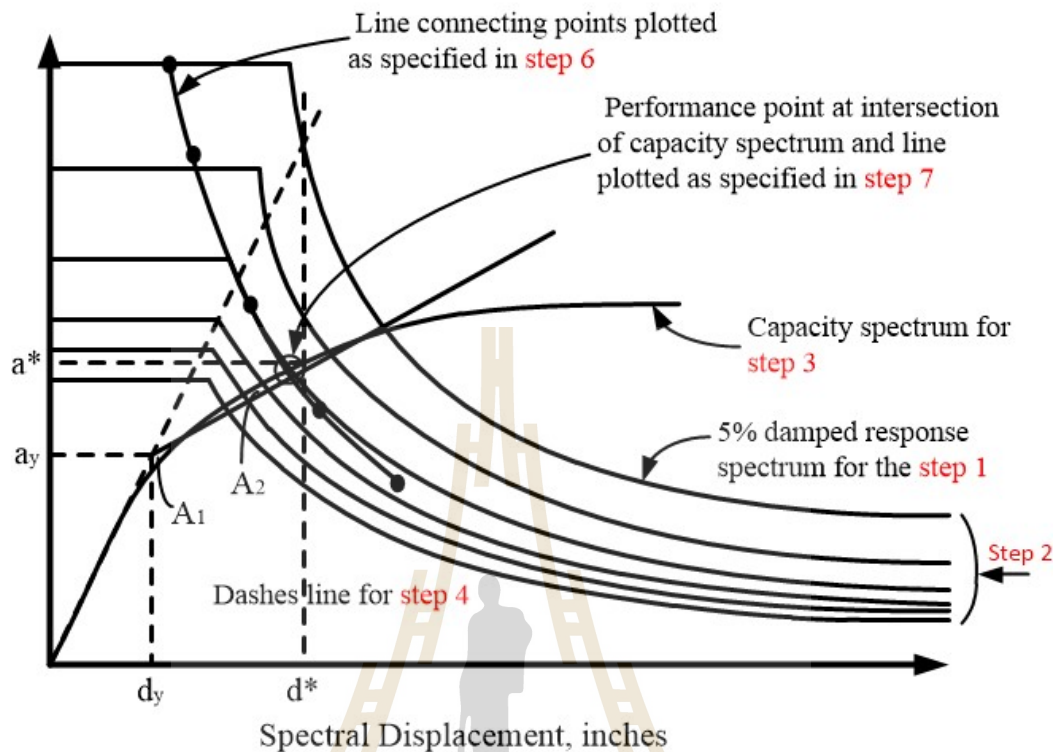


Figure 2.13 Capacity spectrum procedure “B” after step 7. (ATC 40)

## 2.4 Inter-story Drift Method

In inter-story drift is one of the most common methods used to categories the mentioned three qualitative levels as  $>1\%$ ,  $>2\%$ , and  $>4\%$ , respectively, (ASCE 41-06). Besides, the Australian code (Standards Australia,2007) indicates 1.5% as the maximum allowable story drift. in modal response spectrum analysis, combinations of different structural modes are used to calculate the structure response in term of storey deflection (Chopra, 2007). However, in time-history procedure, the following approaches have been proposed to be employed by practicing engineers to calculate inter-story drifts (AS Hokmabadi, B Fatahi† and B Samali, 2012):

1. Calculations of the storey drift according to the maximum absolute storey deflection irrespective of occurrence time (first approach).
2. Calculations of the storey drift according to storey deflection when the maximum deflection at top level occurs (second approach).
3. Calculations of the total maximum storey drift at each level considering all time-steps during the earthquake (third approach).

In this study, we used the third approach to calculate the inter-story drift that followed ASCE 41-06.

## 2.5 Acceptance Criteria

The acceptability of force and deformation actions shall be evaluated for each component that classified as primary or secondary, and each action shall be classified as deformation-controlled (ductile) action or force-controlled (nonductile) action. The primary elements provide the capacity of the structure to resist collapse under seismic forces induced by ground motion in any direction. The secondary elements do not contribute significantly or reliably in resisting earthquake effects in any direction because of low lateral stiffness, strength or deformation capacity.

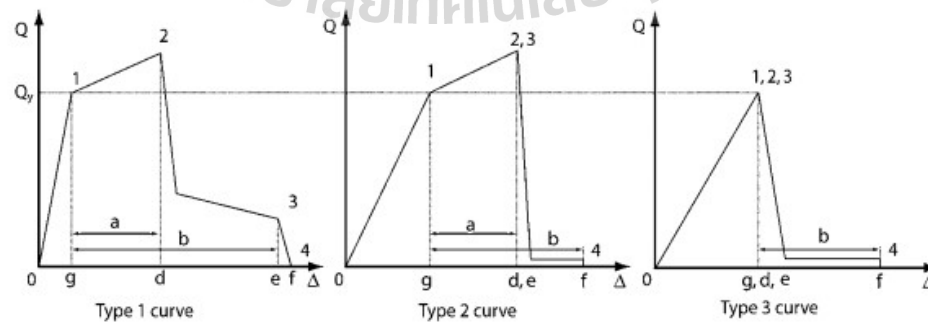


**Figure 2.14** Component force versus deformation curves. (ASCE 41-13)

Deformation-controlled or force-controlled uses the force-deformation curves to classify all the component actions as shown in figure 2.14.

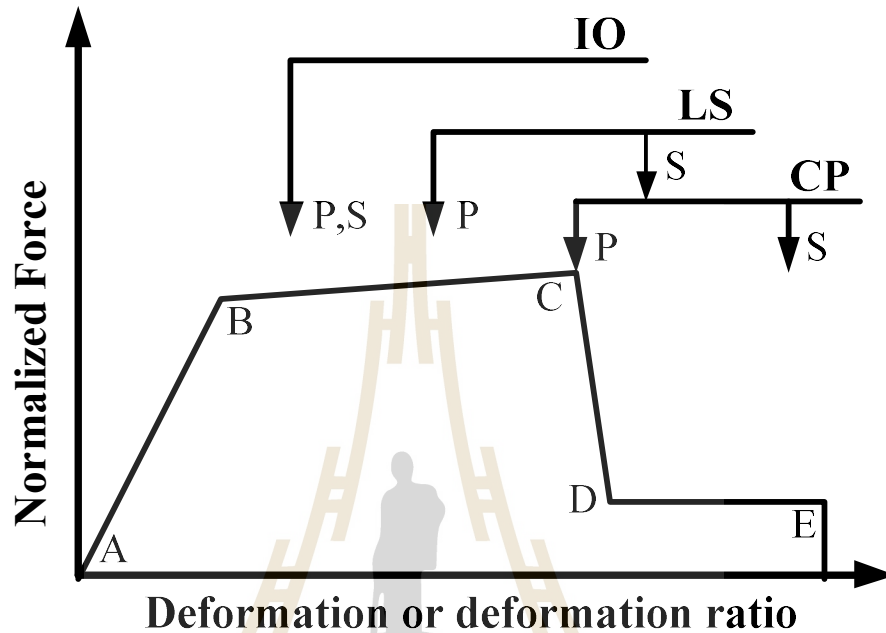


**Figure 2.15** Generalized component force-deformation relations. (ASCE 41-13)

The type 1 curve in figure 2.14 is a ductile behaviour that there is an elastic behaviour range (point 0-1), followed by plastic behaviour range (1-3 on the curve), and non-negligible residual strength and ability to support gravity loads after 3. The plastic range includes a work hardening or softening range (points 1-2-3). Primary component actions with this behaviour that classified as deformation-controlled for the flexural element depended on the plastic range for this value  $d \geq 2g$ . The type-2 curve in figure 2.14 is the ductile behaviour that there is an elastic behaviour range (point 0-1) and a plastic behaviour range (1-3) followed by loss of strength and ability to support gravity loads beyond at point 2. The components with this behavior can categorise as deformation-controlled if the plastic range is such that  $e > 2g$ , otherwise

force-controlled. The type 3 curve as shown in figure 3 is a brittle (non-ductile) behavior that there is an elastic behavior range (0-1 on the curve) followed by loss capacity of seismic-force resistant and able to support gravity loads beyond at point 1. The components with this behavior can consider as force-controlled. As shown in figure 2.15, it explains the acceptance criteria for deformation ratio for primary and secondary components that correspond to the target Structural Performance Levels of CP, LS, IO to be called Collapse Prevention, Life Safety, and Immediate Occupancy, respectively. According to ASCE 41-13, the criteria of earthquake-resistant structures are as follows:

1. Immediate Occupancy, "IO", When an earthquake occurs, the structure is able to withstand the earthquake, the structure does not suffer structural damage and does not experience nonstructural damage. So it can be directly used.
2. Level of life safety (Life Safety), "LS". When an earthquake occurs, the structure is able to withstand earthquakes, with minimum structural damage, humans living / residing in the building is safeguarded from earthquakes.
3. Level of structural stability (Collapse Prevention or Structural Stability), "CP". When an earthquake occurs, the structure undergoes severe structural damage, but has not collapsed.

**Table 2.7** Modeling Parameters and Numerical Acceptance Criteria for Nonlinear Procedures-Reinforced Concrete Beams

Conditions			Acceptance Criteria <sup>a</sup>		
			Plastic Rotations Angle (radians)		
			Performance Level		
			IO	LS	CP
Condition i. Beams controlled by flexure <sup>b</sup>					
$\frac{\rho-\rho'}{\rho_{bal}}$	Transverse Reinforcement <sup>c</sup>	$\frac{V}{b_w d \sqrt{f'_c}}$ <sup>d</sup>			
$\leq 0.0$	C	$\leq 3$ (0.25)	0.010	0.025	0.050
$\leq 0.0$	C	$\geq 6$ (0.5)	0.005	0.020	0.040
$\geq 0.5$	C	$\leq 3$ (0.25)	0.005	0.020	0.030
$\geq 0.5$	C	$\geq 6$ (0.5)	0.005	0.015	0.020
$\leq 0.0$	NC	$\leq 3$ (0.25)	0.005	0.020	0.030
$\leq 0.0$	NC	$\geq 6$ (0.5)	0.0015	0.010	0.015
$\geq 0.5$	NC	$\leq 3$ (0.25)	0.005	0.010	0.015
$\geq 0.5$	NC	$\geq 6$ (0.5)	0.0015	0.005	0.010
Condition ii. Beams controlled by shear <sup>b</sup>					
Stirrup spacing $\leq d/2$			0.0015	0.01	0.02
Stirrup spacing $> d/2$			0.0015	0.005	0.01
Condition iii. Beams controlled by inadequate development or splicing along the span <sup>b</sup>					
Stirrup spacing $\leq d/2$			0.0015	0.01	0.02
Stirrup spacing $> d/2$			0.0015	0.005	0.01
Condition iv. Beams controlled by inadequate embedment into beam-column joint <sup>b</sup>					
			0.01	0.02	0.03

NOTE:  $f'_c$  in lb/in<sup>2</sup> (MPa) units.

<sup>a</sup>Values between those listed in the table should be determined by linear interpolation.



<sup>b</sup>Where more than one of conditions i, ii, iii, and iv occur for a given component, use the minimum appropriate numerical value from the table.

“C” and “NC” are abbreviations for conforming and nonconforming transverse reinforcement, respectively. Transverse reinforcement is conforming if, within the flexural plastic hinge region, hoops are spaced at  $\leq d/3$ , and if, for components of moderate and high ductility demand, the strength provided by the hoops ( $V_s$ ) is at least 3/4 of the design shear. Otherwise, the transverse reinforcement is considered nonconforming.

<sup>d</sup> $V$  is the design shear force from NSP or NDP.

**Table 2.8** Modeling Parameters and Numerical Acceptance Criteria for Nonlinear Procedures-Reinforced Concrete Columns

Conditions			Acceptance Criteria <sup>a</sup>		
			Plastic Rotations Angle (radians)		
			Performance Level		
			IO	LS	CP
Condition i. <sup>b</sup>					
$\frac{P}{A_g f_c}$	$\rho = \frac{A_v}{b_w s}$				
$\leq 0.1$	$\geq 0.006$		0.005	0.045	0.060
$\geq 0.6$	$\geq 0.006$		0.003	0.009	0.010
$\leq 0.1$	$= 0.002$		0.005	0.027	0.034
$\geq 0.6$	$= 0.002$		0.002	0.004	0.005
$\frac{P}{A_g f_c}$	$\rho = \frac{A_v}{b_w s}$	$\frac{V}{b_w d \sqrt{f_c}}^d$			
Condition ii. <sup>b</sup>					
$\leq 0.1$	$\geq 0.006$	$\leq 3$ (0.25)	0.005	0.045	0.060
$\leq 0.1$	$\geq 0.006$	$\geq 6$ (0.5)	0.005	0.045	0.060
$\geq 0.6$	$\geq 0.006$	$\leq 3$ (0.25)	0.003	0.009	0.010
$\geq 0.6$	$\geq 0.006$	$\geq 6$ (0.5)	0.003	0.007	0.008
$\leq 0.1$	$\leq 0.0005$	$\leq 3$ (0.25)	0.005	0.010	0.012

**Table 2.8** Modeling Parameters and Numerical Acceptance Criteria for Nonlinear Procedures-Reinforced Concrete Columns (Continued)

Conditions			Acceptance Criteria <sup>a</sup>		
			Plastic Rotations Angle (radians)		
			Performance Level		
			IO	LS	CP
$\leq 0.1$	$\leq 0.0005$	$\geq 6$ (0.5)	0.004	0.005	0.006
$\geq 0.6$	$\leq 0.0005$	$\leq 3$ (0.25)	0.002	0.003	0.004
$\geq 0.6$	$\leq 0.0005$	$\geq 6$ (0.5)	0.0	0.0	0.0
Condition iii. <sup>b</sup>					
$\frac{P}{A_g f'_c}$	$\rho = \frac{A_v}{b_w s}$				
$\leq 0.1$	$\geq 0.006$		0.00	0.045	0.060
$\geq 0.6$	$\geq 0.006$		0.00	0.007	0.008
$\leq 0.1$	$\leq 0.0005$		0.00	0.005	0.006
$\geq 0.6$	$\leq 0.0005$		0.00	0.0	0.00
Condition iv. Column controlled by inadequate development or splicing along the clear height <sup>b</sup>					
$\frac{P}{A_g f'_c}$	$\rho = \frac{A_v}{b_w s}$				
$\leq 0.1$	$\geq 0.006$		0.00	0.045	0.060
$\geq 0.6$	$\geq 0.006$		0.00	0.007	0.008
$\leq 0.1$	$\leq 0.0005$		0.00	0.005	0.006
$\geq 0.6$	$\leq 0.0005$		0.00	0.0	0.00

NOTE:  $f'_c$  is in lb/in<sup>2</sup> (MPa) units.

<sup>a</sup>Values between those listed in the table should be determined by linear interpolation.

<sup>b</sup>Refer to Section 10.4.2.2.2 for definition of conditions i, ii, and iii. Columns are considered to be controlled by inadequate development or splices where the calculated steel stress at the splice exceeds the steel stress specified by Eq. (10-2). Where more than one of conditions i, ii, iii, and iv occurs for a given component, use the minimum appropriate numerical value from the table.

Where  $P > 0.7A_g f_c'$ , the plastic rotation angles should be taken as zero for all performance levels unless the column has transverse reinforcement consisting of hoops with 135-degree hooks spaced at  $\leq d/3$  and the strength provided by the hoops ( $V_s$ ) is at least 3/4 of the design shear. Axial load  $P$  should be based on the maximum expected axial loads caused by gravity and earthquake loads.

<sup>d</sup> $V$  is the design shear force from NSP or NDP.

According to ASCE/SEI 41-13, Plastic rotation limit criteria for member evaluation of RC frames is provided for each performance level based on member reinforcement ratio, confinement, and shear demand-to-strength ratio for beam and columns controlled by flexure. The ASCE/SEI 41-13 plastic rotation limits for beams and columns and maximum plastic rotations are summarized in table 2.7 and 2.8, respectively.

## 2.6 Braced Steel Frame

Steel bracing is the best method for global retrofit of the existing building that sees much lowrise, mid rise, and highrise building, using many types of steel bracing to resisting the earthquake load. By the way, Soundarya N. Gandhi (2017) studied the strengthening of reinforced concrete and steel structure by using steel bracing systems. The objective of this paper is to evaluate the response of braced and unbraced structure subjected to seismic loads and to identify the suitable bracing system for resisting the seismic load efficiently. There are a numbers of possibilities to arrange steel bracings such as X,V and Inverted V. The analysis of RC & Steel G+14 floors is carried out using ETABS software for frame situated in zone V. The RC & Steel G+14 structure is analyzed without bracings and with different types of bracings system. Story shears, story drifts and story Displacement is compared for all type of structural systems i.e. braced and unbraced structural system. Base won the result, the

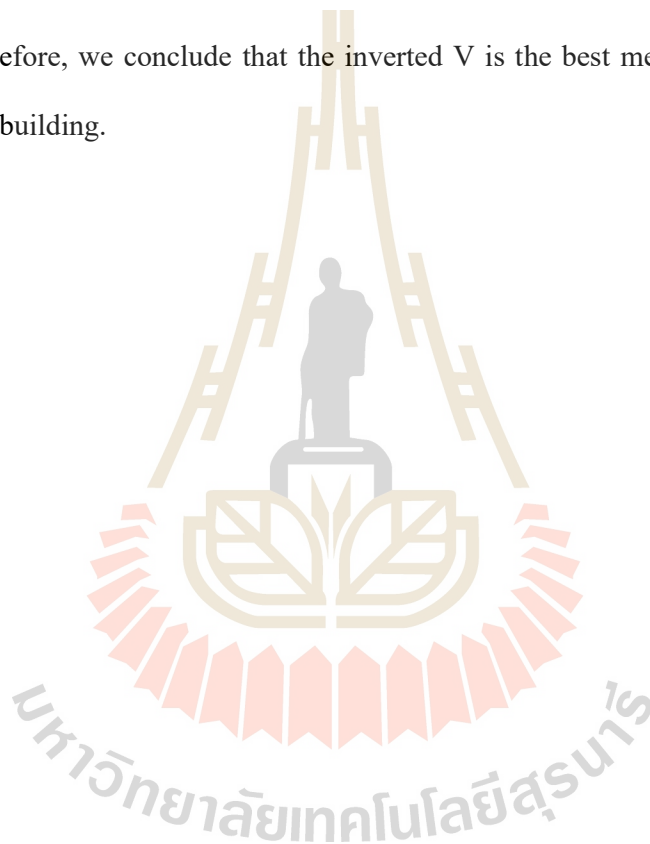
structure with inverted V Bracing gives minimum Storey drift as compared to other X, V in both X and Y direction . The magnitudes of storey drift for all the stories are found to be within limits, i.e. 0.004 times to storey height according to IS 1893:2002 (Part I).

Shachindra Kumar Chadhar (2015) studied the Seismic behavior of RC building frame with steel bracing system using various arrangements. In this study, A G+15 story reinforced concrete building of 4 bays have been considered for investigating the effect of V type and inverted V type bracings and there arrangements in various positions in the building. The reinforced concrete building with V type and inverted V type bracing provided on various positions in the building are analyzed for earthquake loading. Building is designed according to IS: 456-2008 and earthquake loading is applied as per the recommendation of IS: 1893-2002. Building is assumed to be located in seismic zone IV of India and rest on medium soil condition. According to the result, Inverted V bracing system significantly reduces the bending moment and shear force than V type bracing system. Node displacements and storey drifts are minimum for inverted V braced frame as compared to V braced frame.

C. Taenseesaeng studied the Study of the Reinforced Earthquake Resistance Building Structure in Sanklangvittaya School, Chiangrai Thailand. This study aims to investigate the damage of reinforced concrete building brought by the earthquake on 5th of May 2014. This building was basically built following the school building standard of the office of the Basic Education Commission. There are many building like this one built in hazardous area of Thailand before the recent announcement of ministerial orders. To reduce the damage from earthquake, this study investigates how to resist and prevent the severe damage following the standard of Department of

Public Works and Town & Country Planning. The study uses 3 steel frames to strengthen the building and these are as follows: a) Braced b) Inverted c) Knee Braced. ETABS 2013 program is used to analyze the building. The shear force is 23.20% of the total weight. According to the result, Knee Braced strengthening is inappropriate. The inverted V models provide better engineering results and less budget than others.

Therefore, we conclude that the inverted V is the best method for retrofitting the existing building.



## CHAPTER III

### METHOD AND METHODOLOGY

#### 3.1 Structural Modeling

In this study, we have use three-story, six-story, and nine-story building to evaluate the building performance level.

##### 3.1.1 Three-story building modeling

Three-story building that locates in Chiang Rai city, Chiang Rai province, assumes an existing building for studying the structural performance levels, is an ordinary reinforced concrete moment frame. This building are the symmetry configuration, 4x4@6 meters bays in both X and Y directions as shown in figure 3.1, a low-rise structure that located in the high seismic zone in Thailand. The beam and column dimensions are 30x50 cm and 50x50 cm. The slab thickness and story high are 20 cm and 350 cm. The material properties determined to be 23.54 N/mm<sup>2</sup> for concrete compressive strength and to be 392.27 N/mm<sup>2</sup> for both longitudinal and transversal reinforcement bars. Gravity and earthquake load that to be referred from ASCE/SEI 41-13 used to account for the seismic assessment. The soil class for this building is site class D with many parameters to determine earthquake load such as the reduction factor (R) is 3, the overstrength factor ( $\Omega_0$ ) is 3, the deflection amplification factor ( $C_d$ ) is 2.5, and the importance factor (I) is 1.5. The others required parameters are the spectral response acceleration parameter at short period is 0.798g, the spectral response acceleration parameter at 1 s period is 0.232g and the fundamental period of the building T is 0.21 seconds. The site coefficient  $F_a$  and  $F_v$  that got from the spectral

response acceleration parameter short and 1 s period on the site class D are 1.181 and 1.936, respectively. From table 1.6-1 and 1.6-2 of DPT 1302-52 (Thai Code), it shows that  $S_{DS} > 0.5$  and  $S_{D1} > 0.2$  used to point out the risk category, meet the high level of seismicity and high level of seismicity that similar to the risk category D of ASCE 7, respectively. All of the parameters used to calculate the base shear coefficient  $C_s$  is 0.315g to determine the pseudo seismic force then simulate as the pushover static load.

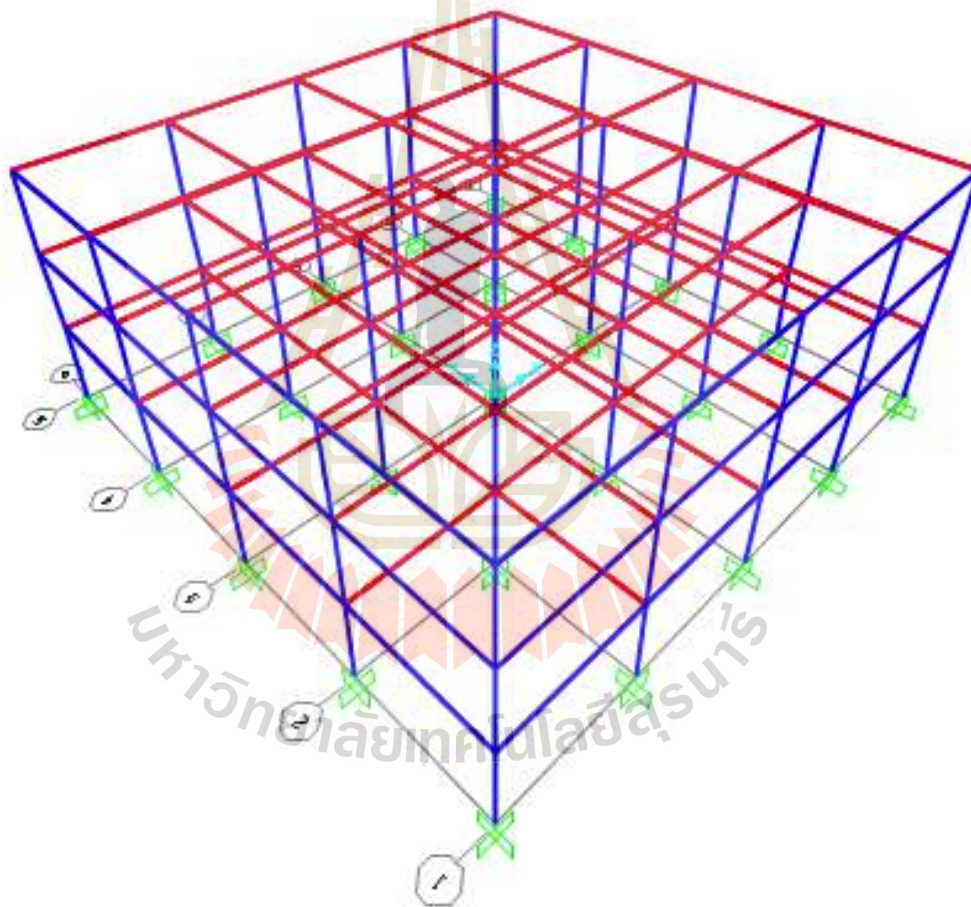


**Figure 3.1** 3D view of three-story building. (SAP2000)

### 3.1.2 Six-story building modeling

Six-story building that locates in Chiang Rai city, Chiang Rai province, assumes an existing building for studying the structural performance levels, is an ordinary reinforced concrete moment frame. This building are the symmetry configuration, 4x4@6 meters bays in both X and Y directions as shown in figure 3.2, a low-rise structure that located in the high seismic zone in Thailand. The beam and column dimensions are 30x50 cm and 55x55 cm. The slab thickness and story high are 20 cm and 350 cm. The material properties determined to be 23.54 N/mm<sup>2</sup> for concrete compressive strength and to be 392.27 N/mm<sup>2</sup> for both longitudinal and transversal reinforcement bars.

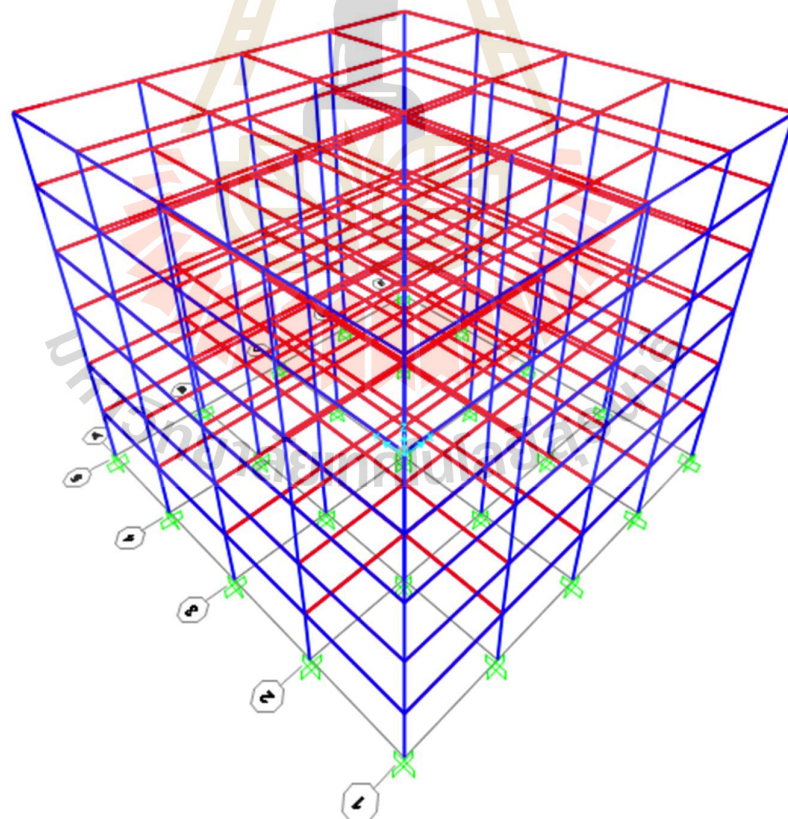


**Figure 3.2** 3D view of six-story building. (SAP2000)



### 3.1.3 Nine-story building modeling

Nine-story building that locates in Chiang Rai city, Chiang Rai province, assumes an existing building for studying the structural performance levels, is an ordinary reinforced concrete moment frame. This building are the symmetry configuration, 4x4@6 meters bays in both X and Y directions as shown in figure 3.3, a low-rise structure that located in the high seismic zone in Thailand. The beam and column dimensions are 30x60 cm and 70x70 cm. The slab thickness and story high are 20 cm and 350 cm. The material properties determined to be 23.54 N/mm<sup>2</sup> for concrete compressive strength and to be 392.27 N/mm<sup>2</sup> for both longitudinal and transversal reinforcement bars.

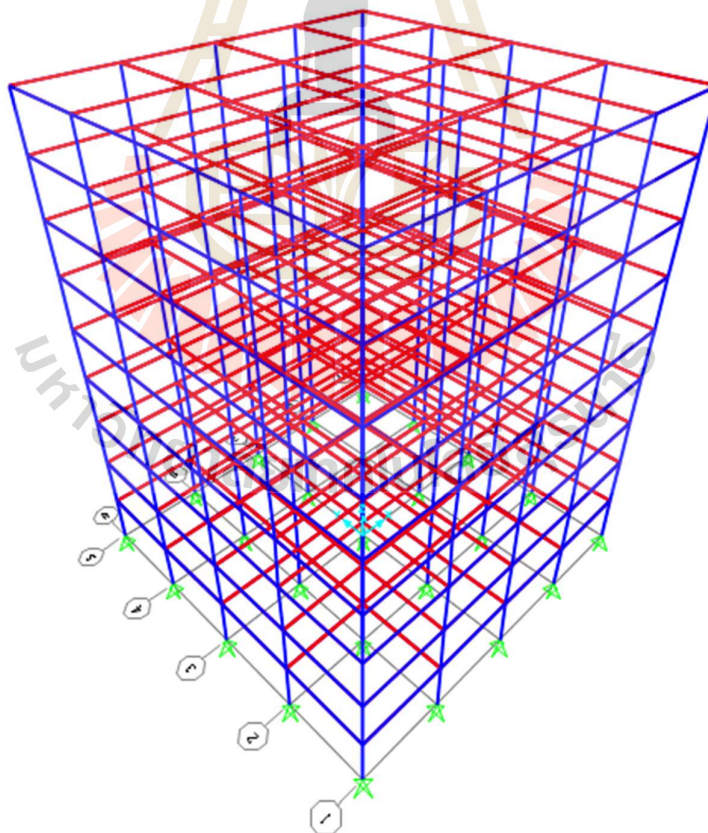


**Figure 3.3** 3D view of nine-story building. (SAP2000)

## 3.2 Structural Modeling of retrofitted building

In this study, we have use three-story, six-story, and nine-story retrofitted building to evaluate the building performance level.

### 3.2.1 Three-story retrofitted building modeling

Steel bracing is the best method for global retrofit of the existing building that sees much low-rise, mid-rise, high-rise building, using many types of steel bracing to resisting the earthquake load. By the way, the structure with inverted V Bracing gives minimum Story drift as compared to other X, V.

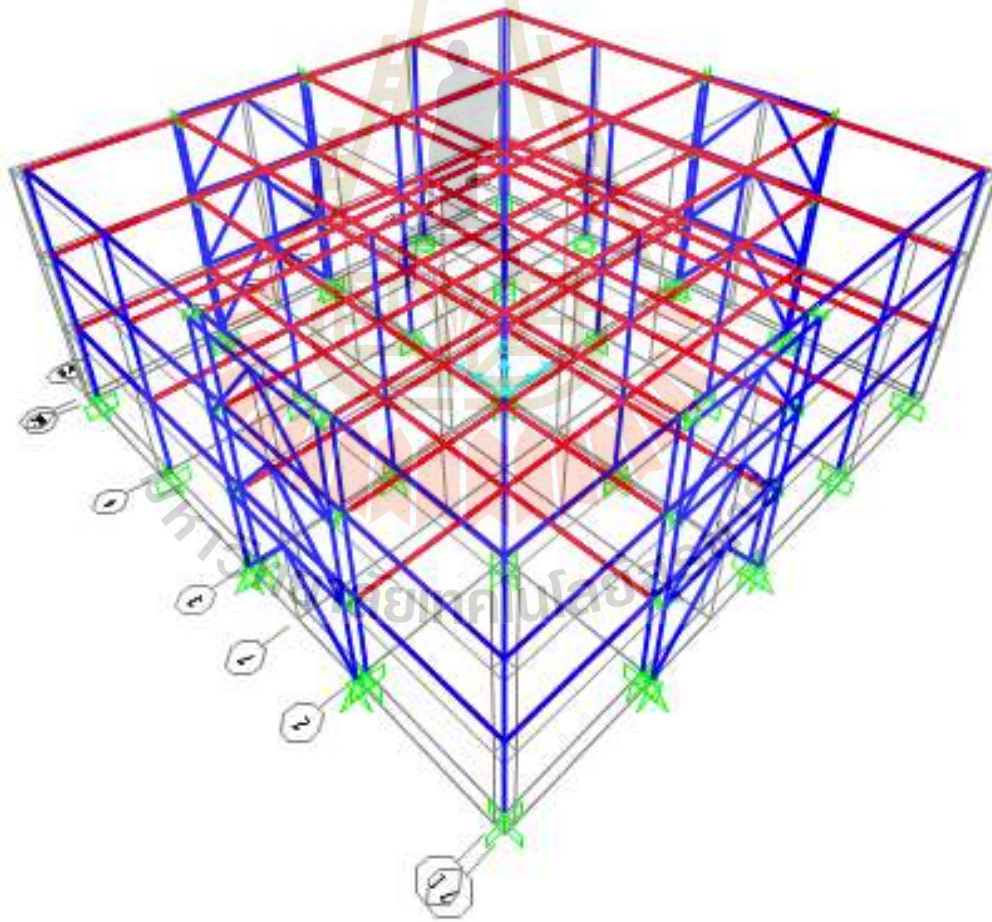


**Figure 3.4** 3D view of the three-story braced steel frame. (SAP2000)

The magnitudes of story drift for all the stories are found to be within limits, i.e. 0.004 times to story height according to IS 1893:2002 (Part I) (Soundarya, 2017). For the story drift, it is not enough to choose inverted V that should be studied for other cases to qualified as the best steel bracing. The results of the study and analysis of the retrofit model to resist earthquakes from all data. Knee Braced strengthening is inappropriate. The inverted V models provide better engineering results and less budget than others (Channarong, 2016). Inverted V bracing system significantly reduces the bending moment and shear force than V type bracing system (Shachindra, 2015). Node displacements and story drifts are minimum for inverted V braced frame as compared to V braced frame (Shachindra, 2015). This study is used inverted V steel bracing that has yield strength is  $245.17 \text{ N/mm}^2$ , ultimate strength is  $392.27 \text{ N/mm}^2$ , and modulus of elasticity is  $200055.66 \text{ N/mm}^2$ . The outer steel frames have the column dimension of W300X300X94, beam dimension of W350X250X79.7, and bracing dimension of HSS200X200X8.0 for both three-story as shown in figure 3.4.

### **3.2.2 Six-story retrofitted building modeling**

This study is used inverted V steel bracing that has yield strength is  $245.17 \text{ N/mm}^2$ , ultimate strength is  $392.27 \text{ N/mm}^2$ , and modulus of elasticity is  $200055.66 \text{ N/mm}^2$ . The outer steel frames have the column dimension of W300X300X94, beam dimension of W350X250X79.7, and bracing dimension of HSS200X200X8.0 of six-story building as shown in figure 3.5.

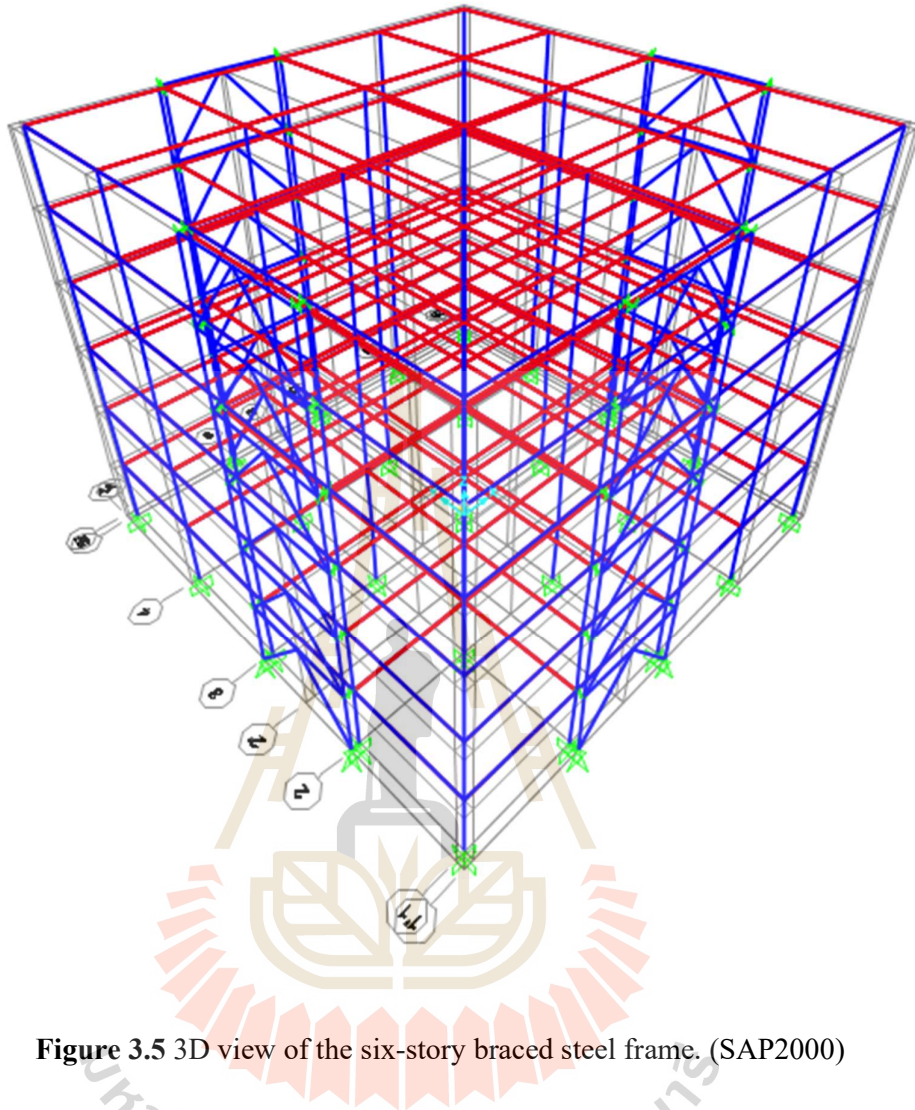


**Figure 3.5** 3D view of the six-story braced steel frame. (SAP2000)

### 3.2.3 Nine-story retrofitted building modeling

This study is used inverted V steel bracing that has yield strength is  $245.17 \text{ N/mm}^2$ , ultimate strength is  $392.27 \text{ N/mm}^2$ , and modulus of elasticity is  $200055.66 \text{ N/mm}^2$ . The outer steel frames have the column dimension of W500X300X114, beam dimension of W350X250X79.7, and bracing dimension of HSS300X300X6.0 of nine-story building as shown in figure 3.6.

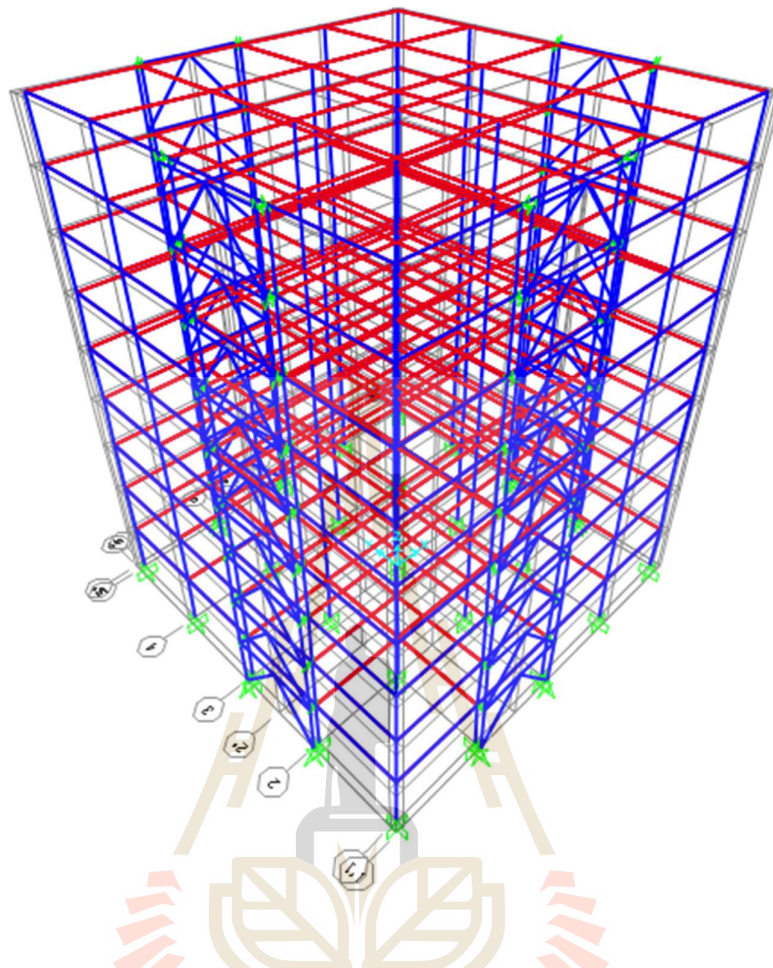


**Figure 3.6** 3D view of the nine-story braced steel frame. (SAP2000)

### **3.3 Performance Evaluation of Existing Building**

#### **3.3.1 Displacement Coefficient Method of the three-story building**

Nonlinear Static Procedure (NSP) use to analyze the Multi-Degree-Of-Freedom system as shown in figure 3.7 to find the seismic response. But the NSPs use “Equivalent” Single-Degree-of-Freedom (ESDOF) representations of structures to estimate roof peak displacement and the response quantities associated with this roof displacement as shown in figure 3.8. These ESDOF systems are generally based on the fundamental mode of response, thus systematically excluding the effects of higher modes (in the case of elastic response) or Multi-Degree-Of-Freedom (MDOF) effects

(in the case of nonlinear response) on response quantities. Displacement coefficient method was used to calculate the target displacement of the control node on the roof that presented in both ASCE 41-13 Eq. 7-28 and FEMA 440 Eq. 3-9 (2005). The building that used to evaluate the performance levels is the symmetry configuration, needed only one direction for qualified its performance. The magnitude of the target displacement that shown in table 3.1 obtained from the maximum value between ASCE 41-13 Eq. 7-28 and FEMA 440 Eq. 3-9.

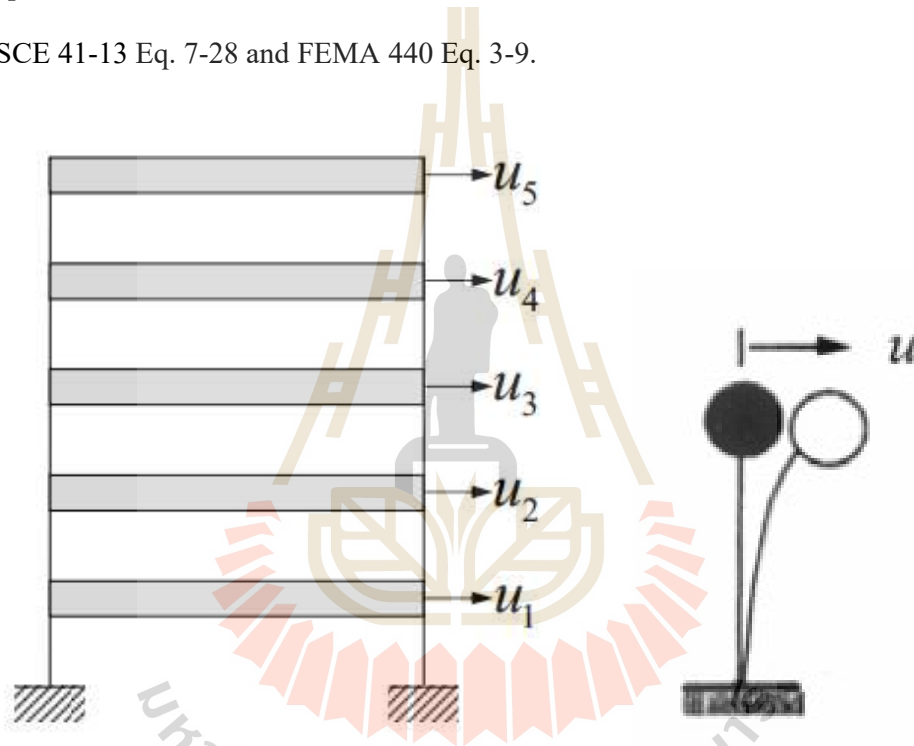


**Figure 3.7** Multi-Degree-Of-Freedom      **Figure 3.8** Single-Degree of Freedom

**Table 3.1** Parameter and target displacement ( $\delta_t$ ) of three-story building

Parameters	FEMA 440	ASCE 41-13	Note
$C_0$	1.233	1.350	ASCE 41-13 Table 7-5. Values for Modification Factor
$C_1$	1.133	1.090	Modification Factor to relate the expected max displacements
$C_2$	1.011	1.009	Values for Modification Factor
$C_3$	1.000		Building with post-yield stiffness
$S_a$	0.628	0.628	Spectral Response Acceleration
$T_e$	0.425	0.472	Effective natural vibration
$G$	9.81	9.81	Gravitational Acceleration
$\delta_t$	0.040	0.0517	FEMA 440: $\delta_t=C_0C_1C_2C_3S_a(T_e/2\pi)^2g$
			ASCE 41-13: $\delta_t=C_0C_1C_2S_a(T_e/2\pi)^2g$

### 3.3.2 Displacement Coefficient Method of the six-story building

For the six-story building, it has the target displacement of the control node on the roof roof that presented in both ASCE 41-13 Eq. 7-28 and FEMA 440 Eq. 3-9 (2005). The building that used to evaluate the performance levels is the symmetry configuration, needed only one direction for qualified its performance. The magnitude of the target displacement that shown in table 3.2 obtained from the maximum value between ASCE 41-13 Eq. 7-28 and FEMA 440 Eq. 3-9.

**Table 3.2** Parameter and target displacement ( $\delta_t$ ) of six-story building

Parameters	FEMA 440	ASCE 41-13	Note
$C_0$	1.2397	1.2407	ASCE 41-13 Table 7-5. Values for Modification Factor
$C_1$	1.0599	1.0	Modification Factor to relate the expected max displacements
$C_2$	1.00	1.00	Values for Modification Factor
$C_3$	1.000		Building with post-yield stiffness
$S_a$	0.628	0.628	Spectral Response Acceleration
$T_e$	0.7852	0.7852	Effective natural vibration
$G$	9.81	9.81	Gravitational Acceleration
$\delta_t$	0.127	0.12	FEMA 440: $\delta_t=C_0C_1C_2C_3S_a(T_e/2\pi)^2g$
			ASCE 41-13: $\delta_t=C_0C_1C_2S_a(T_e/2\pi)^2g$

### 3.3.3 Displacement Coefficient Method of the nine-story building

For the nine-story building, it has the target displacement of the control node on the roof that presented in both ASCE 41-13 Eq. 7-28 and FEMA 440 Eq. 3-9 (2005). The building that used to evaluate the performance levels is the symmetry configuration, needed only one direction for qualified its performance. The magnitude of the target displacement that shown in table 3.3 obtained from the maximum value between ASCE 41-13 Eq. 7-28 and FEMA 440 Eq. 3-9.



**Table 3.3** Parameter and target displacement ( $\delta_t$ ) of nine-story building

Parameters	FEMA 440	ASCE 41-13	Note
$C_0$	1.2787	1.2787	ASCE 41-13 Table 7-5. Values for Modification Factor
$C_1$	1.00	1.00	Modification Factor to relate the expected max displacements
$C_2$	1.00	1.00	Values for Modification Factor
$C_3$	1.00		Building with post-yield stiffness
$S_a$	0.628	0.628	Spectral Response Acceleration
$T_e$	1.0821	1.0821	Effective natural vibration
$G$	9.81	9.81	Gravitational Acceleration
$\delta_t$	0.234	0.234	FEMA 440: $\delta_t=C_0C_1C_2C_3S_a(T_e/2\pi)^2g$
			ASCE 41-13: $\delta_t=C_0C_1C_2S_a(T_e/2\pi)^2g$

### 3.3.4 Capacity Spectrum Method of the three-story building

The nonlinear static analysis procedure has also included the capacity spectrum method (CSM) that uses the intersection of the capacity-demand curve to estimate maximum roof displacement at the performance point. The performance point that found to check the structural performance levels of the IO, LS or CP depended on deformation limits specified in ATC-40 were 0.01, 0.02 and 0.33( $V_b/W$ ) as shown in table 3.4, respectively. Building design needs to consider the performance level that bases upon the importance and function of the building such as the hospital to be considered Immediate Occupancy (IO) level. A case studying the three-story building used SAP2000, analyzed the pushover static analysis, determined performance point that represents in the Acceleration-Displacement Response Spectra (ADRS) as shown

in figure 3.9. To depend on figure 3.9, it shows that the magnitude of base shear and tip displacement at the performance point are 6605789 N and 0.04 m, respectively. To determine the building performance levels, it can use the deformation limits to compare with the roof drift ratio at the performance point as follows: Roof drift ratio at the performance point is  $0.04/10.5 = 0.0038$ .

**Table 3.4** Deformation limits

Standard	Inter-story drift limit	Structural Performance Levels		
		Collapse Prevention	Life Safety	Immediate Occupancy
ATC 40	Maximum total drift	$0.33(V_i/P_i)$	0.02	0.01
	Maximum inelastic drift	No limit	No limit	0.005

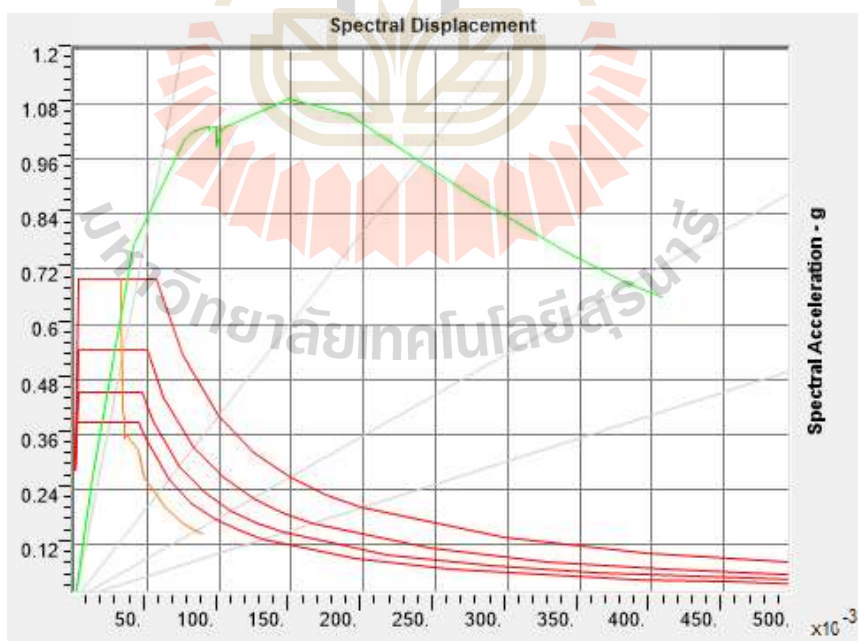


**Figure 3.9** Capacity spectrum curve of the three-story building. (SAP2000)

### 3.3.5 Capacity Spectrum Method of the six-story building

The six-story building used SAP2000, analyzed the pushover static analysis, determined performance point that represents in the Acceleration-Displacement Response Spectra (ADRS) as shown in figure 3.10. To depend on figure 3.10, it shows that the magnitude of base shear and tip displacement at the performance point are 6984303 N and 0.092 m, respectively. To determine the building performance levels, it can use the deformation limits to compare with the roof drift ratio at the performance point as follows: Roof drift ratio at the performance point is  $0.092/21 = 0.0044$ .

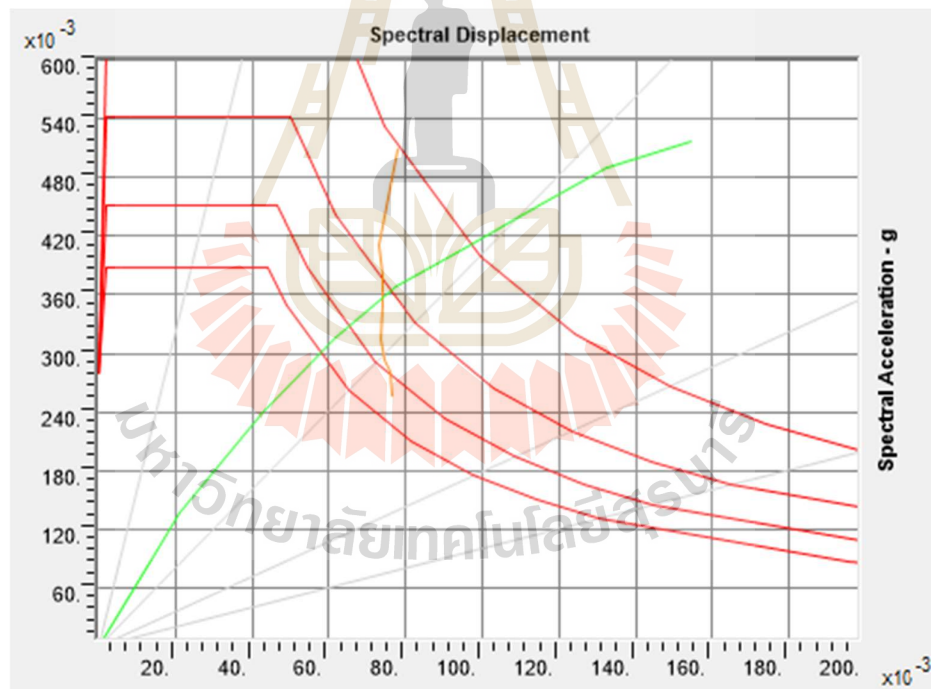


**Figure 3.10** Capacity spectrum curve of the six-story building. (SAP2000)

### 3.3.6 Capacity Spectrum Method of the nine-story building

The nine-story building used SAP2000, analyzed the pushover static analysis, determined performance point that represents in the Acceleration-Displacement Response Spectra (ADRS) as shown in figure 3.11. To depend on figure 3.11, it shows that the magnitude of base shear and tip displacement at the performance point are 8211036 N and 0.14 m, respectively. To determine the building performance levels, it can use the deformation limits to compare with the roof drift ratio at the performance point as follows: Roof drift ratio at the performance point is  $0.14/31.5= 0.0044$ .

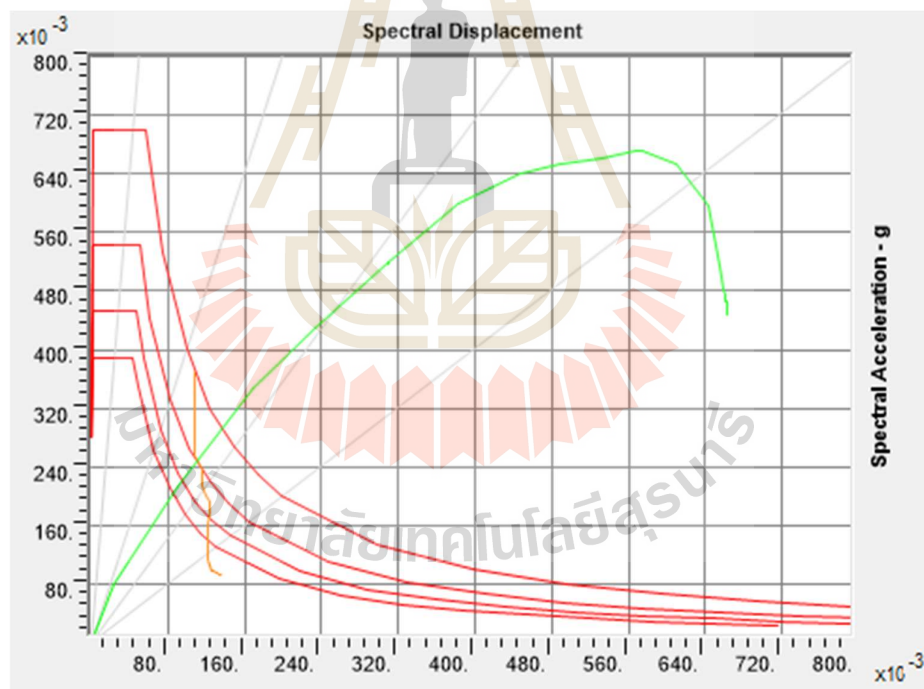


**Figure 3.11** Capacity spectrum curve of the nine-story building. (SAP2000)

### 3.3.7 Inter-story Drift Method of the three-story building

According to ASCE/SEI 41-06, Inter-story drift ratio is determined as the difference between the deflections of two adjacent floors which can be expressed as a percentage of the story height. The inter-story drift is the most acceptable parameter to control the displacement, the resulting damage, and in turn performance of the structure. Thus, the importance of precise prediction of drifts in structural designs is obvious. ASCE/SEI 41-06 suggests typical limits of 1% inter-story drift for immediate occupancy (IO), 2% inter-story drift associated with Life Safety (LS) performance level and 4% inter-story drift for Collapse Prevention (CP) performance. These values are appropriate for well-detailed RC frames. The inter-story drifts of the frames at different building drifts are shown in figure 3.13. Before calculating the inter-story drift, we need to determine the deflection at level  $x$  ( $\delta_x$ ) as shown in equation 3.1. The value of the deflection is shown in figure 3.12 According to ASCE 7-16, the inter-story drift ratio (IDR) as determine in equation 3.2 shall not exceed the performance limit as defined by ASCE/SEI 41-06. The figure 3.14 shows the determination of the inter-story drift by ASCE standard.

$$\delta_x = \frac{C_d \delta_{xe}}{I_e} \quad (3.1)$$

where  $C_d$  : deflection amplification factor in Table 12.2-1 of the ASCE 7-16

$\delta_{xe}$  : deflection at the location required by this section determined by an elastic analysis

$I_e$  : Importance Factor determined in accordance with Section 11.5.1 of the ASCE 7-16

$$\text{IDR} = \frac{(\delta_x - \delta_{x-1})100}{L_x} \quad (3.2)$$

where  $L_x$  : story height at the level  $x$

$\delta_x$  : deflection at the level  $x$

$\delta_{x-1}$  : deflection at the level  $x-1$

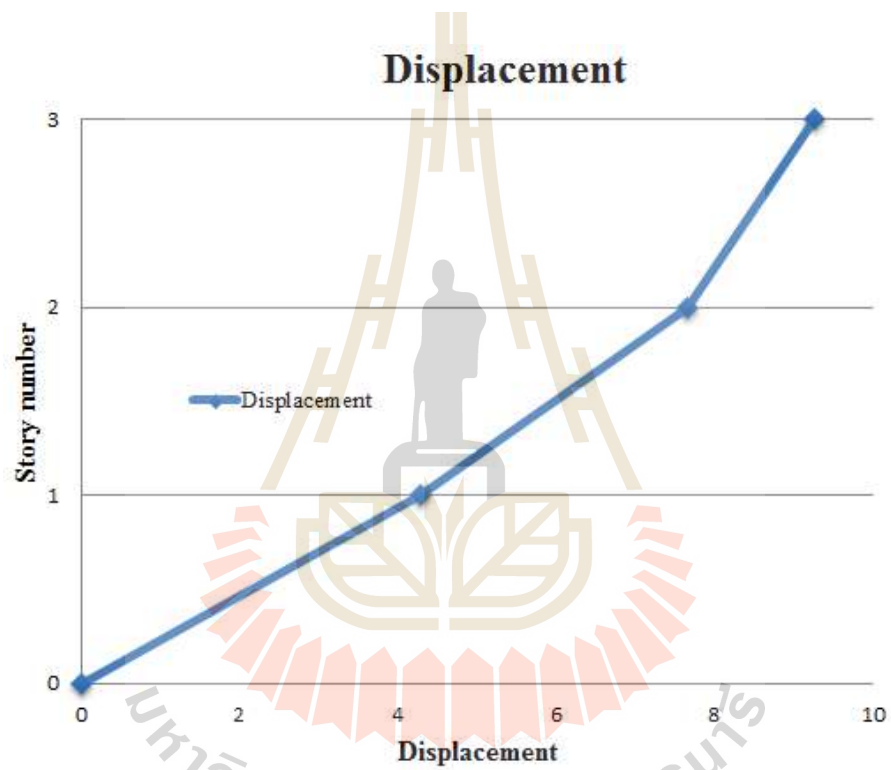


Figure 3.12 Story deflections (cm)

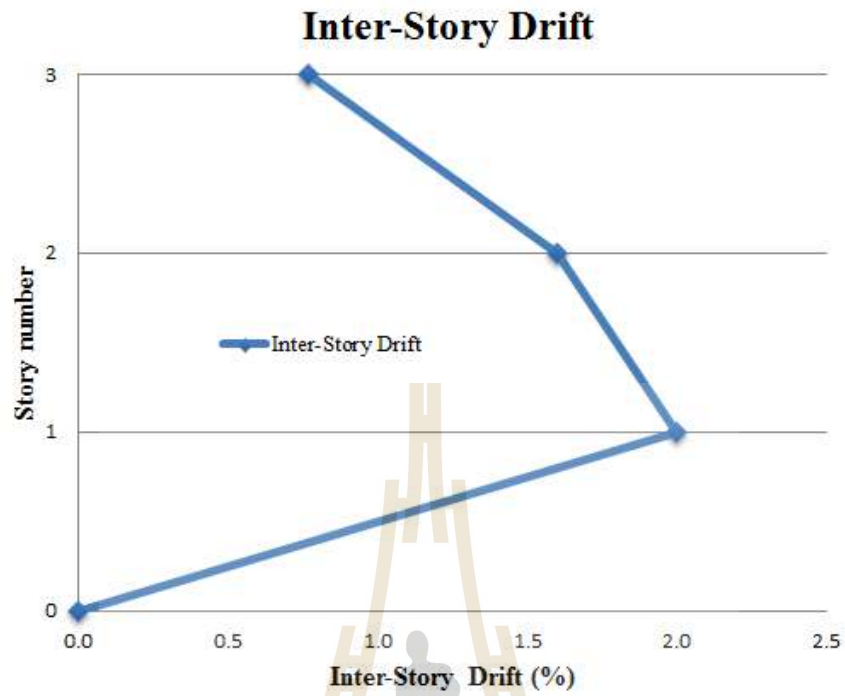


Figure 3.13 Inter-story drift (%)

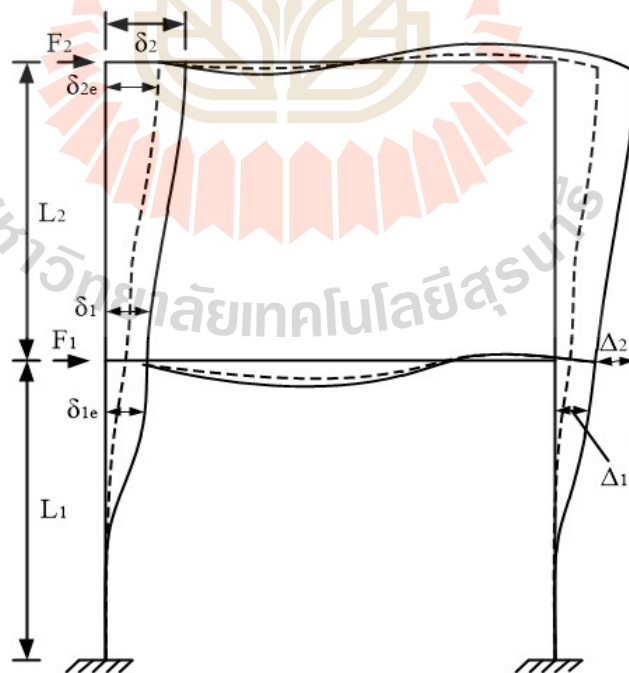


Figure 3.14 Inter-Story Drift Determination. (ASCE 41-13)

### 3.3.8 Inter-story Drift Method of the six-story building

According to ASCE/SEI 41-06, Inter-story drift ratio is determined as the difference between the deflections of two adjacent floors which can be expressed as a percentage of the story height. The inter-story drift is the most acceptable parameter to control the displacement, the resulting damage, and in turn performance of the structure. Thus, the importance of precise prediction of drifts in structural designs is obvious. ASCE/SEI 41-06 suggests typical limits of 1% inter-story drift for immediate occupancy (IO), 2% inter-story drift associated with Life Safety (LS) performance level and 4% inter-story drift for Collapse Prevention (CP) performance. These values are appropriate for well-detailed RC frames.

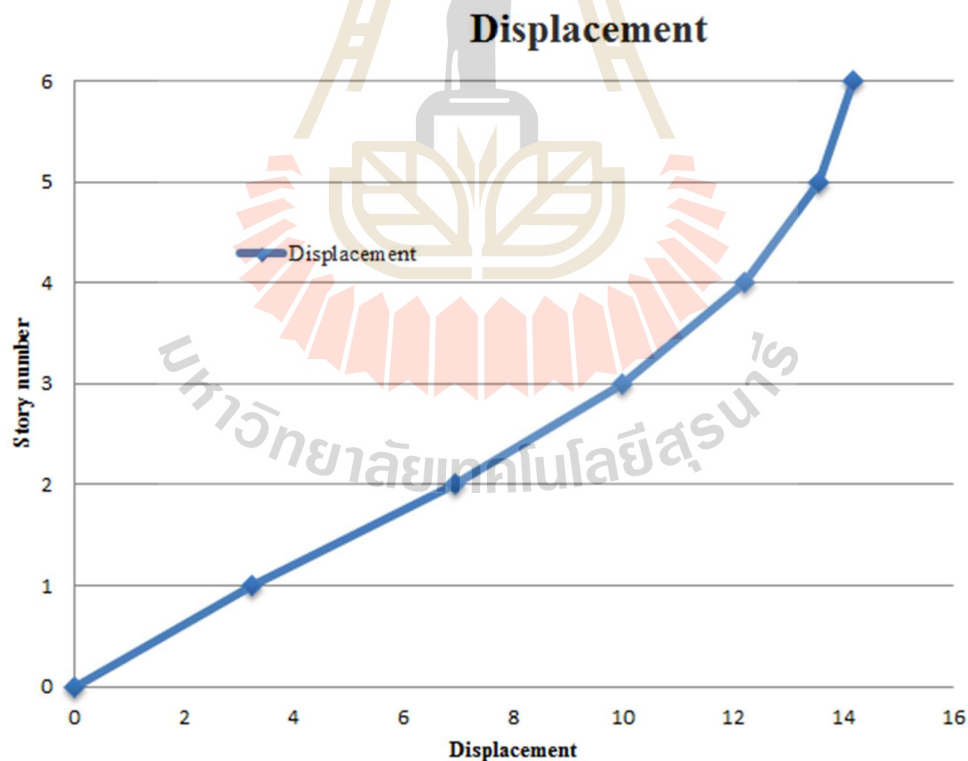
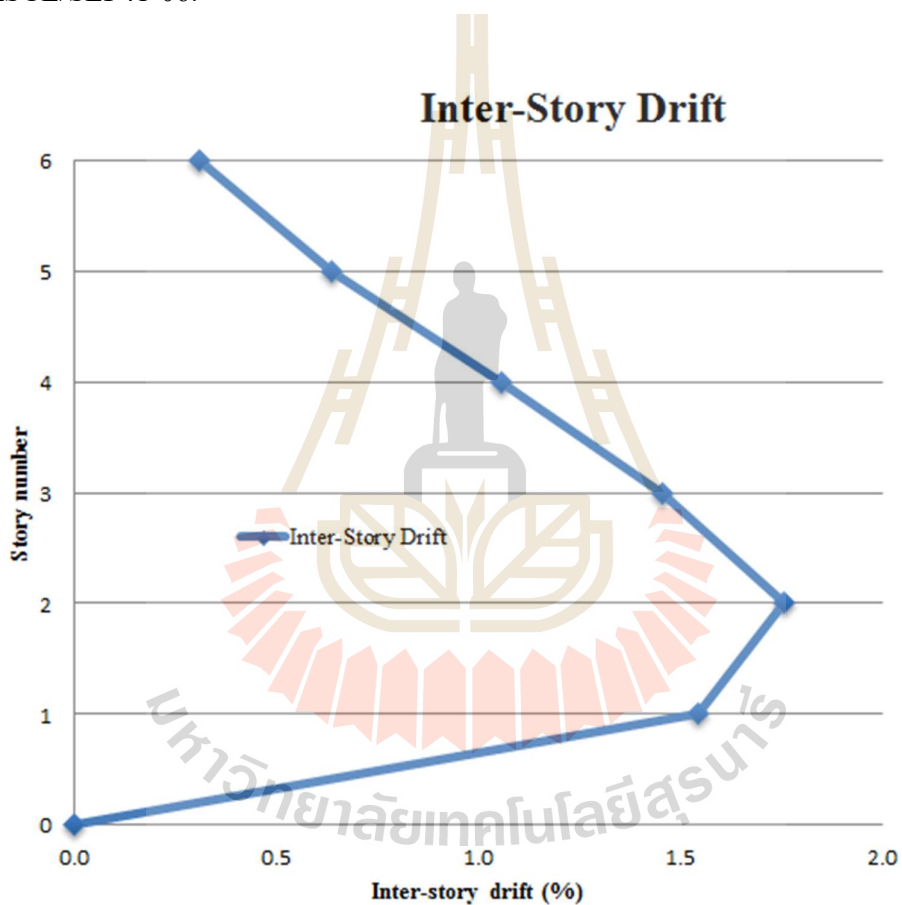


Figure 3.15 Story deflections (cm)



The inter-story drifts of the frames at different building drifts are shown in figure 3.16. Before calculating the inter-story drift, we need to determine the deflection at level  $x$  ( $\delta_x$ ) as shown in equation 3.1. The value of the deflection is shown in figure 3.15 According to ASCE 7-16, the inter-story drift ratio (IDR) as determine in equation 3.2 shall not exceed the performance limit as defined by ASCE/SEI 41-06.



**Figure 3.16** Inter-story drift (%)

### 3.3.9 Inter-story Drift Method of the nine-story building

According to ASCE/SEI 41-06, Inter-story drift ratio is determined as the difference between the deflections of two adjacent floors which can be expressed as a percentage of the story height. The inter-story drift is the most acceptable parameter to control the displacement, the resulting damage, and in turn performance of the structure. Thus, the importance of precise prediction of drifts in structural designs is obvious. ASCE/SEI 41-06 suggests typical limits of 1% inter-story drift for immediate occupancy (IO), 2% inter-story drift associated with Life Safety (LS) performance level and 4% inter-story drift for Collapse Prevention (CP) performance. These values are appropriate for well-detailed RC frames.

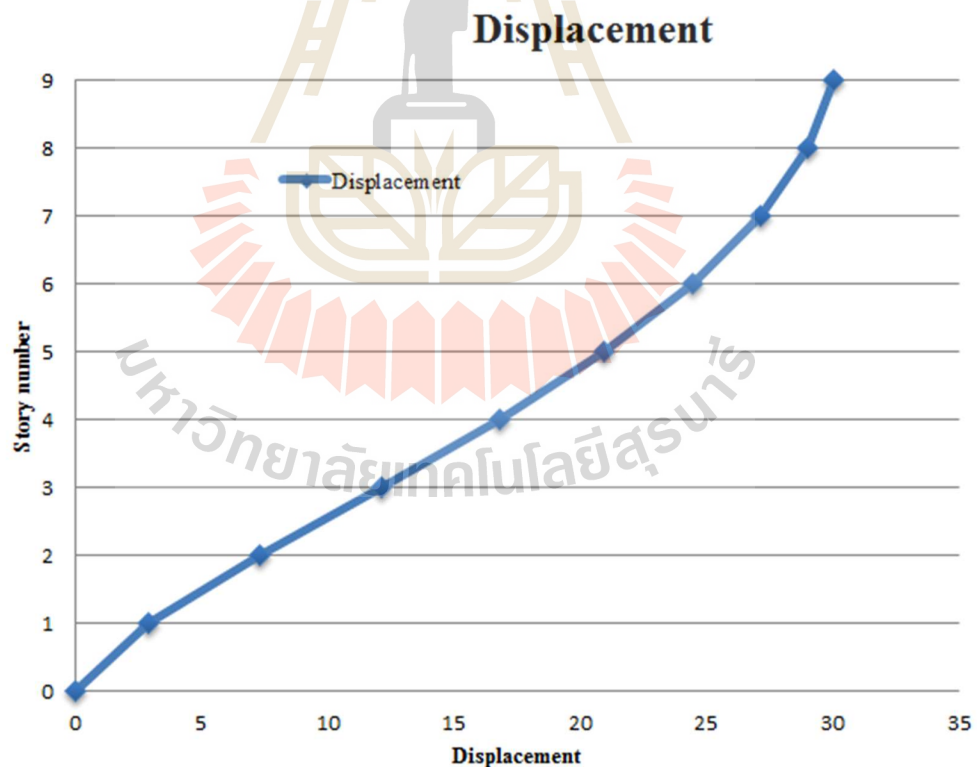
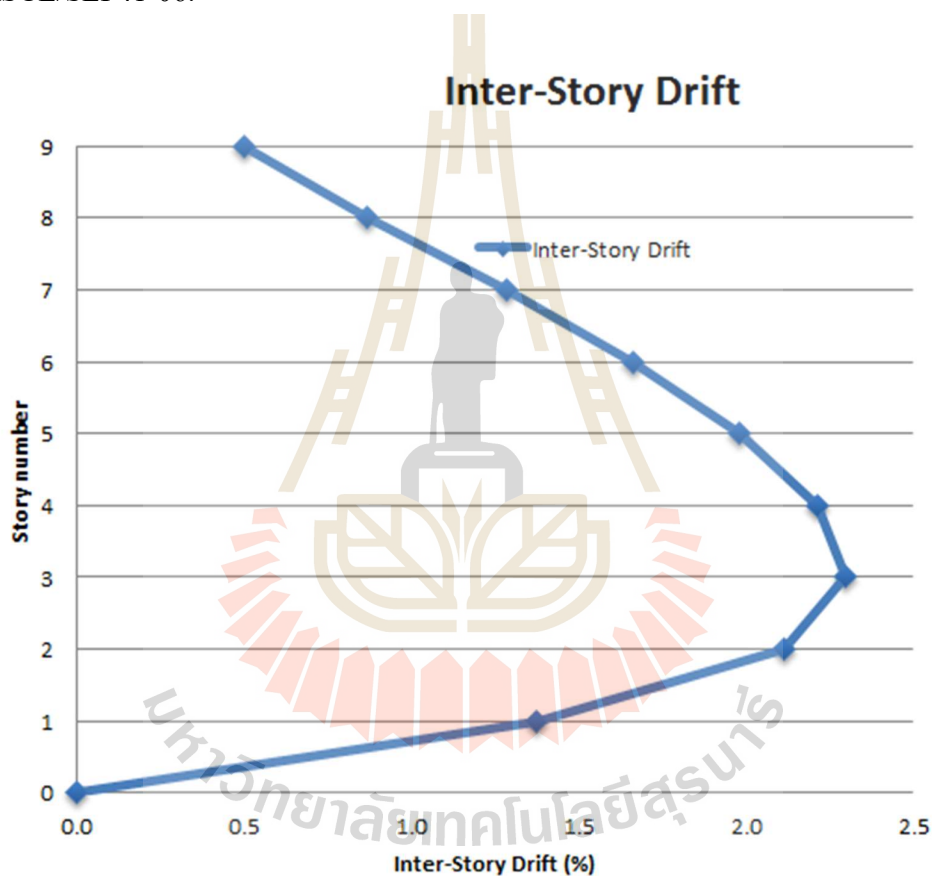


Figure 3.17 Story deflections (cm)

The inter-story drifts of the frames at different building drifts are shown in figure 3.18. Before calculating the inter-story drift, we need to determine the deflection at level  $x$  ( $\delta_x$ ) as shown in equation 3.1. The value of the deflection is shown in figure 3.17 According to ASCE 7-16, the inter-story drift ratio (IDR) as determine in equation 3.2 shall not exceed the performance limit as defined by ASCE/SEI 41-06.



**Figure 3.18** Inter-story drift (%)

### 3.3.10 Acceptance Criteria of the three-story Building

#### 3.3.10.1 Conditions of the Column

According to ASCE 41-13, it shows that the axial compression of the column is classified as a force-controlled action. To know the

column is adequate for axial compression, the lower-bound strength of column must be more than the maximum requirement force at the target displacement. Shear of the column has also classified as a force-controlled action. Both the axial and shear capacity of the column are more than the maximum analysis force at the target displacement. The conditions of the columns were shown in table 3.5. The value of the transverse reinforcement details ( $V_p/V_o \leq 0.6$ ) that is a condition to be used for the columns to which chooses the closed hoops with 90-degree hooks (ii). Other requirement parameters used to determine performance levels of the column as shown in table 3.5.

**Table 3.5** Conditions of the columns of the three-story building

Level	Conditions		
	$\frac{P}{A_g f_c}$	$\frac{A_v}{b_w s}$	$\frac{V}{b_w d \sqrt{f_c}}$
3	0.075	0.005	0.137
2	0.149	0.005	0.255
1	0.221	0.005	0.442

### 3.3.10.2 Conditions of the Beam

The beam shear must be evaluated on three locations of the beam, which are yield zones for two ends of the beam, and the center of the beam known as a non-yield zone. After checking the result, it shows that the lower-bound shear capacity of the beam is more than the shear demand of the beam at the given performance objective. Moreover, the flexural of the beam must be checked at all locations where the loads produce the maximum effects to the beam elements. The

beam was classified as positive and negative flexural demand that examined for adequacy at the left, middle, and right of beam segments and the left and right of beam segments, respectively.

**Table 3.6** Condition of the beams of the three-story building

Level	Condition		
	$\frac{\rho - \rho'}{\rho_{bal}}$	Transverse reinforcement	$\frac{V}{b_w d \sqrt{f_c}}$
3	0.00	C	0.111
2	-0.28	C	0.115
1	-0.42	C	0.115

Before defining the performance levels of the beam, it must be examined for the shear-controlled or flexure-controlled. Base on the result, the beam shear capacity is more than the beam shear requirement, shown that the beam is the flexure-controlled. The transverse reinforcing was classified as conforming and nonconforming transverse reinforcement that abbreviated as "C" and "NC", respectively. The other required parameters are shown in table 3.6.

### 3.3.11 Acceptance Criteria of the six-story Building

#### 3.3.11.1 Conditions of the Column

According to ASCE 41-13, it shows that the axial compression of the column is classified as a force-controlled action. To know the column is adequate for axial compression, the lower-bound strength of column must

be more than the maximum requirement force at the target displacement. Shear of the column has also classified as a force-controlled action.

**Table 3.7** Conditions of the columns of the six-story building

Level	Conditions		
	$\frac{P}{A_g f'_c}$	$\frac{A_v}{b_w s}$	$\frac{V}{b_w d \sqrt{f'_c}}$
6	0.047976	0.00285	0.090017
5	0.096073	0.00285	0.119020
4	0.145851	0.00285	0.150307
3	0.196783	0.00285	0.180887
2	0.248912	0.00285	0.209455
1	0.287078	0.00285	0.258643

Both the axial and shear capacity of the column are more than the maximum analysis force at the target displacement. The conditions of the columns were shown in table 3.7. The value of the transverse reinforcement details ( $V_P/V_O \leq 0.6$ ) that is a condition to be used for the columns to which chooses the closed hoops with 90-degree hooks (ii). Other requirement parameters used to determine performance levels of the column as shown in table 3.7.

### 3.3.11.2 Conditions of the Beam

The beam shear must be evaluated on three locations of the beam, which are yield zones for two ends of the beam, and the center of the beam

known as a non-yield zone. After checking the result, it shows that the lower-bound shear capacity of the beam is more than the shear demand of the beam at the given performance objective. Moreover, the flexural of the beam must be checked at all locations where the loads produce the maximum effects to the beam elements. The beam was classified as positive and negative flexural demand that examined for adequacy at the left, middle, and right of beam segments and the left and right of beam segments, respectively.

**Table 3.8** Condition of the beams of the six-story building

Level	Condition		
	$\frac{\rho - \rho'}{\rho_{bal}}$	Transverse reinforcement	$\frac{V}{b_w d \sqrt{f'_c}}$
6	-0.17278	C	0.60945416
5	-0.38729	C	0.836492274
4	-0.56742	C	0.836565618
3	-0.65247	C	0.835603048
2	-0.71257	C	0.836212111
1	-0.78546	C	0.827938724

Before defining the performance levels of the beam, it must be examined for the shear-controlled or flexure-controlled. Base on the result, the beam shear capacity

is more than the beam shear requirement, shown that the beam is the flexure-controlled. The transverse reinforcing was classified as conforming and nonconforming transverse reinforcement that abbreviated as “C” and “NC”, respectively. The other required parameters are shown in table 3.8.

### 3.3.12 Acceptance Criteria of the nine-story Building

#### 3.3.12.1 Conditions of the Column

According to ASCE 41-13, it shows that the axial compression of the column is classified as a force-controlled action. To know the column is adequate for axial compression, the lower-bound strength of column must be more than the maximum requirement force at the target displacement.

**Table 3.9** Conditions of the columns of the nine-story building

Level	Conditions		
	$\frac{P}{A_g f'_c}$	$\frac{A_v}{b_w s}$	$\frac{V}{b_w d \sqrt{f'_c}}$
9	0.077645622	0.002243	0.088991952
8	0.154426133	0.002243	0.133105603
7	0.231379963	0.002243	0.187004287
6	0.308533819	0.002243	0.232305065
5	0.385974104	0.002243	0.268779468
4	0.463849896	0.002243	0.311109013
3	0.542266918	0.002243	0.320158638
2	0.621679032	0.002243	0.419869743
1	0.699213769	0.002243	0.245487742



Shear of the column has also classified as a force-controlled action. Both the axial and shear capacity of the column are more than the maximum analysis force at the target displacement. The conditions of the columns were shown in table 3.9. The value of the transverse reinforcement details ( $V_p/V_o \leq 0.6$ ) that is a condition to be used for the columns to which chooses the closed hoops with 90-degree hooks (ii). Other requirement parameters used to determine performance levels of the column as shown in table 3.9.

### 3.3.12.2 Conditions of the Beam

The beam shear must be evaluated on three locations of the beam, which are yield zones for two ends of the beam, and the center of the beam known as a non-yield zone. After checking the result, it shows that the lower-bound shear capacity of the beam is more than the shear demand of the beam at the given performance objective. Moreover, the flexural of the beam must be checked at all locations where the loads produce the maximum effects to the beam elements. The beam was classified as positive and negative flexural demand that examined for adequacy at the left, middle, and right of beam segments and the left and right of beam segments, respectively. Before defining the performance levels of the beam, it must be examined for the shear-controlled or flexure-controlled. Base on the result, the beam shear capacity is more than the beam shear requirement, shown that the beam is the flexure-controlled. The transverse reinforcing was classified as conforming and nonconforming transverse reinforcement that abbreviated as “C” and “NC”, respectively. The other required parameters are shown in table 3.10.

**Table 3.10** Condition of the beams of the nine-story building

Level	Condition		
	$\frac{\rho-\rho'}{\rho_{bal}}$	Transverse reinforcement	$\frac{V}{b_w d \sqrt{f_c}}$
9	-0.248	C	0.168998001
8	-0.4839	C	0.182389341
7	-0.5853	C	0.18132613
6	-0.688	C	0.180822911
5	-0.698	C	0.179572727
4	-0.715	C	0.177898254
3	-0.7432	C	0.175893145
2	-0.7643	C	0.173614005
1	-0.798	C	0.17041992

### 3.3.13 Stiffness Calculation Beam-Column Joints

Joint stiffness shall be modelled the joint stiffness implicitly by adjusting the centerline model following by three different types as shown in figure 3.19. Moreover, the interior column was used to calculate the ratio of the column-beam moments as shown in table 3.11. For example, it shows that the first story of the building has  $\Sigma M_{nc} / \Sigma M_{nb} > 1.2$ , Using beam rigid end length offset is 0.00 and column rigid end length offset is 1.00. The other stories of the building were shown in table 3.11.

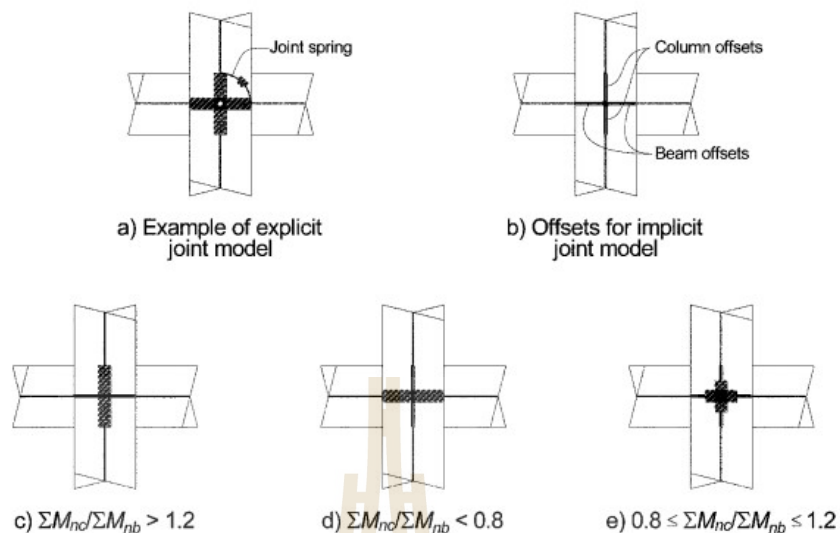


**Figure 3.19** Beam–Column joint stiffness modeling. (ASCE 41-13)

**Table 3.11** Joint stiffness of the interior columns

Level	$M_{nc}$ Kg.m	$M_{nb}^+$ Kg.m	$M_{nb}^-$ Kg.m	$\Sigma M_{nc}$ Kg.m	$\Sigma M_{nb}$ Kg.m	$\frac{\Sigma M_{nc}}{\Sigma M_{nb}}$	Rigid Factor Column	Rigid Factor Beam
3	45500	25962	49493	45500	75454	0.75	0	1
2	94500	25962	49493	140000	75454	1.56	1	0
1	99000	25962	49193	193500	75454	1.64	1	0

1. For  $\Sigma M_{nc} / \Sigma M_{nb} > 1.2$ , column offsets are rigid and beam offsets are not;
  2. For  $\Sigma M_{nc} / \Sigma M_{nb} < 0.8$ , beam offsets are rigid and column offsets are not; and
  3. For  $0.8 \leq M_{nc} / \Sigma M_{nb} \leq 1.2$ , half of the beam and column offsets are considered rigid.
- where  $M_{nc}$  is the nominal moment capacities at column and  $M_{nb}$  is the nominal moment capacities at beam.

### 3.4 Performance Evaluation of Retrofitted Building

#### 3.4.1 Displacement Coefficient Method of the three-story Building

Displacement coefficient method was also used to calculate the target displacement of the retrofitted building at the control node on the roof that similar the procedure as the existing building. The target displacement of the FEMA 440 and ASCE/SEI 41-13 equal 0.02 m and 0.0263 m as shown in table 3.12, respectively. We use the maximum between to two these values to compare to point out the pushover step that gets from the SAP2000.

**Table 3.12** Parameter and target displacement ( $\delta_t$ ) of three-story building

Parameters	FEMA 440	ASCE 41-13	Note
$C_0$	1.218	1.373	ASCE 41-13 Table 7-5. Values for Modification Factor
$C_1$	1.122	1.101	Modification Factor to relate the expected max displacements
$C_2$	1.006	1.005	Values for Modification Factor
$C_3$	1.000		Building with post-yield stiffness
$S_a$	0.628	0.628	Spectral Response Acceleration
$T_e$	0.304	0.333	Effective natural vibration
$G$	9.81	9.81	Gravitational Acceleration
$\delta_t$	0.020	0.0263	FEMA 440: $\delta_t = C_0 C_1 C_2 C_3 S_a (T_e / 2\pi)^2 g$
			ASCE 41-13: $\delta_t = C_0 C_1 C_2 S_a (T_e / 2\pi)^2 g$

### 3.4.2 Displacement Coefficient Method of the six-story Building

Displacement coefficient method was also used to calculate the target displacement of the retrofitted building at the control node on the roof that similar the procedure as the existing building. The target displacement of the FEMA 440 and ASCE/SEI 41-13 equal 0.068673 m and 0.072714 m as shown in table 3.13, respectively. We use the maximum between to two these values to compare to point out the pushover step that gets from the SAP2000.

**Table 3.13** Parameter and target displacement ( $\delta_t$ ) of six-story building

Parameters	FEMA 440	ASCE 41-13	Note
$C_0$	1.2422	1.2371	ASCE 41-13 Table 7-5. Values for Modification Factor
$C_1$	1.000	1.0576	Modification Factor to relate the expected max displacements
$C_2$	1.000	1.0053	Values for Modification Factor
$C_3$	1.000		Building with post-yield stiffness
$S_a$	0.628	0.628	Spectral Response Acceleration
$T_e$	0.5949	0.5949	Effective natural vibration
$G$	9.81	9.81	Gravitational Acceleration
$\delta_t$	0.068673	0.072714	FEMA 440: $\delta_t = C_0 C_1 C_2 C_3 S_a (T_e / 2\pi)^2 g$
			ASCE 41-13: $\delta_t = C_0 C_1 C_2 S_a (T_e / 2\pi)^2 g$

### 3.4.3 Displacement Coefficient Method of the nine-story Building

Displacement coefficient method was also used to calculate the target displacement of the retrofitted building at the control node on the roof that similar the procedure as the existing building. The target displacement of the FEMA 440 and ASCE/SEI 41-13 equal 0.155554 m and 0.163251 m as shown in table 3.14, respectively. We use the maximum between to two these values to compare to point out the pushover step that gets from the SAP2000.

**Table 3.14** Parameter and target displacement ( $\delta_t$ ) of nine-story building

Parameters	FEMA 440	ASCE 41-13	Note
$C_0$	1.2824	1.2825	ASCE 41-13 Table 7-5. Values for Modification Factor
$C_1$	1.000	1.0494	Modification Factor to relate the expected max displacements
$C_2$	1.000	1.00	Values for Modification Factor
$C_3$	1.000		Building with post-yield stiffness
$S_a$	0.628	0.628	Spectral Response Acceleration
$T_e$	0.8812	0.8812	Effective natural vibration
$G$	9.81	9.81	Gravitational Acceleration
$\delta_t$	0.155554	0.163251	FEMA 440: $\delta_t = C_0 C_1 C_2 C_3 S_a (T_e / 2\pi)^2 g$
			ASCE 41-13: $\delta_t = C_0 C_1 C_2 S_a (T_e / 2\pi)^2 g$

### 3.4.4 Capacity Spectrum Method of the three-story building

Capacity Spectrum Method (CSM), primarily described in ATC 40, was also used to evaluate the performance levels of the retrofitted building. Capacity Spectrum Method (CSM) was described in section 2.3 that talked about the Capacity Spectrum Method of the existing building. The structure with inverted V Bracing gives minimum Story drift as compared to other X, V. The magnitudes of story drift for all the stories are found to be within limits, i.e. 0.004 times to story height according to IS 1893:2002 (Part I) [1]. To depend on figure 3.20, it shows that the magnitude of base shear and tip displacement at the performance point are 7218051 N and 0.019 m, respectively. To determine the building performance levels, it can use the deformation limits to compare with the roof drift ratio at the performance point as follows: Roof drift ratio at the performance point is  $0.019/10.5 = 0.0018$ .

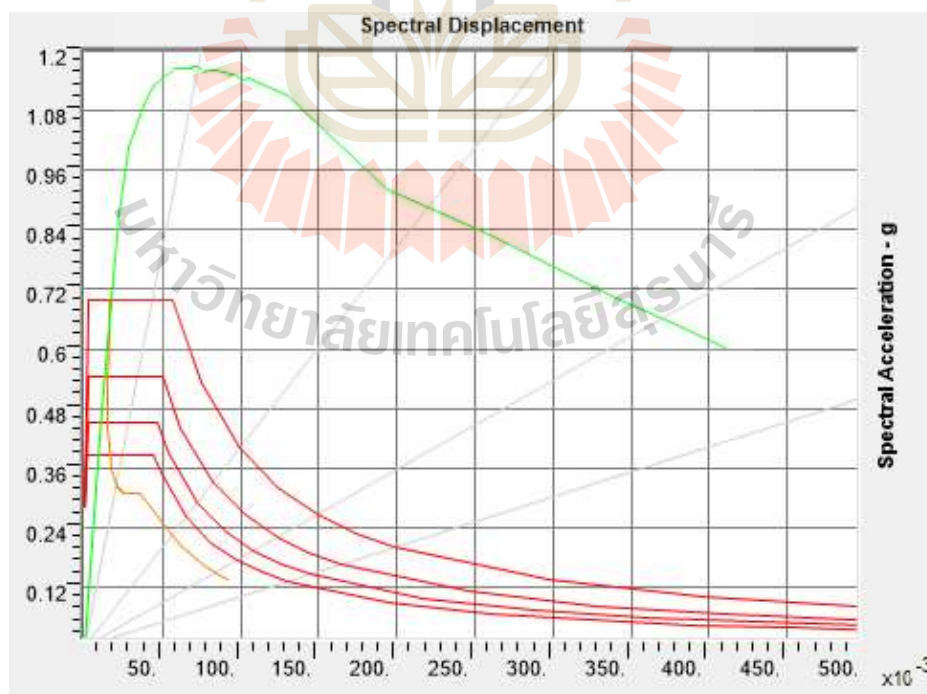


**Figure 3.20** Capacity spectrum curve of three-story building. (SAP2000)

### 3.4.5 Capacity Spectrum Method of the six-story building

To depend on figure 3.21, it shows that the magnitude of base shear and tip displacement at the performance point are 9532797 N and 0.066 m, respectively. To determine the building performance levels, it can use the deformation limits to compare with the roof drift ratio at the performance point as follows: Roof drift ratio at the performance point is  $0.066/21 = 0.00314$ .

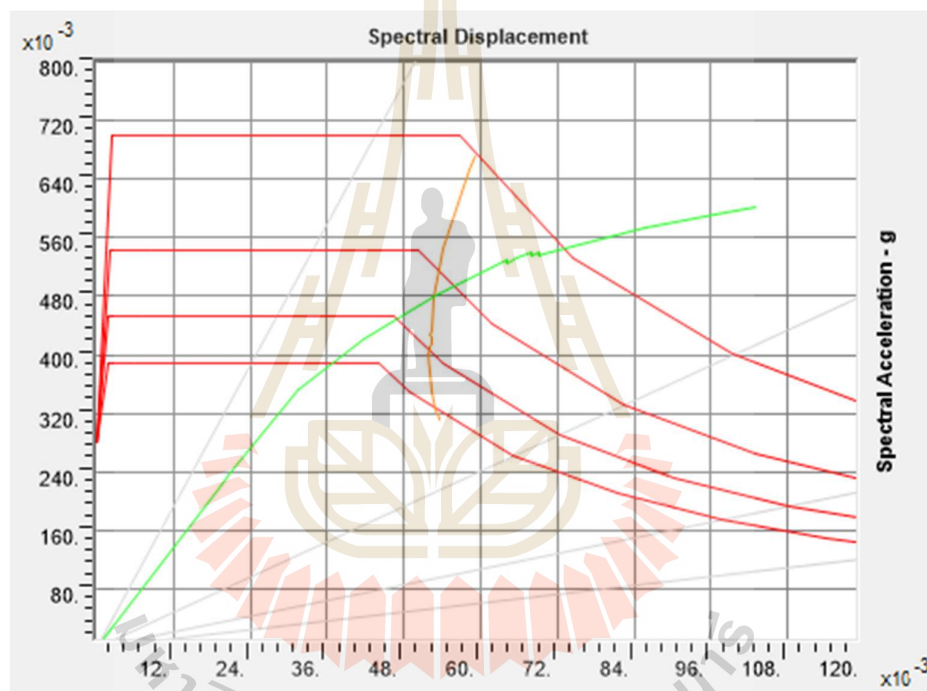


Figure 3.21 Capacity spectrum curve of six-story building. (SAP2000)

### 3.4.6 Capacity Spectrum Method of the nine-story building

To depend on figure 3.22, it shows that the magnitude of base shear and tip displacement at the performance point are 11151768 N and 0.109 m, respectively. To determine the building performance levels, it can use the deformation



limits to compare with the roof drift ratio at the performance point as follows: Roof drift ratio at the performance point is  $0.109/31.5 = 0.00346$ .

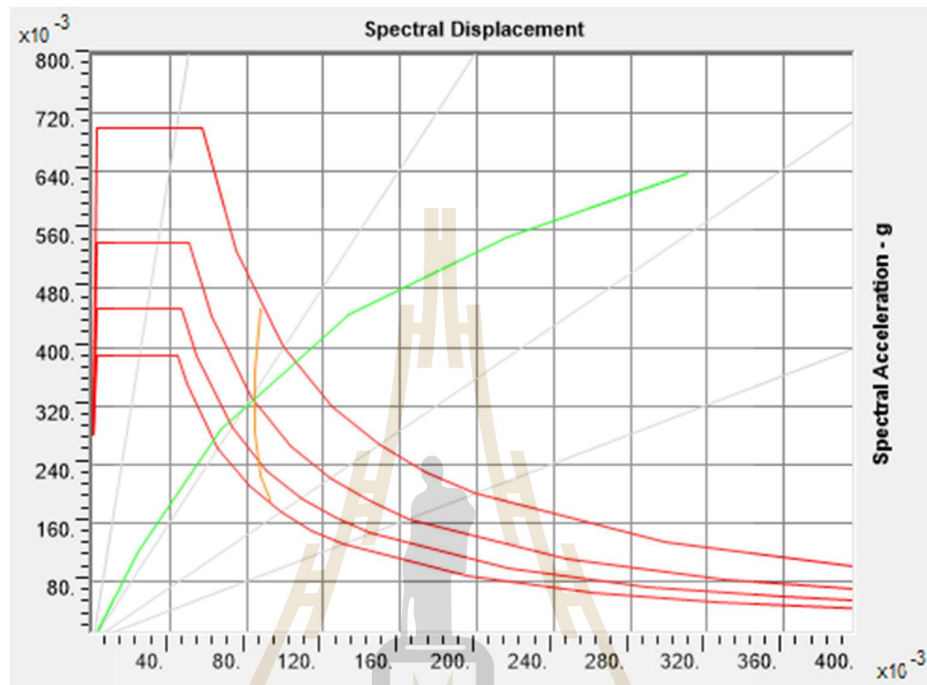


**Figure 3.22** Capacity spectrum curve of nine-story building. (SAP2000)

### 3.4.7 Inter-story Drift Method of the three-story building

According to ASCE/SEI 41-06, Inter-story drift ratio is determined as the difference between the deflections of two adjacent floors which can be expressed as a percentage of the story height. The inter-story drift is the most acceptable parameter to control the displacement, the resulting damage, and in turn performance of the structure. Thus, the importance of precise prediction of drifts in structural designs is obvious. ASCE/SEI 41-06 suggests typical limits of 1% inter-story drift for immediate occupancy (IO), 2% inter-story drift associated with Life Safety (LS) performance level and 4% inter-story drift for Collapse Prevention (CP) performance.

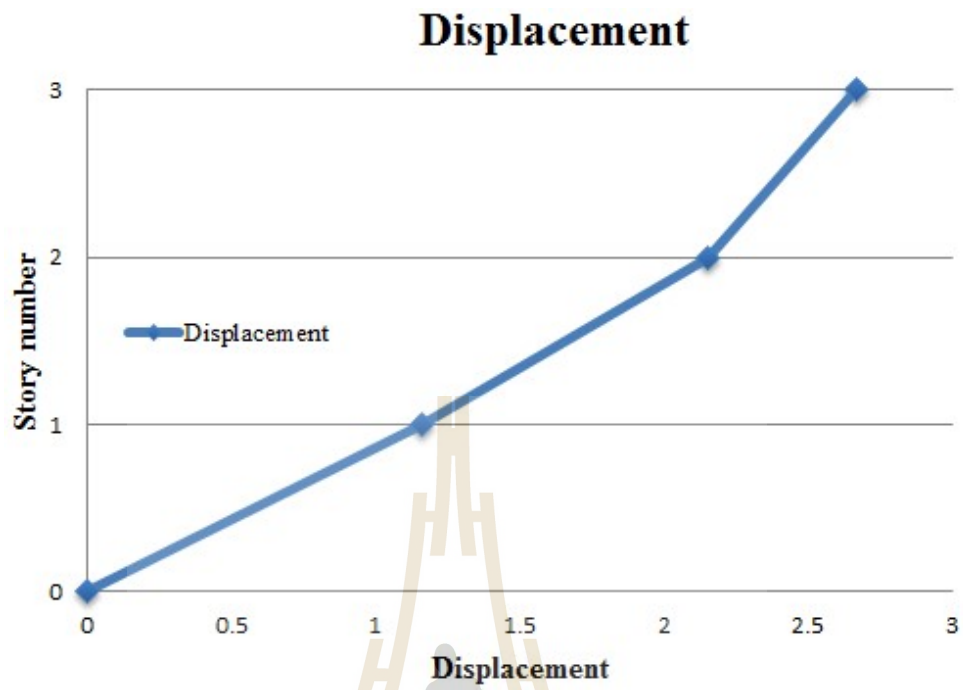


Figure 3.23 Story deflections

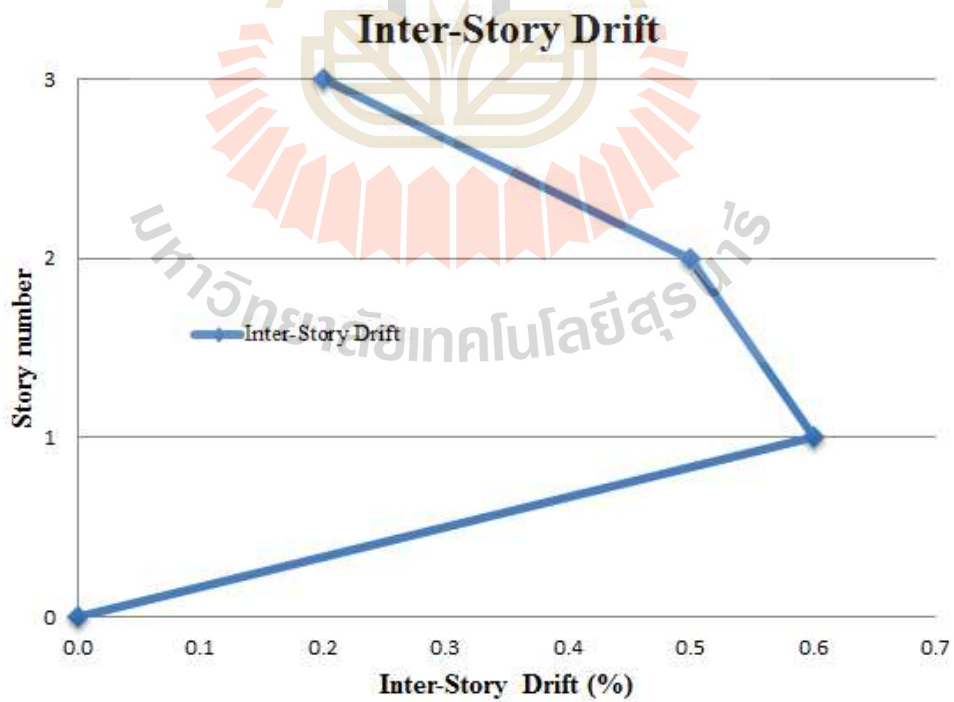


Figure 3.24 Inter-story drift (%)

Before calculating the inter-story drift, we need to determine the deflection as shown in figure 3.23. According to the figure 3.24, it shows that the inter-story drift at the first story, second story, and third story equal to 0.2%, 0.5%, and 0.6%, respectively.

### 3.4.8 Inter-story Drift Method of the six-story building

According to ASCE/SEI 41-06, Inter-story drift ratio is determined as the difference between the deflections of two adjacent floors, which can be expressed as a percentage of the story height. The inter-story drift is the most acceptable parameter to control the displacement, the resulting damage, and in turn performance of the structure. Thus, the importance of precise prediction of drifts in structural designs is obvious.

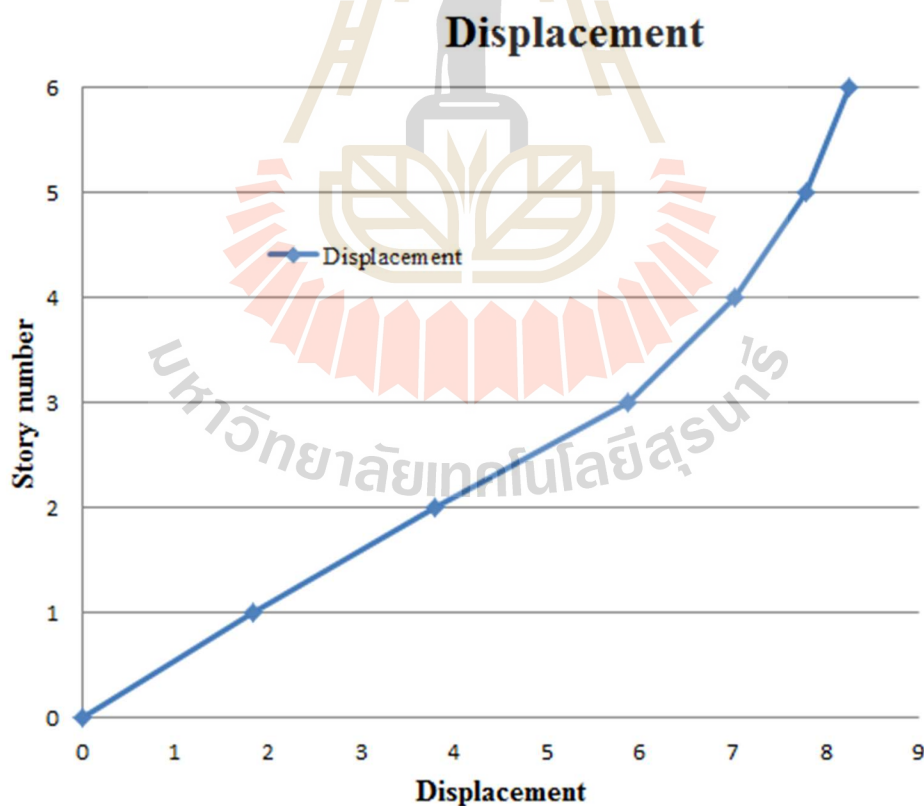
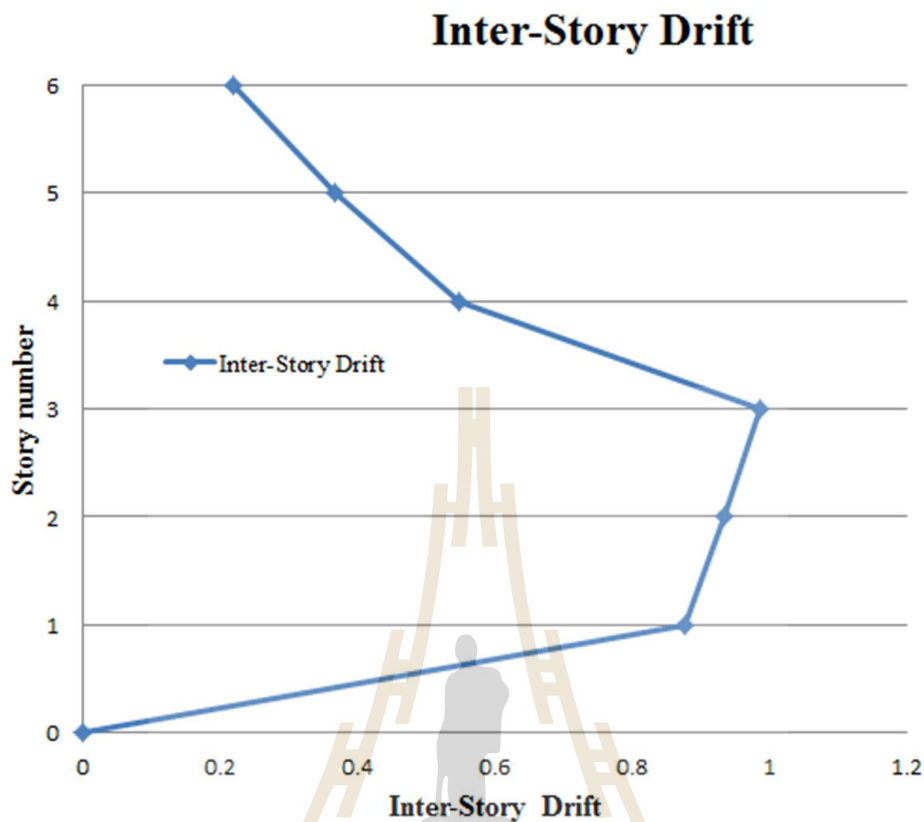


Figure 3.25 Story deflections



**Figure 3.26** Inter-story drift (%)

ASCE/SEI 41-06 suggests typical limits of 1% inter-story drift for immediate occupancy (IO), 2% inter-story drift associated with Life Safety (LS) performance level and 4% inter-story drift for Collapse Prevention (CP) performance. Before calculating the inter-story drift, we need to determine the deflection, as shown in figure 3.25. The inter-story drift of the six-story building was shown in the figure in table 3.26.

#### **3.4.9 Inter-story Drift Method of the nine-story building**

According to ASCE/SEI 41-06, Inter-story drift ratio is determined as the difference between the deflections of two adjacent floors, which can be expressed as a percentage of the story height. The inter-story drift is the most acceptable

parameter to control the displacement, the resulting damage, and in turn performance of the structure. Thus, the importance of precise prediction of drifts in structural designs is obvious. ASCE/SEI 41-06 suggests typical limits of 1% inter-story drift for immediate occupancy (IO), 2% inter-story drift associated with Life Safety (LS) performance level and 4% inter-story drift for Collapse Prevention (CP) performance.

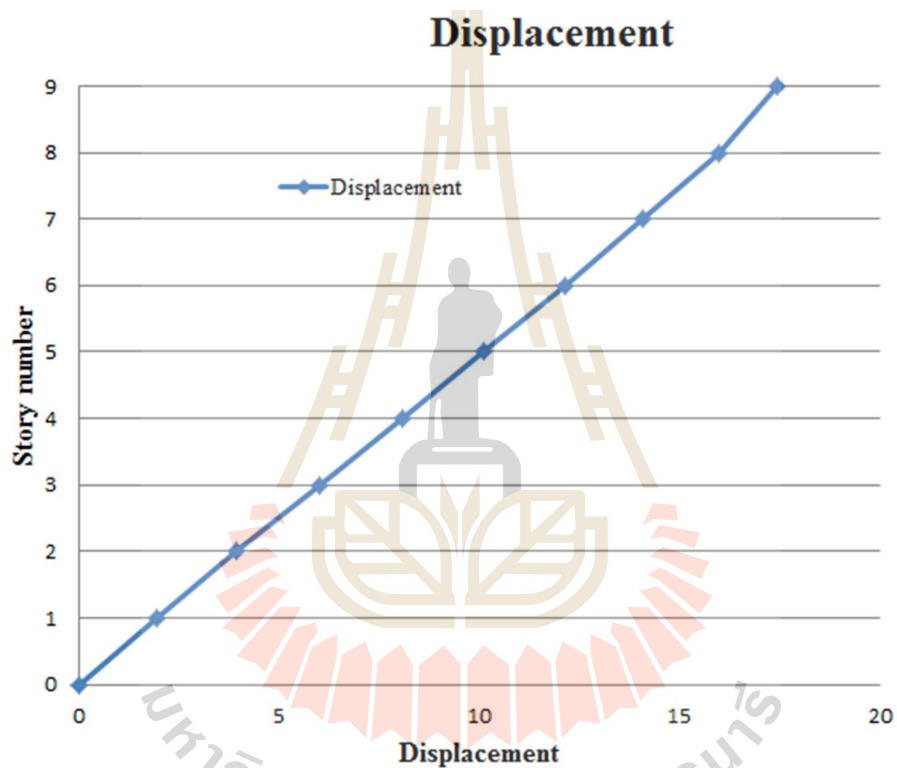
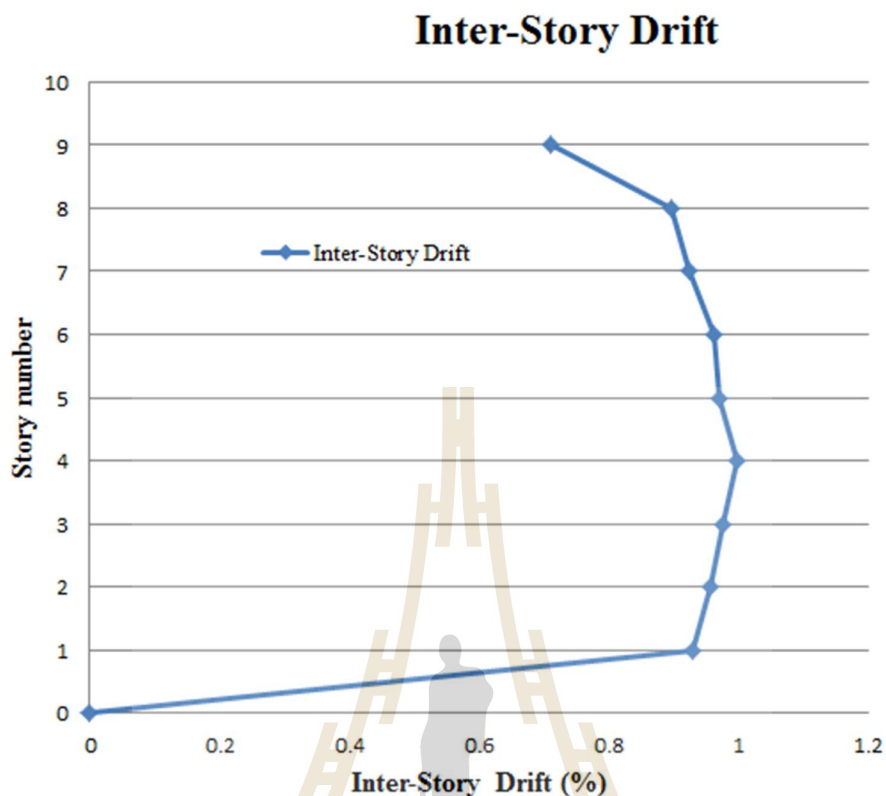


Figure 3.27 Story deflections



**Figure 3.28** Inter-story drift (%)

Before calculating the inter-story drift, we need to determine the deflection, as shown in figure 3.27. The inter-story drift of the nine-story building was shown in the figure in table 3.28.

### 3.4.10 Acceptance Criteria of the Three-story Building

#### 3.4.10.1 Performance Evaluation of the Column

All the conditions that used to evaluate the performance levels of the retrofitted building of the column were performed the same as the performance levels of the existing building of the column. The acceptance criteria of the retrofitted building are quite similar to the acceptance criteria of the existing building. The most of the columns do not have the plastic hinge rotation (radian), and

a little bit of the column has plastic hinge rotation (radian) in the first story. The acceptance criteria were used to compare with the plastic hinge rotation (radian) of the retrofitted building to classify the performance levels of the retrofitted building. Both the axial compression and Shear of the column are classified as a force-controlled action. Both the axial and shear capacity of the column are more than the maximum analysis force at the target displacement. The value of the transverse reinforcement details ( $V_p/V_o \leq 0.6$ ) that is a condition to be used for the columns to which chooses the closed hoops with 90-degree hooks (ii). Other requirement parameters used to determine performance levels of the column as shown in table 3.15.

**Table 3.15** Conditions of the columns of the three-story building

Level	Condition		
	$\frac{P}{A_g f_c}$	$\frac{A_v}{b_w s}$	$\frac{V}{b_w d \sqrt{f_c}}$
3	0.091	0.005	0.065
2	0.181	0.005	0.105
1	0.271	0.005	0.228

#### 3.4.10.2 Performance Evaluation of the Beam

All the conditions that used to evaluate the performance levels of the retrofitted building of the beam were performed the same as the performance levels of the existing building of the beam. The acceptance criteria of the retrofitted building is quite similar to the acceptance criteria of the existing building.

The most of the beams have a little bit the plastic hinge rotation (radian) in the first and second floor, and the columns do not have the plastic hinge rotation (radian) in the third story. The acceptance criteria was used to compare with the plastic hinge rotation (radian) of the retrofitted building to classify the performance levels of the retrofitted building. Before defining the performance levels of the beam, it must be examined for the shear-controlled or flexure-controlled. Base on the result, the beam shear capacity is more than the beam shear requirement, shown that the beam is the flexure-controlled. The transverse reinforcing was classified as conforming and nonconforming transverse reinforcement that abbreviated as “C” and “NC”, respectively. The other required parameters are shown in table 3.16.

**Table 3.16** Condition of the beams of the three-story building

Level	Condition		
	$\frac{\rho-\rho'}{\rho_{bal}}$	Transverse reinforcement	$\frac{V}{b_w d \sqrt{f'_c}}$
3	0.00	C	0.125
2	-0.28	C	0.155
1	-0.42	C	0.162

### 3.4.11 Acceptance Criteria of the Six-story Building

#### 3.4.11.1 Performance Evaluation of the Column

All the conditions that used to evaluate the performance levels of the retrofitted building of the column were performed the same as the performance levels of the existing building of the column. The acceptance criteria of



the retrofitted building are quite similar to the acceptance criteria of the existing building. The most of the columns do not have the plastic hinge rotation (radian), and a little bit of the column has plastic hinge rotation (radian) in the first story.

**Table 3.17** Conditions of the columns of the six-story building

Level	Condition		
	$\frac{P}{A_g f_c}$	$\frac{A_v}{b_w s}$	$\frac{V}{b_w d \sqrt{f_c}}$
6	0.04676	0.00285	0.06867
5	0.09507	0.00285	0.08263
4	0.14195	0.00285	0.08594
3	0.19004	0.00285	0.11519
2	0.23700	0.00285	0.14964
1	0.28439	0.00285	0.22077

The acceptance criteria were used to compare with the plastic hinge rotation (radian) of the retrofitted building to classify the performance levels of the retrofitted building. Both the axial compression and Shear of the column are classified as a force-controlled action. Both the axial and shear capacity of the column are more than the maximum analysis force at the target displacement. The value of the transverse reinforcement details ( $V_P/V_O \leq 0.6$ ) that is a condition to be used for the columns to which chooses the closed hoops with 90-degree hooks (ii). Other requirement parameters used to determine performance levels of the column as shown in table 3.17.

### 3.4.11.2 Performance Evaluation of the Beam

All the conditions that used to evaluate the performance levels of the retrofitted building of the beam were performed the same as the performance levels of the existing building of the beam. The acceptance criteria of the retrofitted building is quite similar to the acceptance criteria of the existing building.

**Table 3.18** Condition of the beams of the six-story building

Level	Condition		
	$\frac{\rho - \rho'}{\rho_{bal}}$	Transverse reinforcement	$\frac{V}{b_w d \sqrt{f'_c}}$
6	-0.17278	C	0.071770926
5	-0.38729	C	0.09405271
4	-0.56742	C	0.101457197
3	-0.65247	C	0.100391389
2	-0.71257	C	0.099388685
1	-0.78546	C	0.097380781

The most of the beams have a little bit the plastic hinge rotation (radian) in the first and second floor, and the columns do not have the plastic hinge rotation (radian) in the third story. The acceptance criteria was used to compare with the plastic hinge rotation (radian) of the retrofitted building to classify the performance levels of the retrofitted building. Before defining the performance levels of the beam, it must be examined for the shear-controlled or flexure-controlled. Base on the result, the beam shear capacity is more than the beam shear requirement, shown that the beam is the flexure-controlled. The transverse reinforcing was classified as

conforming and nonconforming transverse reinforcement that abbreviated as "C" and "NC", respectively. The other required parameters are shown in table 3.18.

### 3.4.12 Acceptance Criteria of the Nine-story Building

#### 3.4.12.1 Performance Evaluation of the Column

All the conditions that used to evaluate the performance levels of the retrofitted building of the column were performed the same as the performance levels of the existing building of the column. The acceptance criteria of the retrofitted building are quite similar to the acceptance criteria of the existing building. The most of the columns do not have the plastic hinge rotation (radian), and a little bit of the column has plastic hinge rotation (radian) in the first story.

**Table 3.19** Conditions of the columns of the nine-story building

Level	Condition		
	$\frac{P}{A_g f_c}$	$\frac{A_v}{b_w s}$	$\frac{V}{b_w d \sqrt{f_c}}$
9	0.157069735	0.002243	0.102645158
8	0.078981389	0.002243	109540.0004
7	0.235420938	0.002243	0.147501559
6	0.314041789	0.002243	0.17119631
5	0.393034058	0.002243	0.198183984
4	0.472466232	0.002243	0.228767807
3	0.552616889	0.002243	0.245246523
2	0.633492521	0.002243	0.241969124
1	0.715468139	0.002243	0.229677905

The acceptance criteria were used to compare with the plastic hinge rotation (radian) of the retrofitted building to classify the performance levels of the retrofitted building. Both the axial compression and Shear of the column are classified as a force-controlled action. Both the axial and shear capacity of the column are more than the maximum analysis force at the target displacement. The value of the transverse reinforcement details ( $V_P/V_O \leq 0.6$ ) that is a condition to be used for the columns to which chooses the closed hoops with 90-degree hooks (ii). Other requirement parameters used to determine performance levels of the column as shown in table 3.19.

#### **3.4.12.2 Performance Evaluation of the Beam**

All the conditions that used to evaluate the performance levels of the retrofitted building of the beam were performed the same as the performance levels of the existing building of the beam. The acceptance criteria of the retrofitted building is quite similar to the acceptance criteria of the existing building. The most of the beams have a little bit the plastic hinge rotation (radian) in the first and second floor, and the columns do not have the plastic hinge rotation (radian) in the third story. The acceptance criteria was used to compare with the plastic hinge rotation (radian) of the retrofitted building to classify the performance levels of the retrofitted building. Before defining the performance levels of the beam, it must be examined for the shear-controlled or flexure-controlled. Base on the result, the beam shear capacity is more than the beam shear requirement, shown that the beam is the flexure-controlled. The transverse reinforcing was classified as conforming and nonconforming transverse reinforcement that abbreviated as "C" and "NC", respectively. The other required parameters are shown in table 3.20.

**Table 3.20** Condition of the beams of the nine-story building

Level	Condition		
	$\frac{\rho-\rho'}{\rho_{bal}}$	Transverse reinforcement	$\frac{V}{b_w d \sqrt{f'_c}}$
9	-0.248	C	0.167021984
8	-0.4839	C	0.182547954
7	-0.5853	C	0.181392311
6	-0.688	C	0.180228881
5	-0.698	C	0.178965643
4	-0.715	C	0.177092685
3	-0.7432	C	0.174423932
2	-0.7643	C	0.171055808
1	-0.798	C	0.16681199



## CHAPTER IV

### RESULT AND COMPARISON

#### 4.1 Introduction

Performance Based Seismic Design (PBSD) is a design concept that is currently being applied in seismic design on a variety of buildings and bridges. Its main goal is to produce structures that will have predictable results in the event of an earthquake. A defining parameter in PBSD is its performance objective: the acceptable level of damage selected for a specified earthquake intensity level. A building may be designed based on one or multiple performance objectives. In this study, we use the four methods to evaluate building performance. The building performance divides into three levels that call Immediate Occupancy (IO), Life Safety (LS), and Collapse Prevention (CP). Immediate Occupancy, "IO," When an earthquake occurs, the structure can withstand the earthquake, the structure does not suffer structural damage and does not experience non-structural damage. So it can be directly used. Level of life safety (Life Safety), "LS," When an earthquake occurs, the structure can withstand earthquakes, with minimum structural damage, humans living/residing in the building is safeguarded from earthquakes. Level of structural stability (Collapse Prevention or Structural Stability), "CP," When an earthquake occurs, the structure undergoes severe structural damage, but has not collapsed. A three storied building is used to assess the building performance using Displacement Coefficient Method, Capacity Spectrum Method, Inter-story Drift Method, and Member-Level Performance Method.

Therefore, the result from the calculation of each method is compared with any standards or codes that specified the performance levels. Base on the result, we can know the performance level of the building that classified as global and local performance.

## 4.2 Performance Evaluation of Existing Building

### 4.2.1 Displacement Coefficient Method of the Three-story Building

From table 3.1, the target displacement of the FEMA 440 and ASCE/SEI 41-13 equal 0.040 m and 0.0517 m, respectively. We choose the maximum value between both values to compare with performance levels that get from the SAP2000 software as shown in table 4.1. The 0.0517 m of the target displacement meets in step 3<sup>rd</sup> of the 0.092645 m displacements in table 4.1. Therefore, the performance level of the building meets in between Immediate Occupancy (IO) to Life Safety (LS) levels.

**Table 4.1** Pushover steps of the three-story building

Step	Displacement (m)	Base-Shear (Kgf)	A to B	B to IO	IO to LS	LS to CP	CP to C	C to D	D to E	>E	Total
0	2.6E-6	0.000	390	0	0	0	0	0	0	0	390
1	0.0149	291624.52	388	2	0	0	0	0	0	0	390
2	0.0499	832423.50	290	100	0	0	0	0	0	0	390
3	0.0926	1127561.68	242	114	34	0	0	0	0	0	390
4	0.0965	1142979.45	238	114	38	0	0	0	0	0	390
5	0.1012	1158335.73	234	106	50	0	0	0	0	0	390
6	0.1083	1174948.23	222	114	54	0	0	0	0	0	390

**Table 4.1** Pushover steps of the three-story building (Continued)

Step	Displacement (m)	Base-Shear (Kgf)	A to B	B to IO	IO to LS	LS to CP	CP to C	C to D	D to E	>E	Total
7	0.1115	1179462.12	218	117	55	0	0	0	0	0	390
8	0.1116	1171650.64	218	117	55	0	0	0	0	0	390
9	0.1117	1171688.29	218	117	55	0	0	0	0	0	390
10	0.1121	1174498.65	218	117	55	0	0	0	0	0	390
11	0.1142	1180434.95	216	115	59	0	0	0	0	0	390
12	0.1167	1183094.61	216	109	65	0	0	0	0	0	390
13	0.1168	1137346.23	216	109	65	0	0	0	0	0	390
14	0.1217	1178674.70	214	111	65	0	0	0	0	0	390
15	0.1267	1194282.24	208	114	68	0	0	0	0	0	390
16	0.1685	1243069.84	202	114	49	0	0	25	0	0	390
17	0.2077	1215594.98	202	114	24	0	0	50	0	0	390
18	0.2921	1040064.96	202	114	24	0	0	50	0	0	390
19	0.3549	910430.01	202	114	24	0	0	50	0	0	390
20	0.3970	828796.53	202	114	24	0	0	50	0	0	390
21	0.4200	788401.09	202	114	24	0	0	50	0	0	390

#### 4.2.2 Displacement Coefficient Method of the Six-story Building

From table 3.2, the target displacement of the FEMA 440 and ASCE/SEI 41-13 equal 0.127 m and 0.12 m, respectively. We choose the maximum value between both values to compare with performance levels that get from the SAP2000 software as shown in table 4.2. The 0.127 m of the target displacement meets in step 7th of the 0.1419 m displacements in table 4.2. Therefore, the



performance level of the building meets in between Immediate Occupancy (IO) to Life Safety (LS) levels.

**Table 4.2** Pushover steps of the six-story building

Step	Displacement (m)	Base-Shear (Kgf)	A to B	B to IO	IO to LS	LS to CP	CP to C	C to D	D to E	>E	Total
0	0	0.000	780	0	0	0	0	0	0	0	780
1	0.019	195538.84	780	0	0	0	0	0	0	0	780
2	0.0265	273106.34	776	4	0	0	0	0	0	0	780
3	0.0530	476687.22	656	124	0	0	0	0	0	0	780
4	0.0766	629265.85	617	163	0	0	0	0	0	0	780
5	0.0964	737180.79	595	185	0	0	0	0	0	0	780
6	0.1177	827406.63	561	219	0	0	0	0	0	0	780
7	0.1419	927677.91	550	203	27	0	0	0	0	0	780
8	0.1633	1010938.92	537	192	51	0	0	0	0	0	780
9	0.1899	1081562.23	516	183	81	0	0	0	0	0	780
10	0.1900	1081639.10	516	183	81	0	0	0	0	0	780

#### 4.2.3 Displacement Coefficient Method of the Nine-story Building

From table 3.3, the target displacement of the FEMA 440 and ASCE/SEI 41-13 equal 0.234 m and 0.234 m, respectively. We choose the maximum value between both values to compare with performance levels that get from the SAP2000 software as shown in table 4.3. The 0.234 m of the target displacement

meets in step 4<sup>th</sup> of the 0.3013 m displacements in table 4.3. Therefore, the performance level of the building meets in between Immediate Occupancy (IO) to Life Safety (LS) levels.

**Table 4.3** Pushover steps of the nine-story building

Step	Displacement (m)	Base-Shear (Kgf)	A to B	B to IO	IO to LS	LS to CP	CP to C	C to D	D to E	> E	Total
0	1.3E-5	0	1170	0	0	0	0	0	0	0	1170
1	0.030	270796.96	1166	4	0	0	0	0	0	0	1170
2	0.116	731388.17	888	282	0	0	0	0	0	0	1170
3	0.216	1177959.4	843	312	15	0	0	0	0	0	1170
4	0.301	1485733.5	797	173	200	0	0	0	0	0	1170
5	0.399	1818421.1	781	130	258	1	0	0	0	0	1170
6	0.399	1820853.1	779	132	258	1	0	0	0	0	1170
7	0.399	1816453.1	779	132	258	0	0	1	0	0	1170
8	0.399	1818225.4	779	132	258	0	0	1	0	0	1170
9	0.492	2122098.5	731	168	259	0	0	12	0	0	1170
10	0.573	2299290.4	686	157	234	0	0	93	0	0	1170
11	0.622	2367856.5	663	150	245	0	0	112	0	0	1170
12	0.672	2416516.5	650	150	248	0	0	122	0	0	1170
13	0.716	2468845.0	633	155	242	0	0	140	0	0	1170
14	0.721	2472397.1	630	158	237	0	0	145	0	0	1170

**Table 4.3** Pushover steps of the nine-story building (Continued)

Step	Displacement (m)	Base-Shear (Kgf)	A to B	B to IO	IO to LS	LS to CP	CP to C	C to D	D to E	> E	Total
15	0.724	2473416.7	627	160	236	0	0	147	0	0	1170
16	0.764	2448202.5	616	157	238	0	0	159	0	0	1170
17	0.798	2292144.3	614	149	235	0	0	172	0	0	1170
18	0.807	2009362.5	614	149	236	0	0	171	0	0	1170
19	0.809	1957066.2	614	149	236	2	0	169	0	0	1170
20	0.811	1892479.8	614	149	236	10	2	159	0	0	1170
21	0.811	1870173.4	614	149	236	18	2	151	0	0	1170
22	0.8111	1831281.9	614	149	236	33	2	136	0	0	1170
23	0.8125	1833695.6	614	149	236	33	2	136	0	0	1170
24	0.8131	1833782.2	614	149	236	33	2	136	0	0	1170
25	0.8120	1767676.9	614	149	236	45	2	124	0	0	1170

#### 4.2.4 Capacity Spectrum Method of the three-story building

To depend on figure 3.9, it shows that the magnitude of base shear and tip displacement at the performance point are 6605789 N and 0.04 m, respectively. To determine the building performance levels, it can use the deformation limits to compare with the roof drift ratio at the performance point as follows: Roof drift ratio at the performance point is  $0.04/10.5 = 0.0038$ . Base on table 3.4, the performance point that found to check the structural performance levels of the IO, LS or CP depended on deformation limits specified in ATC-40 were 0.01, 0.02 and  $0.33(V_b/W)$ , respectively.

Therefore, the performance level of the building meets the Immediate Occupancy (IO) level because of  $0.0038 < 0.01$ .

#### **4.2.5 Capacity Spectrum Method of the six-story building**

To depend on figure 3.10, it shows that the magnitude of base shear and tip displacement at the performance point are 6984303 N and 0.092 m, respectively. To determine the building performance levels, it can use the deformation limits to compare with the roof drift ratio at the performance point as follows: Roof drift ratio at the performance point is  $0.092/21 = 0.0044$ . Base on table 3.4, the performance point that found to check the structural performance levels of the IO, LS or CP depended on deformation limits specified in ATC-40 were 0.01, 0.02 and  $0.33(V_b/W)$ , respectively. Therefore, the performance level of the building meets the Immediate Occupancy (IO) level because of  $0.0044 < 0.01$ .

#### **4.2.6 Capacity Spectrum Method of the nine-story building**

To depend on figure 3.11, it shows that the magnitude of base shear and tip displacement at the performance point are 8211036 N and 0.14 m, respectively. To determine the building performance levels, it can use the deformation limits to compare with the roof drift ratio at the performance point as follows: Roof drift ratio at the performance point is  $0.14/31.5 = 0.0044$ . Base on table 3.4, the performance point that found to check the structural performance levels of the IO, LS or CP depended on deformation limits specified in ATC-40 were 0.01, 0.02 and  $0.33(V_b/W)$ , respectively. Therefore, the performance level of the building meets the Immediate Occupancy (IO) level because of  $0.0044 < 0.01$ .

#### 4.2.7 Inter-story Drift Method of the three-story building

According to table 4.4, the inter-story drift ratio of the existing building equal 2.0% inter-story drift for first floor, 1.6% inter-story drift associated with second floor, and 0.8% inter-story drift for third floor. Depending on table 4.7, ASCE/SEI 41-06 suggests typical limits of 1% inter-story drift for immediate occupancy (IO) performance level, 2% inter-story drift associated with Life Safety (LS) performance level, and 4% inter-story drift for Collapse Prevention (CP) performance level. Therefore, the performance level of the existing building was classified in each story level such as the first story, the second story, and the third story met Life Safety (LS) level, Life Safety (LS) level, and Immediate Occupancy (IO) level, respectively.

**Table 4.4** Inter-story drift ratio (IDR)

Floor	Deflection (cm)	Drift (cm)	Inter-story Drift ratio (%)	Performance Level
3	9.268	15.446	0.8	IO
2	7.657	12.761	1.6	LS
1	4.297	7.161	2.0	LS

#### 4.2.8 Inter-story Drift Method of the six-story building

According to table 4.5, the inter-story drift ratio of the existing building equal 1.5% inter-story drift for first floor, 1.8% inter-story drift associated with second floor, 1.5% inter-story drift for third floor, 1.1% inter-story drift for fourth floor, 0.6% inter-story drift associated with fifth floor, and 0.3% inter-story drift for sixth floor. Depending on table 4.7, ASCE/SEI 41-06 suggests typical limits of 1% inter-story drift for immediate occupancy (IO) performance level, 2% inter-story drift associated

with Life Safety (LS) performance level, and 4% inter-story drift for Collapse Prevention (CP) performance level.

**Table 4.5** Inter-story drift ratio (IDR)

Floor	Deflection (cm)	Drift (cm)	Inter-story Drift ratio (%)	Performance Level
6	14.2	23.67	0.3	IO
5	13.55	22.58	0.6	IO
4	12.21	20.35	1.1	LS
3	9.99	16.65	1.5	LS
2	6.93	11.55	1.8	LS
1	3.24	5.4	1.5	LS

Therefore, the performance level of the existing building was classified in each story level such as the first story, the second story, and the third story, the fourth story, the fifth story, and the sixth story met Life Safety (LS) level, Life Safety (LS) level, Life Safety (LS) level, Life Safety (LS) level, Immediate Occupancy (IO) level, and Immediate Occupancy (IO) level, respectively.

#### 4.2.9 Inter-story Drift Method of the nine-story building

According to table 4.6, the inter-story drift ratio of the existing building equal 1.4% inter-story drift for first floor, 2.1% inter-story drift associated with second floor, 2.3% inter-story drift for third floor, 2.2% inter-story drift for fourth floor, 2.0% inter-story drift associated with fifth floor, 1.7% inter-story drift for sixth floor, 1.3% inter-story drift for seventh floor, 0.9% inter-story drift for eighth floor, and 0.5% inter-story drift for ninth floor. Depending on table 4.7, ASCE/SEI 41-06 suggests

typical limits of 1% inter-story drift for immediate occupancy (IO) performance level, 2% inter-story drift associated with Life Safety (LS) performance level, and 4% inter-story drift for Collapse Prevention (CP) performance level. Therefore, the performance level of the nine-story building was classified in each story level, as shown in table 4.6.

**Table 4.6** Inter-story drift ratio (IDR)

Floor	Deflection (cm)	Drift (cm)	Inter-story Drift ratio (%)	Performance Level
9	30.04	50.07	0.5	IO
8	28.99	48.32	0.9	IO
7	27.16	45.267	1.3	LS
6	24.46	40.767	1.7	LS
5	20.96	34.933	2.0	LS
4	16.80	28.000	2.2	CP
3	12.15	20.250	2.3	CP
2	7.33	12.2167	2.1	CP
1	2.89	4.8167	1.4	LS

**Table 4.7** Structural Performance Levels and Damage<sub>1,2,3</sub>-Vertical Elements

		Structural Performance Levels		
Elements	Type	Collapse Prevention (CP)	Life Safety (LS)	Immediate Occupancy (IO)
Concrete Frames	Drift	4% transient or permanent.	2% transient; 1% permanent.	1% transient; Negligible-permanent.

<sup>1</sup>Damage states indicated in this table are provided to allow an understanding of the severity of damage that may be sustained by various structural elements where present in structures meeting the definitions of the Structural Performance Levels. These damage states are not intended for use in post-earthquake evaluation of damage or for judging the safety of, or required level of repair to, a structure following an earthquake.

<sup>2</sup>Drift values, differential settlements, crack widths, and similar quantities indicated in these tables are not intended to be used as acceptance criteria for evaluating the acceptability of a rehabilitation design in accordance with the analysis procedures provided in this standard; rather, they are indicative of the range of drift that typical structures containing the indicated structural elements may undergo when responding within the various Structural Performance Levels. Drift control of a rehabilitated structure may often be governed by the requirements to protect nonstructural components. Acceptable levels of foundation settlement or movement are highly dependent on the construction of the superstructure. The values indicated are intended to be qualitative descriptions of the approximate behavior of structures meeting the indicated levels.

<sup>3</sup>For limiting damage to frame elements of infilled frames, refer to the rows for concrete or steel frames.

## **4.2.10 Member-Level Performance Method of the three-story building**

### **4.2.10.1 Performance Level of the Column**

From table 3.5, we use the conditions to determine the acceptance criteria of the column at ASCE/SEI 41-13, table 10-8. Values between those listed in the table should be determined by linear interpolation. The acceptance criteria on the first floor have Immediate Occupancy (IO), Life Safety (LS), and Collapse Prevention (CP) that equal 0.004, 0.018, and 0.0231, respectively. The acceptance criteria on the second floor have 0.0041 for immediate occupancy (IO), 0.021 for Life Safety (LS), and 0.0272 for Collapse Prevention (CP). The acceptance criteria on the third floor have Immediate Occupancy (IO), Life Safety (LS), and Collapse Prevention (CP) that equal 0.005, 0.0275, and 0.0360, respectively. Plastic



hinge rotation in table 4.8 gets from SAP2000 that equal 0.0093 for the first floor, 0.0015 for the second floor, and 0.0000 for the third floor. We use the value from the

**Table 4.8** Numerical acceptance criteria for plastic hinge rotation of the columns of the three-story building

Level	Conditions			Acceptance Criteria Plastic Rotations Angle (radians) Performance Level			Plastic Hinge Rotat- ion (radians)	Perform- ance Level
	$\frac{P}{A_g f_c}$	$\rho = \frac{A_v}{b_w s}$	$\frac{V}{b_w d \sqrt{f_c}}$	IO	LS	CP		
3	0.075	0.005	0.137	0.005	0.027	0.036	0.0000	IO
2	0.149	0.005	0.255	0.004	0.021	0.027	0.0015	IO
1	0.221	0.005	0.442	0.004	0.018	0.023	0.0093	LS

acceptance criteria compare with plastic hinge rotation to determine the performance level of the column. The columns of the three stories building were classified in each story level such as the first story, the second story, and the third story met Life Safety (LS) level, Immediate Occupancy (IO) level, and Immediate Occupancy (IO) level, respectively. The 3<sup>rd</sup> step of the pushover analysis of the column with plastic hinge rotation was shown in figure 4.1.

#### 4.2.10.2 Performance Level of the Beam

From table 3.6, we use the conditions to determine the acceptance criteria of the beam at ASCE/SEI 41-13, table 10-7. Values between those listed in the table should be determined by linear interpolation. The acceptance criteria on the first floor have Immediate Occupancy (IO), Life Safety (LS), and Collapse

Prevention (CP) that equal 0.01, 0.025, and 0.05, respectively. The acceptance criteria on the second floor have 0.01 for immediate occupancy (IO), 0.025 for Life Safety (LS), and 0.05 for Collapse Prevention (CP). The acceptance criteria on the third floor have Immediate Occupancy (IO), Life Safety (LS), and Collapse Prevention (CP) that equal 0.01, 0.025, and 0.05, respectively. Plastic hinge rotation in table 4.9 gets from SAP2000 that equal 0.0101 for the first floor, 0.0047 for the second floor, and 0.0006 for the third floor.

**Table 4.9** Numerical acceptance criteria for plastic hinge rotation of the beams of the three-story building

Level	Conditions			Acceptance Criteria Plastic Rotations Angle (radians) Performance Level			Plastic Hinge Rotat- ion (radians)	Perfor- Mance Level
	$\frac{\rho-\rho'}{\rho_{bal}}$	TR <sup>1</sup>	$\frac{V}{b_w d \sqrt{f_c}}$	IO	LS	CP		
3	0.00	C	0.111	0.01	0.025	0.05	0.0006	IO
2	-0.28	C	0.115	0.01	0.025	0.05	0.0047	IO
1	-0.42	C	0.115	0.01	0.025	0.05	0.0101	LS

<sup>1</sup>TR (Transverse Reinforcement)

We use the value from the acceptance criteria compare with plastic hinge rotation to determine the performance level of the beam. The beams of the three stories building were classified in each story level such as the first story, the second story, and the third story met Life Safety (LS) level, Immediate Occupancy (IO) level, and Immediate Occupancy (IO) level, respectively. The 3rd step of the

pushover analysis of the beam with plastic hinge rotation was shown in figure 4.1.

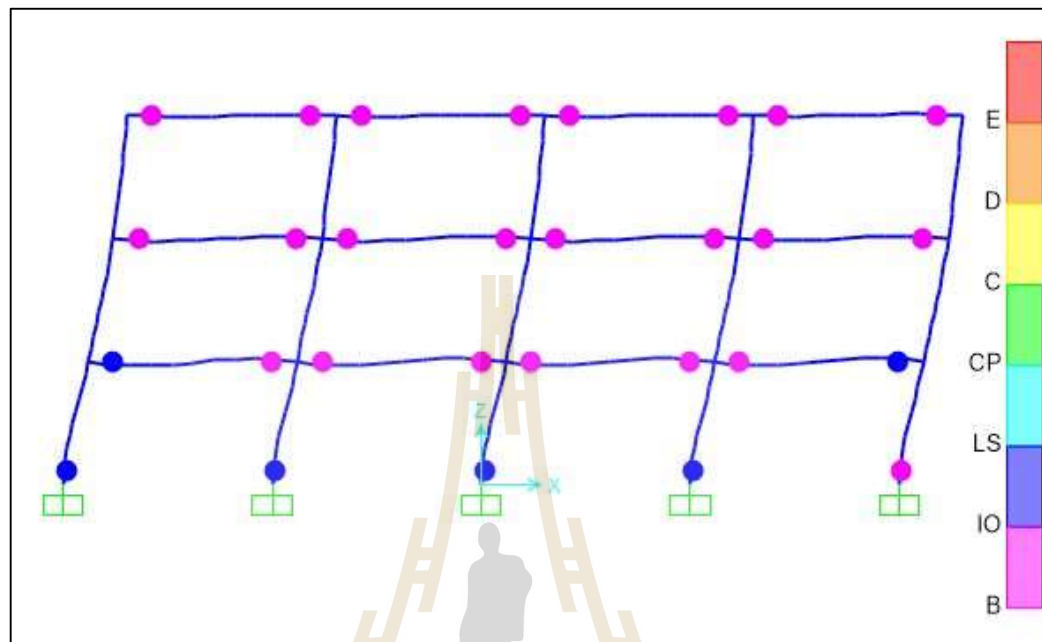


**Figure 4.1** Performance levels of the three-story building

#### 4.2.11 Member-Level Performance Method of the six-story building

##### 4.2.11.1 Performance Level of the column

From table 3.7, we use the conditions to determine the acceptance criteria of the column at ASCE/SEI 41-13, table 10-8. Values between those listed in the table should be determined by linear interpolation. The acceptance criteria of the six-story building were shown in table 4.10. Plastic hinge rotation in table 4.10 gets from SAP2000 that equal 0.006 for the first floor, and 0.0000 for the second to sixth floor. We use the value from the acceptance criteria compare with plastic hinge rotation to determine the performance level of the column. The performance evaluation of the columns of the six-stories building was classified the

performance level in table 4.10. The 7th step of the pushover analysis of the column with plastic hinge rotation was shown in figure 4.2.

**Table 4.10** Numerical acceptance criteria for plastic hinge rotation of the columns of the six-story building

Level	Conditions			Acceptance Criteria Plastic Rotations Angle (radians) Performance Level			Plastic Hinge Rotation (radians)	Perform- Ance Level
	$\frac{P}{A_g f_c}$	$\rho = \frac{A_v}{b_w s}$	$\frac{V}{b_w d \sqrt{f_c}}$	IO	LS	CP		
6	0.048	0.00285	0.090	0.0047	0.041	0.054	0.000	IO
5	0.096	0.00285	0.119	0.0044	0.036	0.049	0.000	IO
4	0.146	0.00285	0.150	0.0041	0.032	0.043	0.000	IO
3	0.197	0.00285	0.181	0.0038	0.028	0.038	0.000	IO
2	0.249	0.00285	0.209	0.0035	0.024	0.032	0.000	IO
1	0.287	0.00285	0.259	0.0033	0.021	0.027	0.006	LS

#### 4.2.11.2 Performance Level of the Beam

From table 3.8, we use the conditions to determine the acceptance criteria of the beam at ASCE/SEI 41-13, table 10-7. Values between those listed in the table should be determined by linear interpolation. The acceptance criteria on the first floor to sixth floor have Immediate Occupancy (IO), Life Safety (LS), and Collapse Prevention (CP) that equal 0.01, 0.025, and 0.05, respectively. Plastic hinge rotation in table 4.11 gets from SAP2000 that equal 0.0109 for the first floor, 0.0091

for the second floor, 0.0066 for the third floor, 0.0036 for the fourth floor, 0.0008 for the fifth floor, and 0.0000 for the sixth floor. We use the value from the acceptance criteria compare with plastic hinge rotation to determine the performance level of the beam. The beams of the six stories building were classified in each story of the performance level, as shown in table 4.11. The 7th step of the pushover analysis of the beam with plastic hinge rotation was shown in figure 4.2.

**Table 4.11** Numerical acceptance criteria for plastic hinge rotation of the beams of the six-story building

Level	Conditions			Acceptance Criteria			Plastic Hinge Rotation (radians)	Performance Level
				Plastic Rotations Angle (radians) Performance Level				
	$\frac{\rho-\rho'}{\rho_{bal}}$	TR <sup>1</sup>	$\frac{V}{b_w d \sqrt{f'_c}}$	IO	LS	CP		
6	-0.17	C	0.00152	0.01	0.025	0.05	0.0000	IO
5	-0.39	C	0.00209	0.01	0.025	0.05	0.0008	IO
4	-0.57	C	0.00209	0.01	0.025	0.05	0.0036	IO
3	-0.65	C	0.00209	0.01	0.025	0.05	0.0066	IO
2	-0.71	C	0.00209	0.01	0.025	0.05	0.0091	IO
1	-0.79	C	0.00207	0.01	0.025	0.05	0.0109	LS

<sup>1</sup>TR (Transverse Reinforcement)

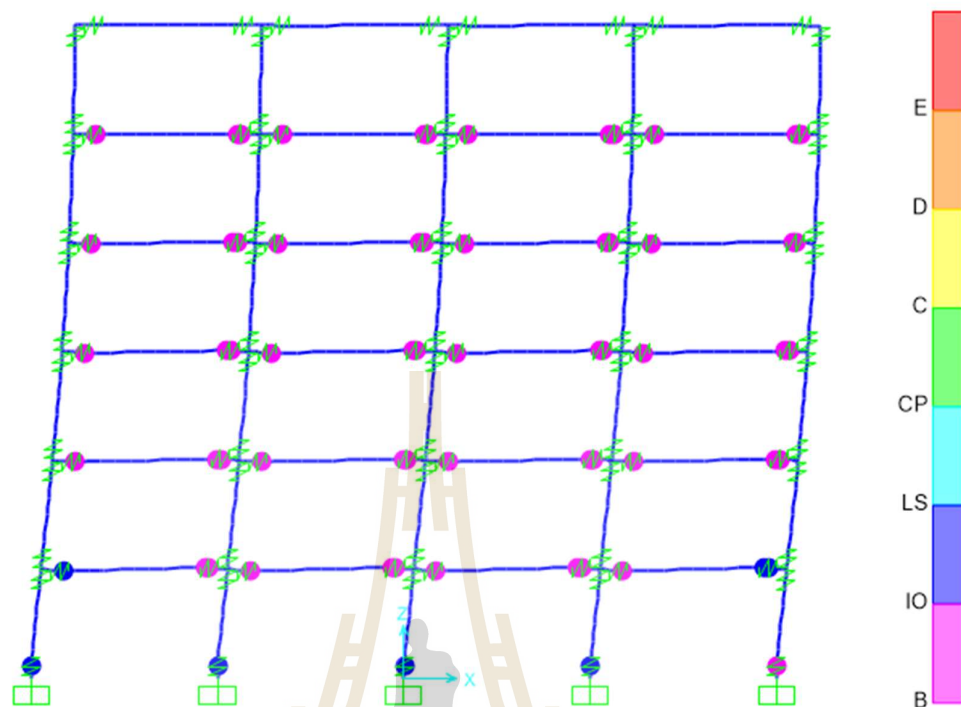


Figure 4.2 Performance levels of the six-story building

#### 4.2.12 Member-Level Performance Method of the nine-story building

##### 4.2.12.1 Performance Level of the Column

From table 3.9, we use the conditions to determine the acceptance criteria of the column at ASCE/SEI 41-13, table 10-8. Values between those listed in the table should be determined by linear interpolation. The acceptance criteria of the nine-story building were shown in table 4.12. Plastic hinge rotation in table 4.12 gets from SAP2000 that equal 0.0051 for the first floor, and 0.0000 for the second to nine floor. We use the value from the acceptance criteria compare with plastic hinge rotation to determine the performance level of the column. The performance evaluation of the columns of the six-stories building was classified the

performance level in table 4.12. The 4th step of the pushover analysis of the column with plastic hinge rotation was shown in figure 4.3.

**Table 4.12** Numerical acceptance criteria for plastic hinge rotation of the columns of the nine-story building

Level	Conditions			Acceptance Criteria Plastic Rotations Angle (radians) Performance Level			Plastic Hinge Rotation (radians)	Perform- ance Level
	$\frac{P}{A_g f_c}$	$\frac{A_v}{b_w s}$	$\frac{V}{b_w d \sqrt{f_c}}$	IO	LS	CP		
9	0.078	0.0024	0.08899	0.0045	0.039	0.051	0.000	IO
8	0.154	0.0024	0.13311	0.0041	0.032	0.043	0.000	IO
7	0.231	0.0024	0.18700	0.0036	0.026	0.034	0.000	IO
6	0.309	0.0024	0.23231	0.0031	0.019	0.025	0.000	IO
5	0.386	0.0024	0.26878	0.0027	0.013	0.017	0.000	IO
4	0.464	0.0024	0.31111	0.0022	0.006	0.008	0.000	IO
3	0.542	0.0024	0.32016	0.0026	0.007	0.008	0.000	IO
2	0.622	0.0024	0.41987	0.0026	0.007	0.008	0.000	IO
1	0.699	0.0024	0.24549	0.0026	0.007	0.008	0.0041	LS

#### 4.2.12.2 Performance Level of the Beam

From table 3.10, we use the conditions to determine the acceptance criteria of the beam at ASCE/SEI 41-13, table 10-7. Values between those listed in the table should be determined by linear interpolation. The acceptance criteria on the first floor to sixth floor have Immediate Occupancy (IO), Life Safety (LS), and

Collapse Prevention (CP) that equal 0.01, 0.025, and 0.05, respectively. Plastic hinge rotations get from SAP2000, as shown in table 4.13. We use the value from the acceptance criteria compare with plastic hinge rotation to determine the performance level of the beam. The beams of the six stories building were classified in each story of the performance level, as shown in table 4.13. The 4<sup>th</sup> step of the pushover analysis of the beam with plastic hinge rotation was shown in figure 4.3.

**Table 4.13** Numerical acceptance criteria for plastic hinge rotation of the beams of the nine-story building

Level	Conditions			Acceptance Criteria Plastic Rotations Angle (radians) Performance Level			Plastic Hinge Rotation (radians)	Performance Level
	$\frac{\rho-\rho'}{\rho_{bal}}$	TR <sup>1</sup>	$\frac{V}{b_w d \sqrt{f'_c}}$	IO	LS	CP		
9	-0.25	C	0.16899	0.01	0.025	0.05	0.00064	IO
8	-0.48	C	0.18239	0.01	0.025	0.05	0.0029	IO
7	-0.59	C	0.18133	0.01	0.025	0.05	0.0056	IO
6	-0.69	C	0.18082	0.01	0.025	0.05	0.0084	IO
5	-0.70	C	0.17957	0.01	0.025	0.05	0.0109	LS
4	-0.72	C	0.17790	0.01	0.025	0.05	0.0129	LS
3	-0.74	C	0.17589	0.01	0.025	0.05	0.0141	LS
2	-0.76	C	0.17361	0.01	0.025	0.05	0.0139	LS
1	-0.80	C	0.17042	0.01	0.025	0.05	0.0117	LS

<sup>1</sup>TR (Transverse Reinforcement)



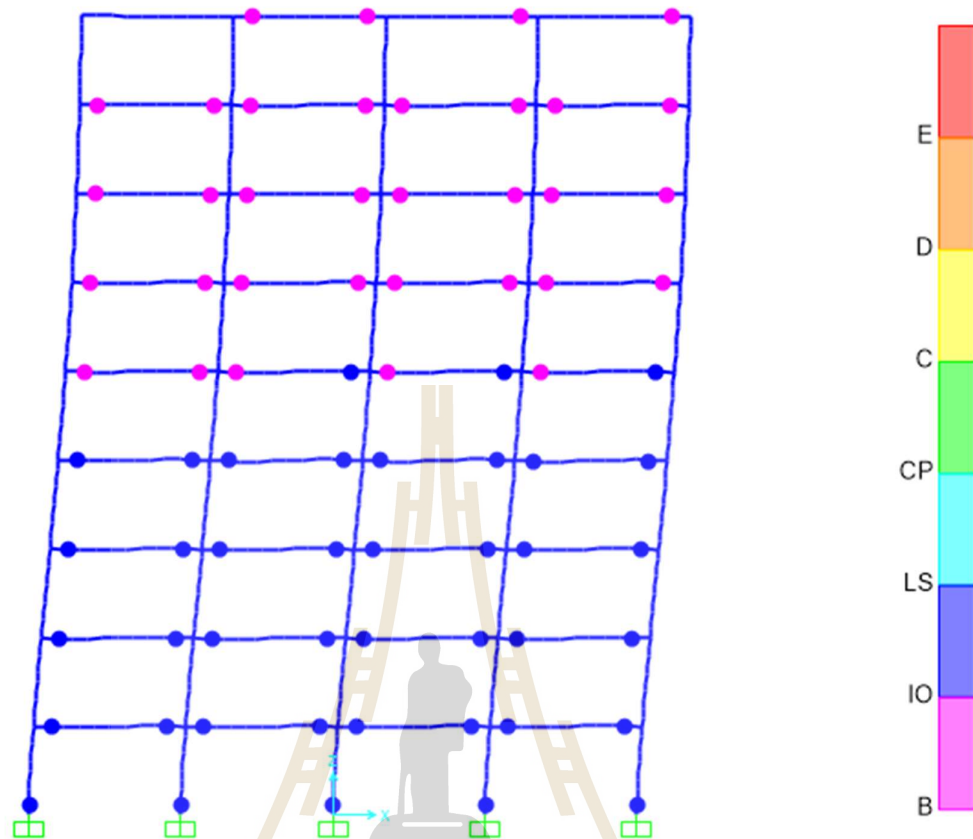


Figure 4.3 Performance levels of the nine-story building

### 4.3 Performance Evaluation of Strengthening Building

#### 4.3.1 Displacement Coefficient Method of the three-story building

From table 3.12, the target displacement of the FEMA 440 and ASCE/SEI 41-13 equal 0.020 m and 0.0263 m, respectively. We choose the maximum value between both values to compare with performance levels that get from the SAP2000 software as shown in table 4.10. The 0.0263 m of the target displacement meets in step 2<sup>nd</sup> of the 0.0266 m displacements in table 4.14. Therefore, the performance level of the building meets the Immediate Occupancy (IO) level.

**Table 4.14** Pushover steps of the three-story building

Step	Displacement (m)	Base Shear (Kgf)	A to B	B to IO	IO to LS	LS to CP	CP to C	C to D	D to E	> E	Total
0	7.0E-06	0	558	0	0	0	0	0	0	0	558
1	0.01355	5240.9	556	2	0	0	0	0	0	0	558
2	0.0266	9600.6	495	63	0	0	0	0	0	0	558
3	0.03438	11104.0	462	90	0	0	0	6	0	0	558
4	0.04489	12222.1	446	102	0	0	0	10	0	0	558
5	0.04489	12222.3	446	102	0	0	0	10	0	0	558
6	0.05221	12795.3	420	126	2	0	0	10	0	0	558
7	0.06750	13433.0	408	111	29	0	0	10	0	0	558
8	0.07056	13498.4	406	104	38	0	0	10	0	0	558
9	0.07875	13489.8	406	91	51	0	0	10	0	0	558
10	0.07895	13499.6	406	91	51	0	0	10	0	0	558
11	0.07932	13511.2	406	90	52	0	0	10	0	0	558
12	0.07990	13536.2	406	90	52	0	0	10	0	0	558
13	0.08367	13628.0	402	90	56	0	0	10	0	0	558
14	0.08845	13643.9	402	86	60	0	0	10	0	0	558
15	0.08966	13682.9	399	89	60	0	0	10	0	0	558
16	0.09062	13703.4	396	91	61	0	0	10	0	0	558
17	0.09424	13686.3	396	91	61	0	0	10	0	0	558
18	0.09523	13700.5	394	93	61	0	0	10	0	0	558
19	0.09695	13713.3	393	92	63	0	0	10	0	0	558
20	0.09959	13685.3	392	93	63	0	0	10	0	0	558

**Table 4.14** Pushover steps of the three-story building (Continued)

Step	Displacement (m)	Base Shear (Kgf)	A to B	B to IO	IO to LS	LS to CP	CP to C	C to D	D to E	> E	Total
21	0.09963	13686.5	391	94	63	0	0	10	0	0	558
22	0.10041	13698.5	390	95	63	0	0	10	0	0	558
23	0.10280	13700.0	386	98	64	0	0	10	0	0	558
24	0.10480	13690.1	386	98	64	0	0	10	0	0	558
25	0.10539	13701.5	386	98	64	0	0	10	0	0	558
26	0.10572	13705.1	386	98	64	0	0	10	0	0	558
27	0.10573	13670.3	386	98	64	0	0	10	0	0	558
28	0.10573	13668.1	386	98	64	0	0	10	0	0	558
29	0.10467	13687.2	386	98	62	0	0	12	0	0	558
30	0.10749	13692.0	386	98	62	0	0	12	0	0	558
31	0.11401	13608.7	386	98	61	0	0	13	0	0	558
32	0.11847	13631.6	385	97	62	0	0	14	0	0	558
33	0.12277	13564.0	384	96	64	0	0	14	0	0	558
34	0.14291	13385.3	380	96	37	0	0	45	0	0	558
35	0.20574	11139.3	380	96	10	4	0	62	0	6	558
36	0.26859	10070.8	376	98	12	0	0	66	0	6	558
37	0.35192	8509.50	374	96	14	0	0	68	0	6	558
38	0.39436	7753.20	374	96	14	0	0	68	0	6	558
39	0.42005	7278.13	374	96	14	0	0	66	2	6	558

### 4.3.2 Displacement Coefficient Method of the six-story building

From table 3.13, the target displacement of the FEMA 440 and ASCE/SEI 41-13 equal 0.068673 m and 0.072714 m, respectively. We choose the maximum value between both values to compare with performance levels that get from the SAP2000 software as shown in table 4.15. The 0.072714 m of the target displacement meets in step 7<sup>th</sup> of the 0.08251 m displacements in table 4.15. Therefore, the performance level of the building meets the Immediate Occupancy (IO) level.

**Table 4.15** Pushover steps of the six-story building

Step	Displacement (m)	Base Shear (Kgf)	A to B	B to IO	IO to LS	LS to CP	CP to C	C to D	D to E	>E	Total
0	0	0	1068	0	0	0	0	0	0	0	1068
1	0.0125	2383.75	1068	0	0	0	0	0	0	0	1068
2	0.025	4767.50	1066	2	0	0	0	0	0	0	1068
3	0.02642	5037.38	1064	4	0	0	0	0	0	0	1068
4	0.03899	7259.03	974	94	0	0	0	0	0	0	1068
5	0.05414	9180.56	924	144	0	0	0	0	0	0	1068
6	0.06715	10330.1	889	171	0	0	0	8	0	0	1068
7	0.08251	11326.5	863	193	0	0	0	12	0	0	1068
8	0.08237	11175.9	863	191	2	0	0	12	0	0	1068

### 4.3.3 Displacement Coefficient Method of the nine-story building

From table 3.14, the target displacement of the FEMA 440 and ASCE/SEI 41-13 equal 0.155554 m and 0.163251 m, respectively. We choose the maximum value between both values to compare with performance levels that get from the SAP2000 software as shown in table 4.16. The 0.163251 m of the target displacement meets in step 3<sup>rd</sup> of the 0.176885 m displacements in table 4.16. Therefore, the performance level of the building meets the Immediate Occupancy (IO) level.

**Table 4. 16** Pushover steps of the nine-story building

Step	Displacement (m)	Base Shear (Kgf)	A to B	B to IO	IO to LS	LS to CP	CP to C	C to D	D to E	> E	Total
0	8.7E-05	0	1602	0	0	0	0	0	0	0	1602
1	0.030175	414161.24	1599	3	0	0	0	0	0	0	1602
2	0.085106	984365.31	1312	290	0	0	0	0	0	0	1602
3	0.176885	1579450.1	1201	363	31	0	0	7	0	0	1602
4	0.246495	1882413.5	1143	293	141	0	0	25	0	0	1602
5	0.349343	2220528.1	1092	190	288	0	0	32	0	0	1602
6	0.362324	2259457.2	1089	189	291	1	0	32	0	0	1602

### 4.3.4 Capacity Spectrum Method of the three-story Building

To depend on figure 3.20, it shows that the magnitude of base shear and tip displacement at the performance point are 7218051 N and 0.019 m, respectively. To determine the building performance levels, it can use the deformation limits to

compare with the roof drift ratio at the performance point as follows: Roof drift ratio at the performance point is  $0.019/10.5 = 0.0018$ . Base on table 3.4, the performance point that found to check the structural performance levels of the IO, LS or CP depended on deformation limits specified in ATC-40 were 0.01, 0.02 and  $0.33(V_b/W)$ , respectively. Therefore, the performance level of the building meets the Immediate Occupancy (IO) level because of  $0.0018 < 0.01$ .

#### **4.3.5 Capacity Spectrum Method of the six-story Building**

To depend on figure 3.21, it shows that the magnitude of base shear and tip displacement at the performance point are 9532797 N and 0.066 m, respectively. To determine the building performance levels, it can use the deformation limits to compare with the roof drift ratio at the performance point as follows: Roof drift ratio at the performance point is  $0.066/21 = 0.00314$ . Base on table 3.4, the performance point that found to check the structural performance levels of the IO, LS or CP depended on deformation limits specified in ATC-40 were 0.01, 0.02 and  $0.33(V_b/W)$ , respectively. Therefore, the performance level of the building meets the Immediate Occupancy (IO) level because of  $0.00314 < 0.01$ .

#### **4.3.6 Capacity Spectrum Method of the nine-story Building**

To depend on figure 3.22, it shows that the magnitude of base shear and tip displacement at the performance point are 11151768 N and 0.109 m, respectively. To determine the building performance levels, it can use the deformation limits to compare with the roof drift ratio at the performance point as follows: Roof drift ratio at the performance point is  $0.109/31.5 = 0.00346$ . Base on table 3.4, the performance point that found to check the structural performance levels of the IO, LS or CP depended on deformation limits specified in ATC-40 were 0.01, 0.02 and  $0.33(V_b/W)$ ,

respectively. Therefore, the performance level of the building meets the Immediate Occupancy (IO) level because of  $0.00346 < 0.01$ .

#### 4.3.7 Inter-story Drift Method of the three-story building

According to table 4.17, the inter-story drift ratio of the existing building equal 0.6% inter-story drift for first floor, 0.5% inter-story drift associated with second floor, and 0.2% inter-story drift for third floor. Depending on table 4.7, ASCE/SEI 41-06 suggests typical limits of 1% inter-story drift for immediate occupancy (IO) performance level, 2% inter-story drift associated with Life Safety (LS) performance level, and 4% inter-story drift for Collapse Prevention (CP) performance level. Therefore, the performance level of the existing building was classified in each story level such as the first story, the second story, and the third story met Immediate Occupancy (IO) level, Immediate Occupancy (IO) level, and Immediate Occupancy (IO) level, respectively.

**Table 4.17** Inter-story drift ratio (IDR)

Floor	Deflection (cm)	Drift (cm)	Inter-story Drift ratio (%)	Performance Level
3	2.67	4.45	0.2	IO
2	2.15	3.58	0.5	IO
1	1.16	1.93	0.6	IO

#### 4.3.8 Inter-story Drift Method of the six-story building

According to table 4.18, the inter-story drift ratio of the six-story building equals 0.876% inter-story drift for first floor, 0.933% inter-story drift

associated with second floor, 0.986% inter-story drift for third floor, 0.548% inter-story drift for fourth floor, 0.367% inter-story drift associated with fifth floor, and 0.219% inter-story drift for sixth floor. Depending on table 4.7, ASCE/SEI 41-06 suggests typical limits of 1% inter-story drift for immediate occupancy (IO) performance level, 2% inter-story drift associated with Life Safety (LS) performance level, and 4% inter-story drift for Collapse Prevention (CP) performance level. Therefore, the performance level of the six-story building was classified in each story level such as the first story, the second story, and the third story, the fourth story, the fifth story, and the sixth story met Immediate Occupancy (IO) level, Immediate Occupancy (IO) level, Immediate Occupancy (IO) level, Life Safety (LS) level, Immediate Occupancy (IO) level, and Immediate Occupancy (IO) level, respectively.

**Table 4.18** Inter-story drift ratio (IDR)

Floor	Deflection (cm)	Drift (cm)	Inter-story Drift ratio (%)	Performance Level
6	8.25	13.75	0.219	IO
5	7.79	12.98	0.367	IO
4	7.02	11.70	0.548	IO
3	5.87	9.78	0.986	IO
2	3.80	6.33	0.933	IO
1	1.84	3.07	0.876	IO

#### 4.3.9 Inter-story Drift Method of the nine-story building

According to table 4.19, the inter-story drift ratio of the existing building equal 0.9286% inter-story drift for first floor, 0.9571% inter-story drift



associated with second floor, 0.9752% inter-story drift for third floor, 0.9971% inter-story drift for fourth floor, 0.9705% inter-story drift associated with fifth floor, 0.9619% inter-story drift for sixth floor, 0.9238% inter-story drift for seventh floor, 0.8952% inter-story drift for eighth floor, and 0.7095% inter-story drift for ninth floor. Depending on table 4.7, ASCE/SEI 41-06 suggests typical limits of 1% inter-story drift for immediate occupancy (IO) performance level, 2% inter-story drift associated with Life Safety (LS) performance level, and 4% inter-story drift for Collapse Prevention (CP) performance level. Therefore, the performance level of the nine-story building was classified in each story level, as shown in table 4.19.

**Table 4.19** Inter-story drift ratio (IDR)

Floor	Deflection (cm)	Drift (cm)	Inter-story Drift ratio (%)	Performance Level
9	17.47	29.1167	0.7095	IO
8	15.98	26.633	0.8952	IO
7	14.1	23.50	0.9238	IO
6	12.16	20.267	0.9619	IO
5	10.14	16.90	0.9705	IO
4	8.102	13.5033	0.9971	IO
3	6.008	10.0133	0.9752	IO
2	3.96	6.60	0.9571	IO
1	1.95	3.25	0.9286	IO

### 4.3.10 Member-Level Performance Method of the three-story building

#### 4.3.10.1 Performance Level of the Column

From table 3.15, we use the conditions to determine the acceptance criteria of the column at ASCE/SEI 41-13, table 10-8. Values between those listed in the table should be determined by linear interpolation. The acceptance criteria on the first floor have Immediate Occupancy (IO), Life Safety (LS), and Collapse Prevention (CP) that equal 0.0037, 0.0159, and 0.0200, respectively. The acceptance criteria on the second floor have 0.0038 for immediate occupancy (IO), 0.0196 for Life Safety (LS), and 0.0252 for Collapse Prevention (CP). The acceptance criteria on the third floor have Immediate Occupancy (IO), Life Safety (LS), and Collapse Prevention (CP) that equal 0.005, 0.0275, and 0.0360, respectively.

**Table 4.20** Numerical acceptance criteria for plastic hinge rotation of the columns of the three-story building

Level	Conditions			Acceptance Criteria Plastic Rotations Angle (radians) Performance Level			Plastic Hinge Rotation (radians)	Perform- ance Level
	$\frac{P}{A_g f'_c}$	$\rho = \frac{A_v}{b_w s}$	$\frac{V}{b_w d \sqrt{f'_c}}$	IO	LS	CP		
3	0.091	0.005	0.065	0.005	0.028	0.036	0.0000	IO
2	0.181	0.005	0.105	0.004	0.02	0.025	0.0000	IO
1	0.271	0.005	0.228	0.004	0.016	0.020	0.0004	IO

Plastic hinge rotation in table 4.20 gets from SAP2000 that equal 0.0004 for the first floor, 0.0000 for the second floor, and 0.0000 for the third floor. We use the value from the acceptance criteria compare with plastic hinge rotation to determine the performance level of the column. The columns of the three stories building were classified in each story level such as the first story, the second story, and the third story met Immediate Occupancy (IO) level, Immediate Occupancy (IO) level, and Immediate Occupancy (IO) level, respectively. The 2nd step of the pushover analysis of the column with plastic hinge rotation was shown in figure 4.4.

#### **4.3.10.2 Performance Level of the Beam**

From table 3.16, we use the conditions to determine the acceptance criteria of the beam at ASCE/SEI 41-13, table 10-7. Values between those listed in the table should be determined by linear interpolation. The acceptance criteria on the first floor have Immediate Occupancy (IO), Life Safety (LS), and Collapse Prevention (CP) that equal 0.01, 0.025, and 0.05, respectively. The acceptance criteria on the second floor have 0.01 for immediate occupancy (IO), 0.025 for Life Safety (LS), and 0.05 for Collapse Prevention (CP). The acceptance criteria on the third floor have Immediate Occupancy (IO), Life Safety (LS), and Collapse Prevention (CP) that equal 0.01, 0.025, and 0.05, respectively. Plastic hinge rotation in table 4.21 gets from SAP2000 that equal 0.0025 for the first floor, 0.0003 for the second floor, and 0.0000 for the third floor. We use the value from the acceptance criteria compare with plastic hinge rotation to determine the performance level of the beam. The beams of the three stories building were classified in each story level such as the first story, the second story, and the third story met Immediate Occupancy (IO) level, Immediate Occupancy (IO) level, and Immediate Occupancy (IO) level, respectively.

**Table 4.21** Numerical acceptance criteria for plastic hinge rotation of the beams of the three-story building

Level	Conditions			Acceptance Criteria			Plastic Hinge Rotation (radians)	Performance Level
	$\frac{\rho-\rho'}{\rho_{bal}}$	TR <sup>1</sup>	$\frac{V}{b_w d \sqrt{f'_c}}$	IO	LS	CP		
3	0.00	C	0.125	0.01	0.025	0.05	0.0000	IO
2	-0.28	C	0.155	0.01	0.025	0.05	0.0003	IO
1	-0.42	C	0.162	0.01	0.025	0.05	0.0025	IO

<sup>1</sup>TR is Transverse Reinforcement

The 2<sup>nd</sup> step of the pushover analysis of the beam with plastic hinge rotation was shown in figure 4.4.

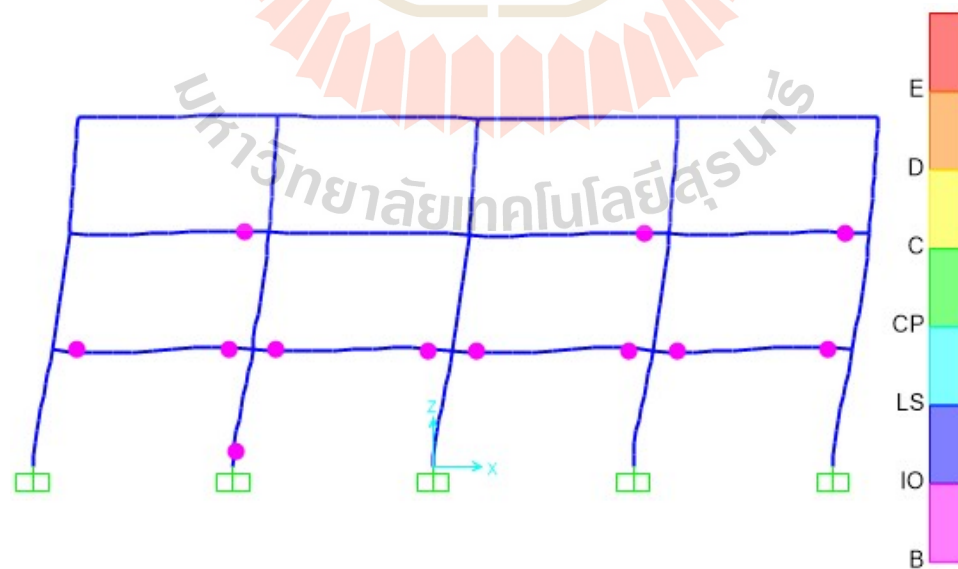


**Figure 4.4** Performance levels of the three-story building

### 4.3.11 Member-Level Performance Method of the six-story building

#### 4.3.11.1 Performance Level of the Column

From table 3.17, we use the conditions to determine the acceptance criteria of the column at ASCE/SEI 41-13, table 10-8. Values between those listed in the table should be determined by linear interpolation. The acceptance criteria of the first to the sixth floor were shown in table 4.22.

**Table 4.22** Numerical acceptance criteria for plastic hinge rotation of the columns of the six-story building

Level	Conditions			Acceptance Criteria Plastic Rotations Angle (radians) Performance Level			Plastic Hinge Rotation (radians)	Perform- ance Level
	$\frac{P}{A_g f_c}$	$\rho = \frac{A_v}{b_w s}$	$\frac{V}{b_w d \sqrt{f_c}}$	IO	LS	CP		
6	0.047	0.0029	0.06867	0.004	0.041	0.054	0.000	IO
5	0.095	0.0029	0.08263	0.004	0.037	0.049	0.000	IO
4	0.142	0.0029	0.08594	0.004	0.033	0.044	0.000	IO
3	0.190	0.0029	0.11519	0.003	0.029	0.038	0.000	IO
2	0.237	0.0029	0.14964	0.003	0.025	0.033	0.000	IO
1	0.284	0.0029	0.22077	0.003	0.021	0.028	0.0012	IO

Plastic hinge rotation got from SAP2000 that equal 0.00123 for the first floor, and 0.000 for the second to the sixth floor. We use the value from the acceptance criteria compare with plastic hinge rotation to determine the performance level of the column. The columns of the six stories building were classified in each

story level, as shown in table 4.22. The 7<sup>th</sup> step of the pushover analysis of the column with plastic hinge rotation was shown in figure 4.5.

#### **4.3.11.2 Performance Level of the Beam**

From table 3.18, we use the conditions to determine the acceptance criteria of the beam at ASCE/SEI 41-13, table 10-7. Values between those listed in the table should be determined by linear interpolation. The acceptance criteria of the first to the sixth floor had Immediate Occupancy (IO), Life Safety (LS), and Collapse Prevention (CP) that equal 0.01, 0.025, and 0.05, respectively. Plastic hinge rotations got from SAP2000, as shown in table 4.23. We use the value from the acceptance criteria compare with plastic hinge rotation to determine the performance level of the beam. The beams of the three stories building were classified in each story level such as the first story, the second story, and the third story met Immediate Occupancy (IO) level, Immediate Occupancy (IO) level, and Immediate Occupancy (IO) level, respectively. The 7<sup>th</sup> step of the pushover analysis of the beam with plastic hinge rotation was shown in figure 4.5.

#### **4.3.11.3 Braced steel frames of six-story building**

The author had a trial and error a lot of the steel section properties to find the appropriate section properties. The author got the steel section that made the existing RC building met immediate occupancy (IO) level. It means that the load was transferred to the braced steel frames instead of the existing RC structure. If the author uses a small steel section, It will make the existing RC building don't meet immediate occupancy (IO) level. If the author uses a big steel section, It will make the existing RC building don't meet immediate occupancy (IO) level. In this research, some braced steel frames met C to D for a rectangular box. The line from C

to D shows the starting failure of the component/element (A.Q. Bhatti & H.Varum., 2012), as shown in figure 2.15. The braced steel frame was shown in figure 4.6.

**Table 4.23** Numerical acceptance criteria for plastic hinge rotation of the beams of the six-story building

Level	Conditions			Acceptance Criteria Plastic Rotations Angle (radians) Performance Level			Plastic- Hinge Rotation (radians)	Perform- ance Level
	$\frac{\rho-\rho'}{\rho_{bal}}$	TR <sup>1</sup>	$\frac{V}{b_w d \sqrt{f'_c}}$	IO	LS	CP		
6	-0.17	C	0.00018	0.01	0.025	0.05	0.000	IO
5	-0.39	C	0.00024	0.01	0.025	0.05	0.000	IO
4	-0.57	C	0.00025	0.01	0.025	0.05	0.00052	IO
3	-0.65	C	0.00025	0.01	0.025	0.05	0.0022	IO
2	-0.71	C	0.00024	0.01	0.025	0.05	0.0042	IO
1	-0.79	C	0.00024	0.01	0.025	0.05	0.0053	IO

<sup>1</sup>TR is Transverse Reinforcement

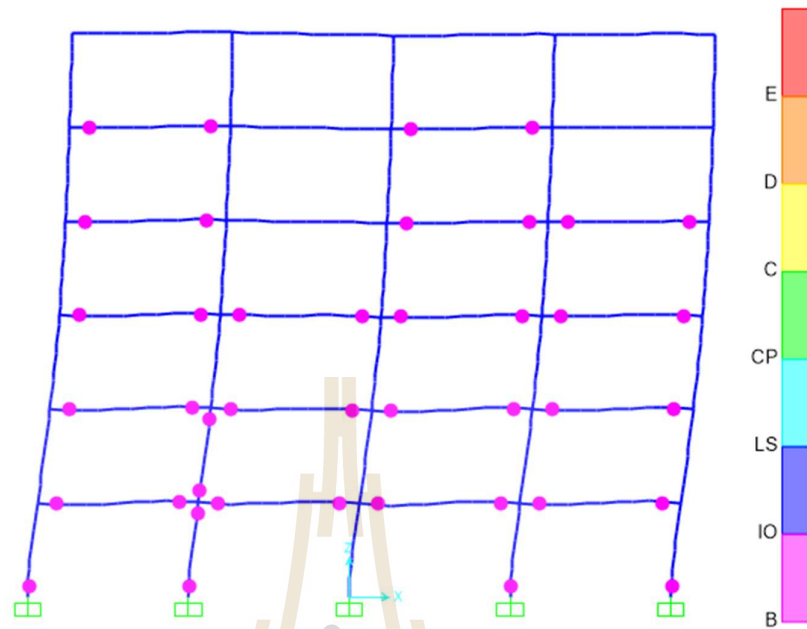


Figure 4.5 Performance levels of the six-story building

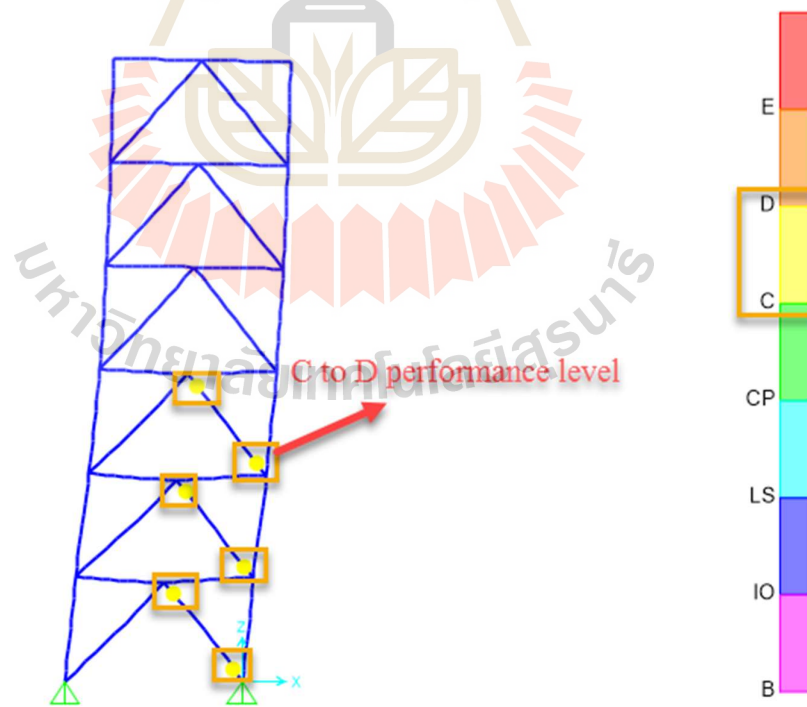


Figure 4.6 Plastic hinges of the braced steel frame



### 4.3.12 Member-Level Performance Method of the nine-story building

#### 4.3.12.1 Performance Level of the Column

From table 3.19, we use the conditions to determine the acceptance criteria of the column at ASCE/SEI 41-13, table 10-8. Values between those listed in the table should be determined by linear interpolation. The acceptance criteria of the first to the sixth floor were shown in table 4.24. Plastic hinge rotations got from SAP2000, as shown in table 4.24.

**Table 4.24** Numerical acceptance criteria for plastic hinge rotation of the columns of the nine-story building

Level	Conditions			Acceptance Criteria Plastic Rotations Angle (radians) Performance Level			Plastic Hinge Rotation (radians)	Perform ance Level
	$\frac{P}{A_g f_c}$	$\rho = \frac{A_v}{b_w s}$	$\frac{V}{b_w d \sqrt{f_c}}$	IO	LS	CP		
9	0.079	0.0024	0.10265	0.0045	0.038	0.051	0.000	IO
8	0.157	0.0024	0.11936	0.0041	0.032	0.042	0.000	IO
7	0.235	0.0024	0.14750	0.0036	0.025	0.034	0.000	IO
6	0.314	0.0024	0.17119	0.0031	0.019	0.025	0.000	IO
5	0.393	0.0024	0.19818	0.0027	0.012	0.016	0.000	IO
4	0.472	0.0024	0.22877	0.0022	0.005	0.007	0.000	IO
3	0.553	0.0024	0.24525	0.0020	0.003	0.004	0.000	IO
2	0.002	0.0024	0.24197	0.0026	0.007	0.008	0.000	IO
1	0.002	0.0024	0.22968	0.0026	0.007	0.008	0.000	IO

We use the value from the acceptance criteria compare with plastic hinge rotation to determine the performance level of the column. The columns of the three stories building were classified in each story level such as the first story, the second story, and the third story met Immediate Occupancy (IO) level, Immediate Occupancy (IO) level, and Immediate Occupancy (IO) level, respectively. The 3rd step of the pushover analysis of the column with plastic hinge rotation was shown in figure 4.7.

#### **4.3.12.2 Performance Level of the Beam**

From table 3.20, we use the conditions to determine the acceptance criteria of the beam at ASCE/SEI 41-13, table 10-7. Values between those listed in the table should be determined by linear interpolation. The acceptance criteria of the first to the sixth floor had Immediate Occupancy (IO), Life Safety (LS), and Collapse Prevention (CP) that equal 0.01, 0.025, and 0.05, respectively. Plastic hinge rotations got from SAP2000, as shown in table 4.25. We use the value from the acceptance criteria compare with plastic hinge rotation to determine the performance level of the beam. The beams of the three stories building were classified in each story level such as the first story, the second story, and the third story met Immediate Occupancy (IO) level, Immediate Occupancy (IO) level, and Immediate Occupancy (IO) level, respectively. The 3rd step of the pushover analysis of the beam with plastic hinge rotation was shown in figure 4.7.

**Table 4.25** Numerical acceptance criteria for plastic hinge rotation of the beams of the nine-story building

Level	Conditions			Acceptance Criteria Plastic Rotations Angle (radians) Performance Level			Plastic Hinge Rotation (radians)	Perform- ance Level
	$\frac{\rho-\rho'}{\rho_{bal}}$	TR <sup>1</sup>	$\frac{V}{b_w d \sqrt{f_c}}$	IO	LS	CP		
9	-0.25	C	0.16702	0.01	0.025	0.05	0.00002	IO
8	-0.48	C	0.18255	0.01	0.025	0.05	0.0015	IO
7	-0.59	C	0.18139	0.01	0.025	0.05	0.0029	IO
6	-0.69	C	0.18023	0.01	0.025	0.05	0.0043	IO
5	-0.70	C	0.17897	0.01	0.025	0.05	0.0056	IO
4	-0.72	C	0.17709	0.01	0.025	0.05	0.0069	IO
3	-0.74	C	0.17442	0.01	0.025	0.05	0.0078	IO
2	-0.76	C	0.17106	0.01	0.025	0.05	0.0077	IO
1	-0.80	C	0.16681	0.01	0.025	0.05	0.0057	IO

<sup>1</sup>TR is Transverse Reinforcement

#### 4.3.12.3 Braced steel frames of nine-story building

The author had a trial and error a lot of the steel section properties to find the appropriate section properties. The author got the steel section that made the existing RC building met immediate occupancy (IO) level. It means that the load was transferred to the braced steel frames instead of the existing RC structure. If the author uses a small steel section, It will make the existing RC building don't meet immediate occupancy (io) level. If the author uses a big steel section, It will

make the existing RC building don't meet immediate occupancy (IO) level. In this research, some braced steel frames met Life Safety (LS) level for a circle box and C to D for a rectangular box. The line from C to D shows the starting failure of the component/element (A.Q. Bhatti & H.Varum.,2012), as shown in figure 2.15. The braced steel frame was shown in figure 4.8.

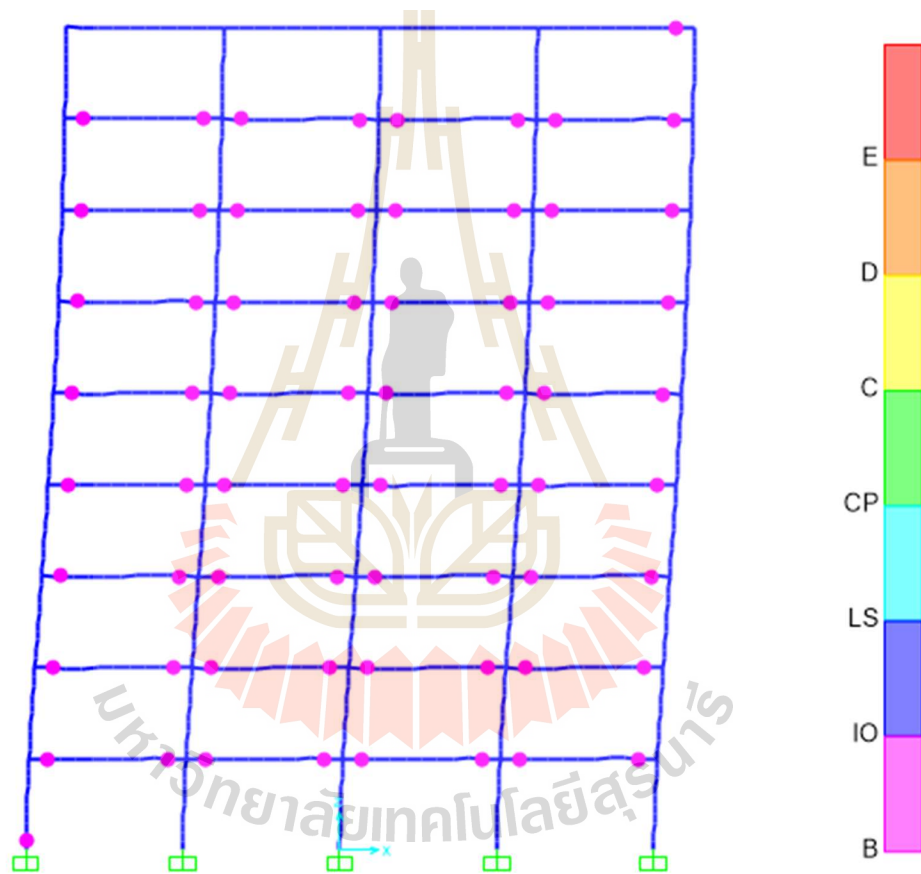


**Figure 4.7** Performance levels of the nine-story building



Figure 4.8 Plastic hinges of the braced steel frame

## 4.4 Comparison of the result

### 4.4.1 Existing and strengthening of the three-story building

From the result, the first floor of the existing building met the Life Safety (LS) level for three methods except the capacity spectrum method met Immediate Occupancy (IO) level. But the second floor met the Immediate Occupancy (IO) level for the three methods except for the inter-story drift method met the Life Safety (LS) level. The third floor met the Immediate Occupancy (IO) level for the four methods. For the strengthening building, the first, second, and third floors met the Immediate Occupancy (IO) level for the four methods.

#### **4.4.2 Existing and strengthening of the six-story building**

From the result, the three methods met Life Safety (LS) level except the capacity spectrum method met Immediate Occupancy (IO) level for the existing building. For the result of the strengthening building, it met the Immediate Occupancy (IO) level for the four methods.

#### **4.4.3 Existing and strengthening of the nine-story building**

From the result, the two methods met Life Safety (LS) level for the existing building. The capacity spectrum method met Immediate Occupancy (IO) level for the existing building. The inter-story drift method met Collapse Prevention (CP) level for the existing building. For the result of the strengthening building, it met the Immediate Occupancy (IO) level for the four methods.

Therefore, all method is a good tool for strengthening the structure when we compared these methods. Because all methods met Immediate Occupancy (IO) level for strengthening the structure.

# CHAPTER V

## CONCLUSION

### 5.1 Conclusion

This case study was evaluated the seismic performance of the three-story, six-story, and nine-story R/C existing building located in Thailand considering to use steel bracing to improve the structural performance levels of the existing building. It was used many standards such as ASCE/SEI 41-13, ASCE/SEI 41-06, ACT 40, FEMA 440, FEMA356, and FEMA 273 that separates into four different methods for the first method is displacement coefficient method, the second method is capacity spectrum method, the third method Inter-story Drift Method, and the four method is member-level performance Method to determine the performance levels. Depend on the result of these four methods, and it shows that the building meets the Immediate Occupancy (IO) after using the steel bracing to improve the seismic performance in the following.

1. The displacement coefficient method can improve the performance levels from Life Safety (LS) to Immediate Occupancy (IO).
2. The capacity spectrum method meets the Immediate Occupancy (IO) for both existing and retrofitted building.
3. The performance of the column changes from the Life Safety (LS) of the existing building to Immediate Occupancy (IO) of the retrofitted building.
4. The performance of the beam changes from Life Safety (LS) of the existing building to Immediate Occupancy (IO) of the retrofitted building.

5. The braced steel frames could be designed to the desired performance limit states specified in FEMA, ASCE, ATC and Thai earthquake standard, and utilized for seismic retrofitting the existing building in Thailand.

6. The braced steel frames were rigidly connected to the foundations and columns of the existing building, but this study did not detail the type of the connection that used to connect between the braced steel frames to the existing structure.

7. The braced steel frames can improve the performance level of the structure from Life Safety (LS) of the existing building to Immediate Occupancy (IO) of the retrofitted building.

8. The inter-story drift changes from Collapse Prevention (CP) of the existing building to Immediate Occupancy (IO) of the retrofitted building.

Therefore, the displacement coefficient and member-level performance methods met the Life Safety (LS) for the existing building and the Immediate Occupancy (IO) for the retrofitted building. However, the capacity spectrum method met the Immediate Occupancy (IO) for both existing and retrofitted building. On the other hand, Inter-story drift method met the collapse prevention (CP) for the existing building and the Immediate Occupancy (IO) for the retrofitted building.

## **5.2 Recommendation**

This research used the same shape as the existing and strengthening building. The author thinks that the other researchers should change the position of the strengthening structure and the shape of the existing building.



## REFERENCES

- Soundarya, N.G., Pawar, Y.P., Pise, C.P., Kadam, S.S., Deshmukh, C.M., Mohite, D.D. (2017). Strengthening of reinforced concrete and steel structure by using steel bracing systems. **International Research Journal of Engineering and Technology (IRJET)**, (pp. 517-522).
- Channarong, T., and Mongkol, J. (2016). **The Study of the Reinforced Earthquake Resistance Building Structure in Sanklangvittaya School, Chiangrai Thailand**. The 21<sup>st</sup> National Convention on Civil Engineering, Songkhla, Thailand, June 28<sup>th</sup>-30<sup>th</sup>, 2016, pp. 1-8.
- Shachindra, K.C., and Abhay, S. (2015). Seismic behavior of RC building frame with steel bracing system using various arrangements. **International Research Journal of Engineering and Technology (IRJET)**, (pp. 479-483).
- FEMA-440. (2005). Improvement of Nonlinear Static Seismic Analysis Procedures. **Federal Emergency Management Agency**, Redwood City, California.
- ATC-40. (1996). Seismic Evaluation and Retrofitting of concrete Buildings. Volume 1 and 2. **Applied Technology Council**, Seismic Safety Commission, Redwood City.
- ASCE 41-13. (2013). Seismic Evaluation and Retrofit of Existing Buildings. **American Society of Civil Engineers**, Reston, VA.
- ACI 318. (2011). Building Code Requirements for Structural Concrete and Commentary. American Concrete Institute, Farmington Hills, MI.

- ACI 369. (2011). Guide for Seismic Rehabilitation of Existing Concrete Frame Buildings and Commentary. American Concrete Institute, Farmington Hills, MI.
- Joint ACI-ASCE Committee 352R. (2003). Recommendations for Design of Beam – Column Connections in Monolithic Reinforced Concrete Structures. **American Concrete Institute, USA.**
- DPT 1302. (2009). Standard of earthquake resistant design of building. **Department of Public Works and Town & Country Planning, Bangkok, Thailand.**
- Mehmet, I., Hayri, B. O., and Huseyin, B. (2007). Re-evaluation of building damage during recent earthquakes in Turkey. **Engineering Structures**, 412-427.
- Dhangar, L. B., and Venu, M. (2008). Pushover analysis of high rise building with and without bracings. **IJCIET**, 9, 759–767.
- Haijuan, D., and Mary B.D.H. (2012). Seismic performance of a reinforced concrete frame building in China. **Engineering Structures**, 41: 77-89.
- Dilip J.C., and Gopal, O.D. (2016). Performance Based Seismic Design of Reinforced Concrete Building. **Open Journal of Civil Engineering**, 6, 188-194.
- Chandrasekaram, S., Serino, G., and Gupta, V. (2008). Performance evaluation and damage assessment of buildings subjected to seismic loading. **WIT Press**, 98: 313-322.
- Waiel, M. (2015). Simple strengthening techniques and new technologies for seismic safety of existing building: recent research and applications in turkey. **International Burdur Earthquake and Environment Symposium (IBEES).**

- Mehmet, I., and Hayri, B.O. (2006). Effects of plastic hinge properties in nonlinear analysis of reinforced concrete buildings. **Engineering Structures**, 28: 1494–1502.
- Bhatti, A.Q., and Varum, H. (2012). Application of Performance Based Nonlinear Seismic Design and Simulation static Pushover Analysis for Seismic Design of RC Buildings. **15<sup>th</sup> WCEE, LISBOA**.
- Reddy, B.B. (2018). Analytical investigation on seismic strengthening of RC frame using steel cage and viscous damper. **IRJET**, 9, 644–653.
- Ramasundaram, S., and Agilesh, K. (2017). Effect of bracings on tall buildings for seismic loads using pushover analysis. **International Research Journal of Engineering and Technology (IRJET)**, 8, 891–897.
- Chakraphan, W. (2013). **Seismic rehabilitation by linear and nonlinear analysis: case study of an RC building in Chiang Mai**. Chulalongkorn University.
- DPT 1303. (2014). Standard of assessment and strengthening of the building structures in areas of the earthquake zone. **Department of Public Works and Town & Country Planning**, Bangkok, Thailand.
- Hendramawat, A.S., Kristiawan, S.A., and Basuki, A. (2013). Evaluation of the Use of Steel Bracing to Improve Seismic Performance of Reinforced Concrete Building. **Procedia Engineering**, 54: 447-456.



**APPENDIX A**  
**SIX-STORY BUILDING MODELING**

มหาวิทยาลัยเทคโนโลยีสุรนารี

## Structural modeling using SAP2000

### 1. Beam section property

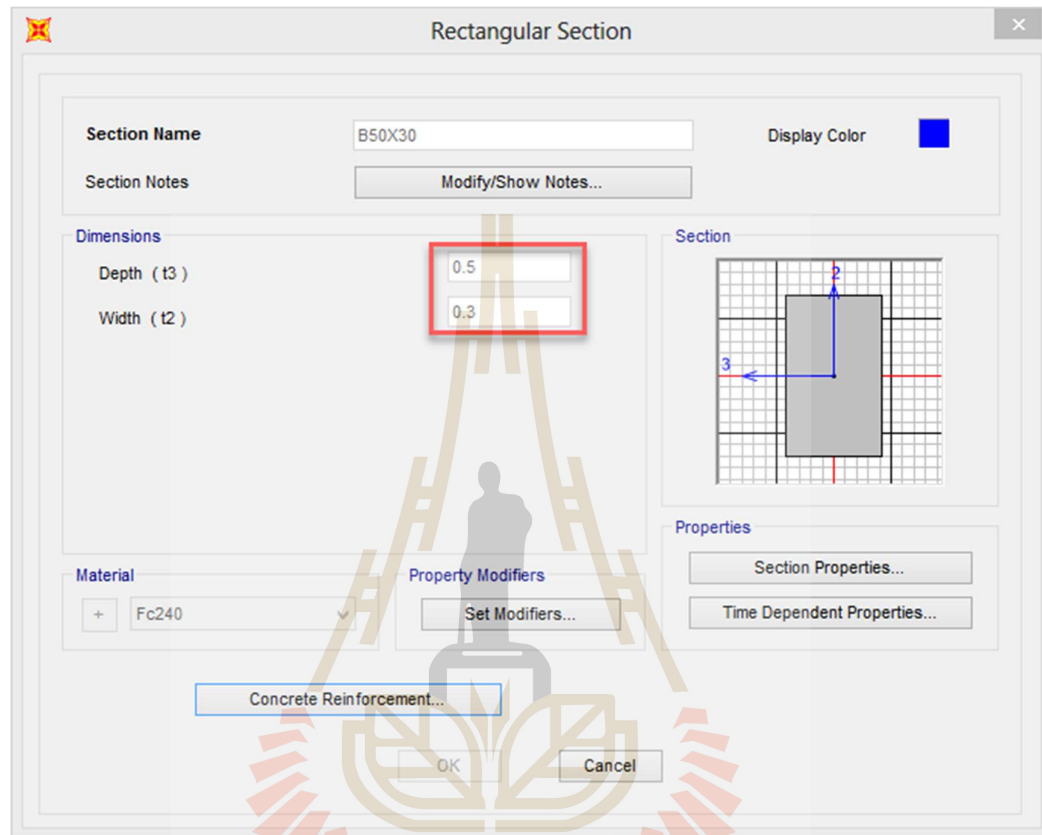


Figure A.1 Beam section property

## 2. Reinforcement property data

**Reinforcement Data**

**Rebar Material**

Longitudinal Bars	+ SD40
Confinement Bars (Ties)	+ SD40

**Design Type**

Column (P-M2-M3 Design)

Beam (M3 Design Only)

**Concrete Cover to Longitudinal Rebar Center**

Top	0.04
Bottom	0.04

**Reinforcement Overrides for Ductile Beams**

	Left	Right
Top	0.	0.
Bottom	0.	0.

OK Cancel

Figure A.2 Reinforcement property

## 3. Column section property

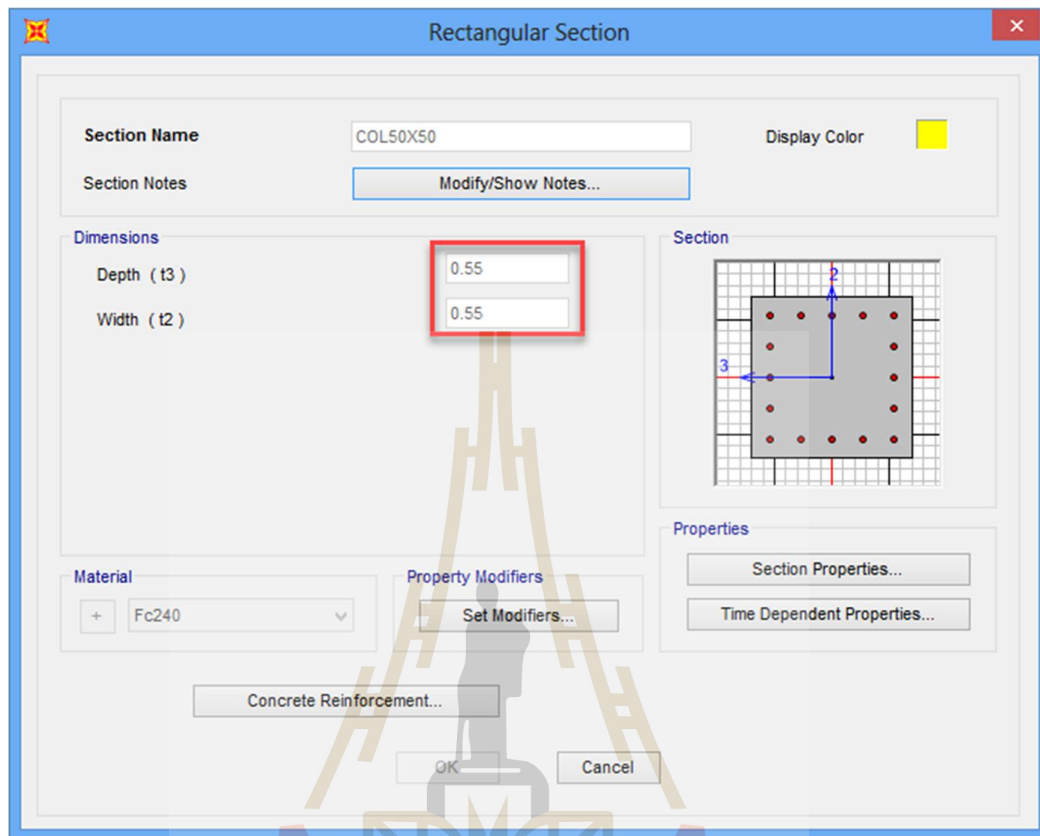


Figure A.3 Column section property

## 4. Reinforcement property data

**Reinforcement Data**

**Rebar Material**

Longitudinal Bars + SD40

Confinement Bars (Ties) + SD40

**Design Type**

Column (P-M2-M3 Design)

Beam (M3 Design Only)

**Reinforcement Configuration**      **Confinement Bars**

Rectangular       Ties

Circular       Spiral

**Longitudinal Bars - Rectangular Configuration**

Clear Cover for Confinement Bars 0.04

Number of Longit Bars Along 3-dir Face 5

Number of Longit Bars Along 2-dir Face 5

Longitudinal Bar Size + 25d

**Confinement Bars**

Confinement Bar Size + 10d

Longitudinal Spacing of Confinement Bars 0.15

Number of Confinement Bars in 3-dir 3

Number of Confinement Bars in 2-dir 3

**Check/Design**

Reinforcement to be Checked

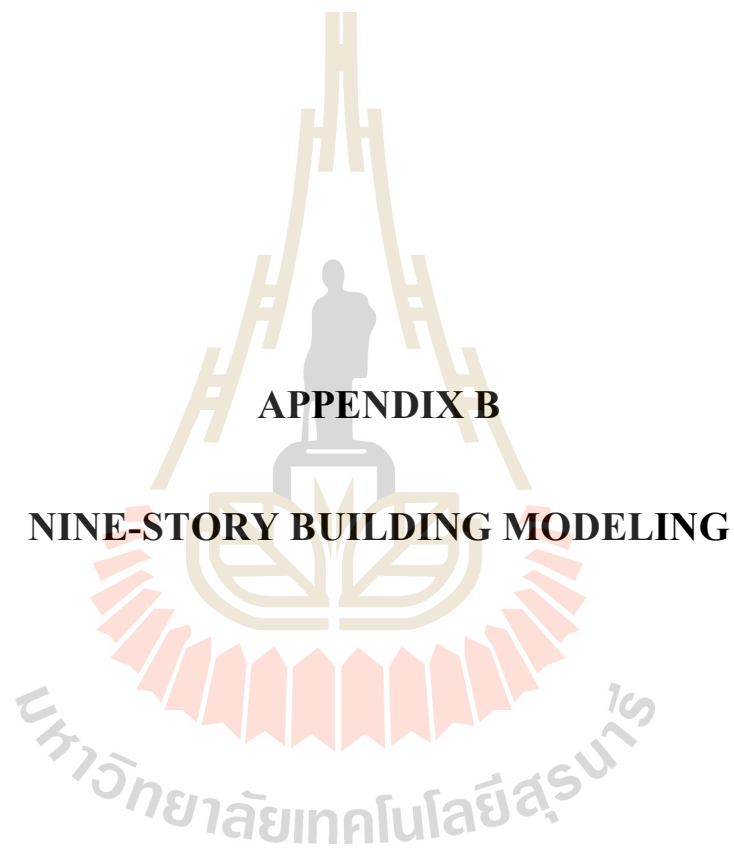
Reinforcement to be Designed

OK

Cancel

Figure A.4 Reinforcement property





**APPENDIX B**

**NINE-STORY BUILDING MODELING**

## Structural modeling using SAP2000

### 1. Beam section property

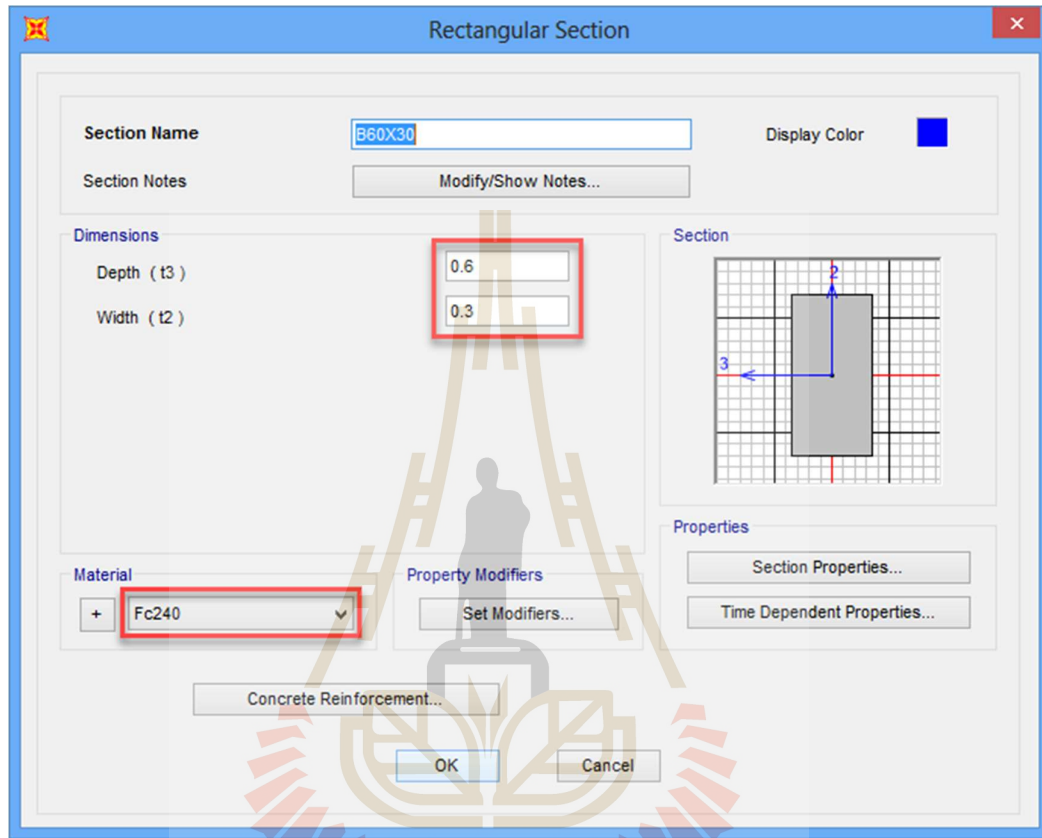


Figure B.1 Beam section property

## 2. Reinforcement property data

**Reinforcement Data**

**Rebar Material**

Longitudinal Bars: + SD40

Confinement Bars (Ties): + SD40

**Design Type**

Column (P-M2-M3 Design)

Beam (M3 Design Only)

**Concrete Cover to Longitudinal Rebar Center**

Top: 0.04

Bottom: 0.04

**Reinforcement Overrides for Ductile Beams**

	Left	Right
Top	0.	0.
Bottom	0.	0.

OK Cancel

Figure B.2 Reinforcement property

มหาวิทยาลัยเทคโนโลยีสุรนารี

## 3. Column section property

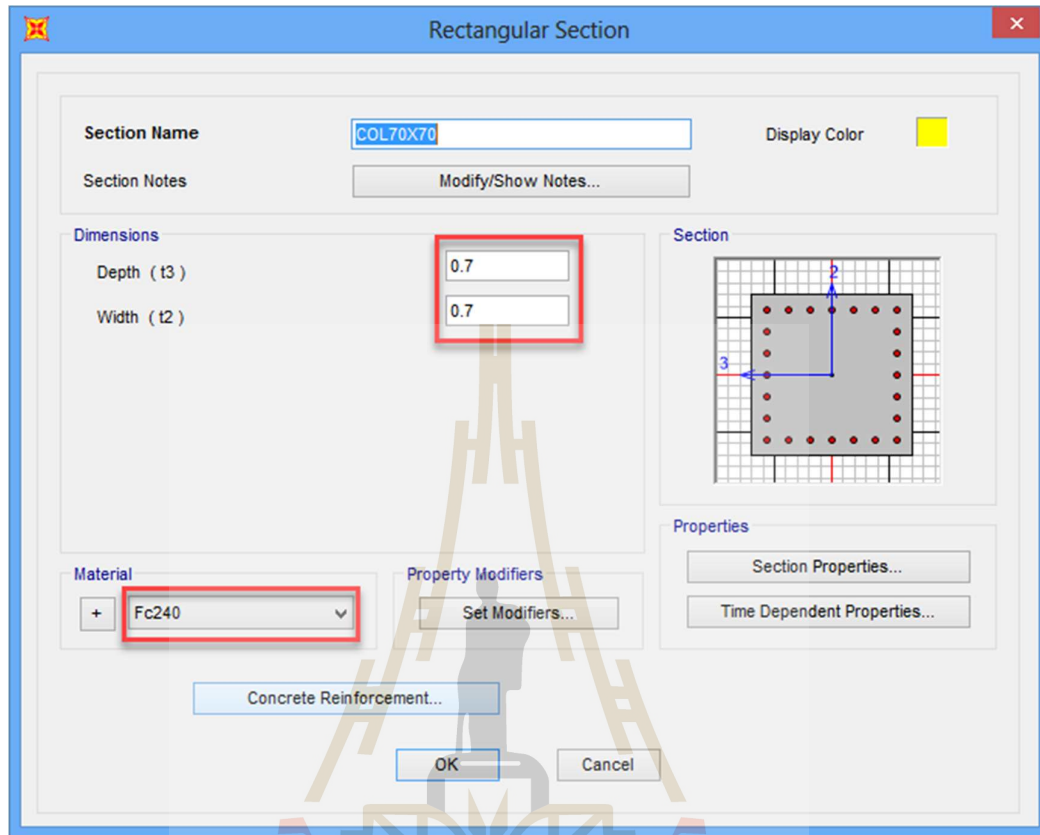


Figure B.3 Column section property

## 4. Reinforcement property data

**Reinforcement Data**

**Rebar Material**

Longitudinal Bars	+ SD40
Confinement Bars (Ties)	+ SD40

**Design Type**

Column (P-M2-M3 Design)

Beam (M3 Design Only)

**Reinforcement Configuration**

Rectangular

Circular

**Confinement Bars**

Ties

Spiral

**Longitudinal Bars - Rectangular Configuration**

Clear Cover for Confinement Bars: 0.04

Number of Longit Bars Along 3-dir Face: 7

Number of Longit Bars Along 2-dir Face: 7

Longitudinal Bar Size: 25d

**Confinement Bars**

Confinement Bar Size: 10d

Longitudinal Spacing of Confinement Bars: 0.15

Number of Confinement Bars in 3-dir: 3

Number of Confinement Bars in 2-dir: 3

**Check/Design**

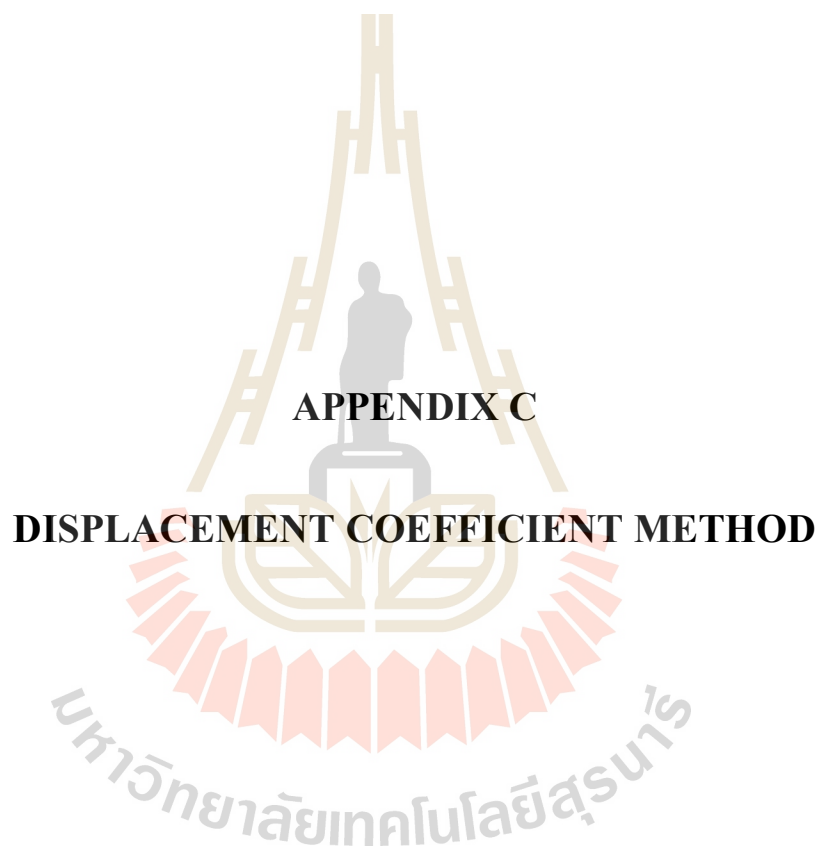
Reinforcement to be Checked

Reinforcement to be Designed

OK

Cancel

Figure B.4 Reinforcement property



**APPENDIX C**

**DISPLACEMENT COEFFICIENT METHOD**

### C.1 Displacement Coefficient Method

Depend on DPT 1302-2009, Thai standard defines the spectral response acceleration at short period ( $S_s$ ) and the spectral response acceleration at 1 s period ( $S_1$ ) for each district all of the province in Thailand. The three stories building locates in Chiang Rai city, Chiang Rai province. The  $S_s$  and  $S_1$  of the Chiang Rai city are shown in table C. 1. In this method, we need to change the  $S_s$  and  $S_1$  as shown in figure C.1.

**Table C.1** Spectral response acceleration  $S_s$  and  $S_1$

Province	Districts	Acceleration (g)	
		$S_s$	$S_1$
Chiang Rai	Doi Luang	0.924	0.270
	Wiang Chiang Rung	0.833	0.241
	Khun Tan	0.650	0.169
	Chiang Khong	0.706	0.191
	Chiang Saen	0.935	0.273
	Thoeng	0.619	0.157
	Pa Daet	0.618	0.154
	Phaya Mengrai	0.672	0.180
	Phan	0.656	0.173
	Mueang Chiang Rai	0.798	0.232
	Mae Chan	0.940	0.278
	Mae Fa Luang	0.929	0.275
	Mae Lao	0.735	0.211
	Mae Suai	0.749	0.209

Province	Districts	Acceleration (g)	
		S <sub>s</sub>	S <sub>1</sub>
Chiang Rai	Mae Sai	0.933	0.273
	Wiang Kaen	0.683	0.175
	Wiang Chai	0.753	0.215
	Wiang Pa Pao	0.759	0.194

Parameters For FEMA 440 Displacement Modification

Pushover Parameters Name  
Name: F440PODM1 Units: KN, m, C

Demand Spectrum Definition  
Effective Viscous Damping (0 < Damp < 1): 0.05

Defined Function  
Scale Factor:   
Characteristic Period of Resp Spec, T<sub>s</sub>:

FEMA 356 General Response Spectrum  
Mapped Spectral Accel at Short Period, S<sub>s</sub>: 0.798  
Mapped Spectral Accel at 1 Sec Period, S<sub>1</sub>: 0.232  
Site Class: D

Include Soil-Structure Interaction Effects Modify/Show/SSI...

**Figure C.1** Spectral response acceleration S<sub>s</sub> and S<sub>1</sub> of the Chiang Rai city





**APPENDIX D**  
**CAPACITY SPECTRUM METHOD**

มหาวิทยาลัยเทคโนโลยีสุรนารี

## D.1 Capacity Spectrum Method

The three stories building locates in Chiang Rai city, Chiang Rai province. Depend on the Department of Mineral Resource, Thailand 2005, this province is in the seismic zone factor Z “2B” as shown in figure D. 1. The seismic zone factor 2B equals to 0.20 as shown in table D.1. In SAP2000, we need to change some parameters for adapting to the Thai zone. The parameters have seismic coefficient  $C_v$  and  $C_a$ , as shown in table D.2 and D.3, respectively. We can see the changing of the  $C_a$  and  $C_v$  as shown in figure. D. 2.

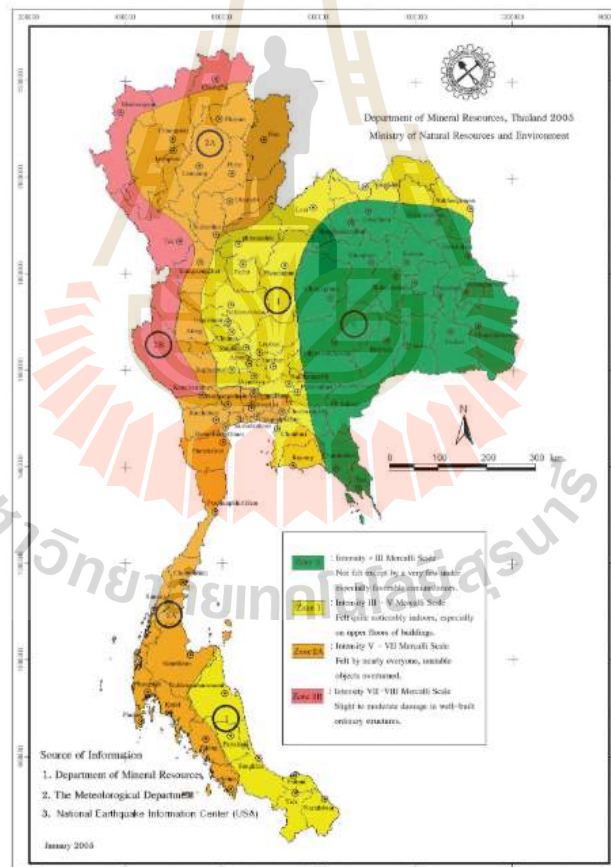


Figure D.1 seismic zone factor Z

**Table D.1** seismic zone factor Z

Zone	1 <sup>1</sup>	2A <sup>1</sup>	2B <sup>1</sup>	3	4
Z	0.075	0.15	0.2	0.3	0.4

1 Seismic zones I, 2A and 2B are not applicable to sites in California

**Table D.2** Seismic Coefficient, C<sub>A</sub>

Soil Profile Type	Shaking Intensity, ZEN <sup>1,2</sup>					
	=0.075	=0.15	=0.20	=0.30	=0.40	=0.40
S <sub>a</sub>	0.08	0.15	0.20	0.30	0.40	1.0(ZEN)
S <sub>C</sub>	0.09	0.18	0.24	0.33	0.40	1.0(ZEN)
S <sub>D</sub>	0.12	0.22	0.28	0.36	0.44	1.1(ZEN)
S <sub>E</sub>	0.19	0.30	0.34	0.36	0.36	0.9(ZEN)
S <sub>F</sub>	Site-specific geotechnical investigation required to determine C <sub>A</sub>					

- 1 The value of E "used to determine the product, ZEN, -should be taken to be equal to 0.5 for the Serviceability Earthquake, 1.0 for the Design Earthquake, and 1.25 (Zone 4 sites), or 1.5 (Zone 3 sites) for the Maximum Earthquake.
- 2 Seismic coefficient C<sub>A</sub> should be determined by linear interpolation for values of the product ZEN other than those shown in the table.

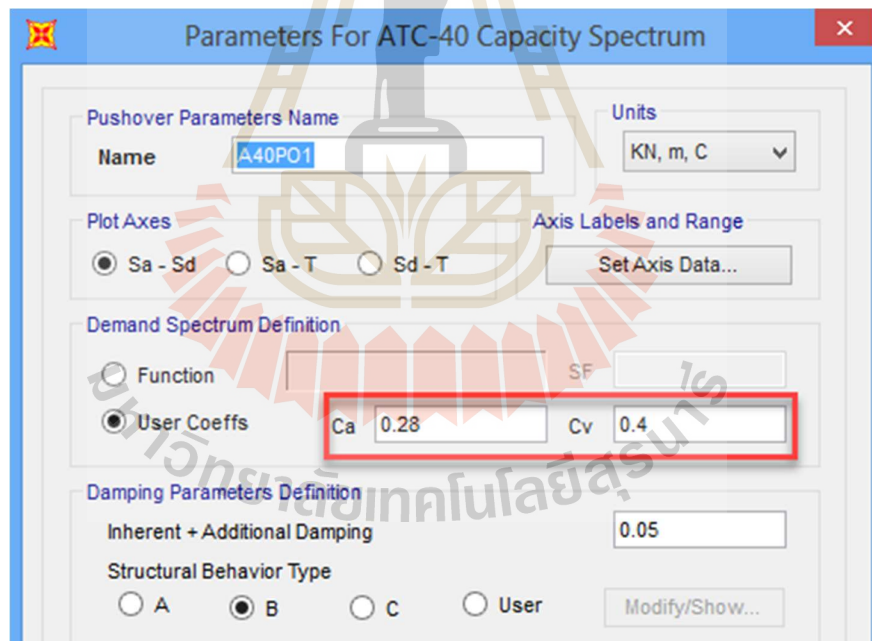
**Table D.3** Seismic Coefficient, C<sub>V</sub>

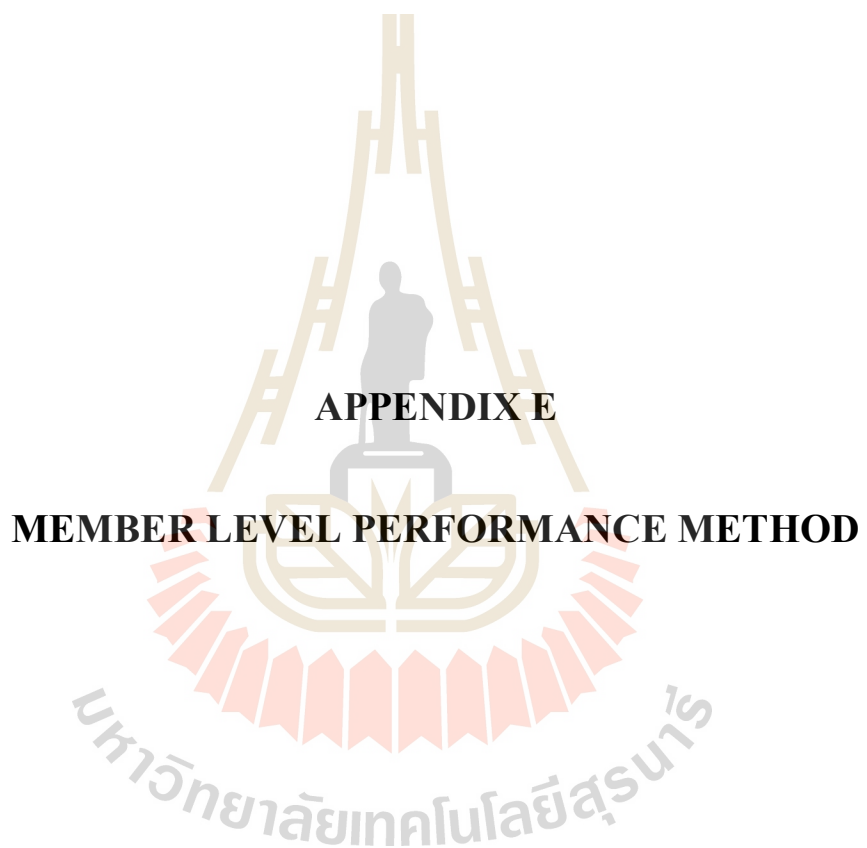
Soil Profile Type	Shaking Intensity, ZEN <sup>1,2</sup>					
	=0.075	=0.15	=0.20	=0.30	=0.40	=0.40
S <sub>a</sub>	0.08	0.15	0.20	0.30	0.40	1.0(ZEN)
S <sub>C</sub>	0.13	0.25	0.32	0.45	0.56	1.4(ZEN)
S <sub>D</sub>	0.18	0.32	0.40	0.54	0.64	1.6(ZEN)

**Table D.3** Seismic Coefficient,  $C_v$  (Continued)

Soil Profile Type	Shaking Intensity, $ZEN^{1,2}$					
	=0.075	=0.15	=0.2	=0.3	=0.4	=0.4
$S_E$	0.26	0.50	0.64	0.84	0.96	2.6(ZEN)
$S_F$	Site-specific geotechnical investigation required to determine $C_v$					

- The value of E used to determine the product, ZEN, should be taken to be equal to 0.5 for the Serviceability Earthquake, 1.0 for the Design Earthquake and 1.5 (Zone 4 sites) or 1.5 (Zone 3 sites) for the Maximum Earthquake.
- Seismic coefficient  $C_v$  should be based on the linear interpolation of values for shaking intensities other than those shown in the table.

**Figure D.2** Seismic coefficient  $C_v$  and  $C_a$



**APPENDIX E**

**MEMBER LEVEL PERFORMANCE METHOD**

## E.1 Member-Level Performance Method

Shear force at grid 5-D

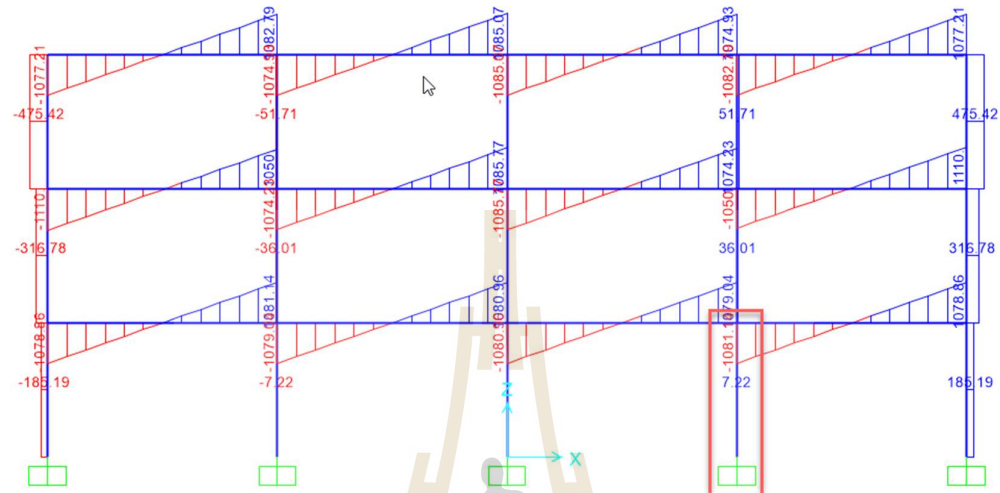


**Figure E.1** Dead load case shear force of the column as shown in the rectangular box

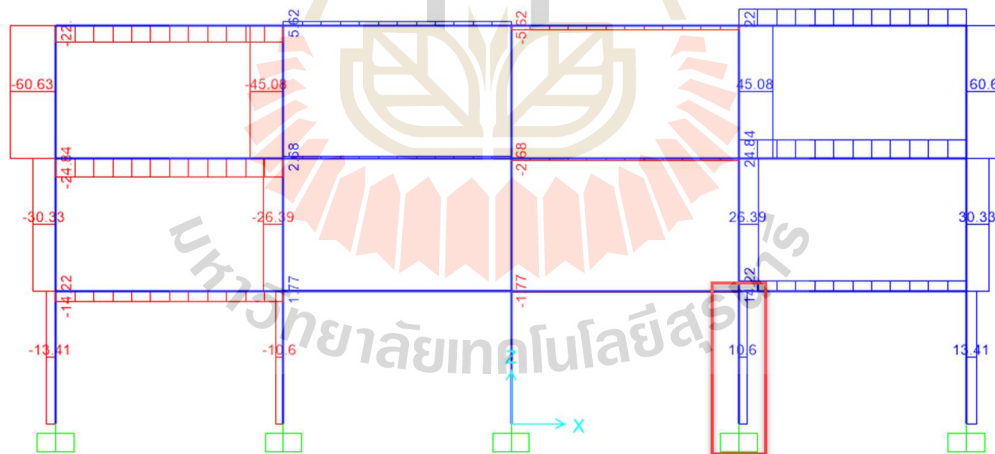


**Figure E.2** Live load case shear force of the column as shown in the rectangular box

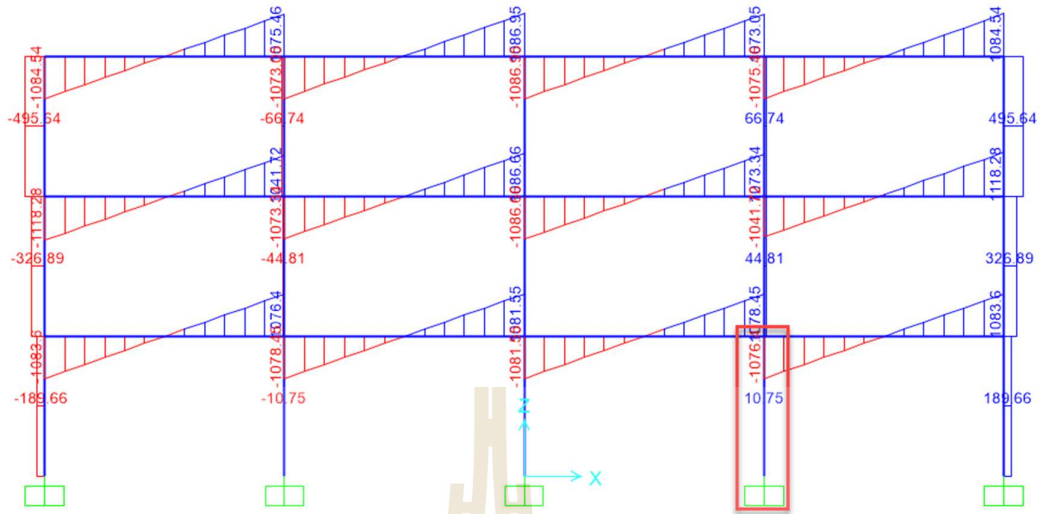


**Figure E.3** Super impose dead load case shear force of the column as shown in the rectangular box

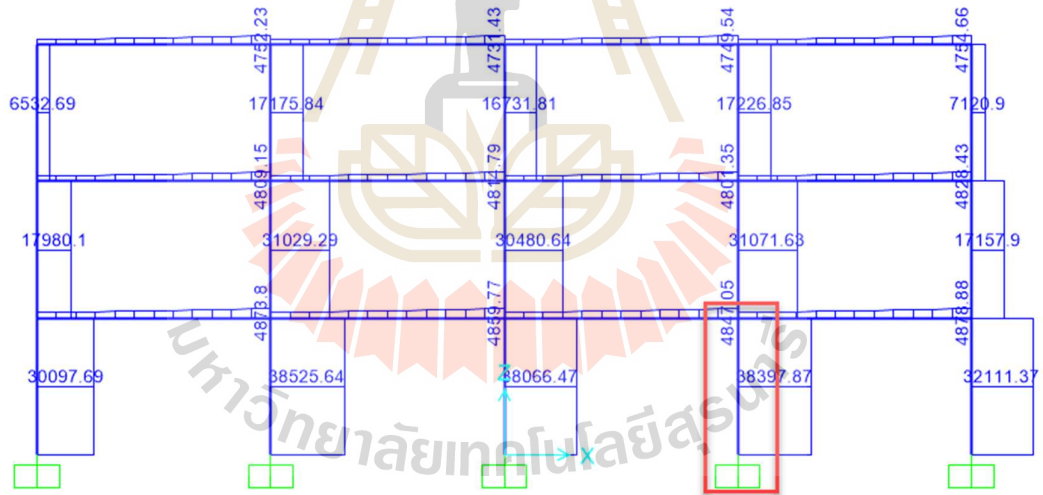


**Figure E.4** Lateral load case shear force of the column as shown in the rectangular box

**Axial force at grid 5-D**

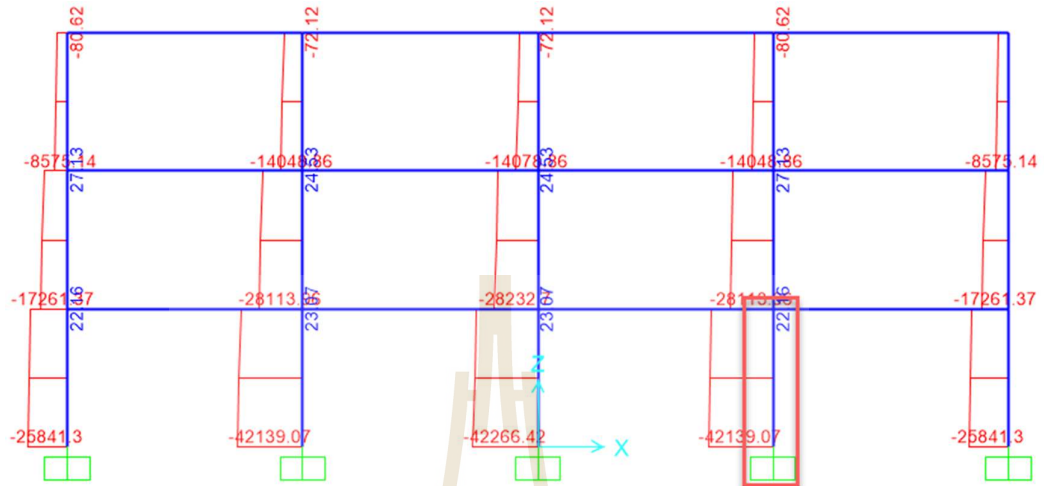


**Figure E.5** Dead load case axial force of the column as shown in the rectangular box

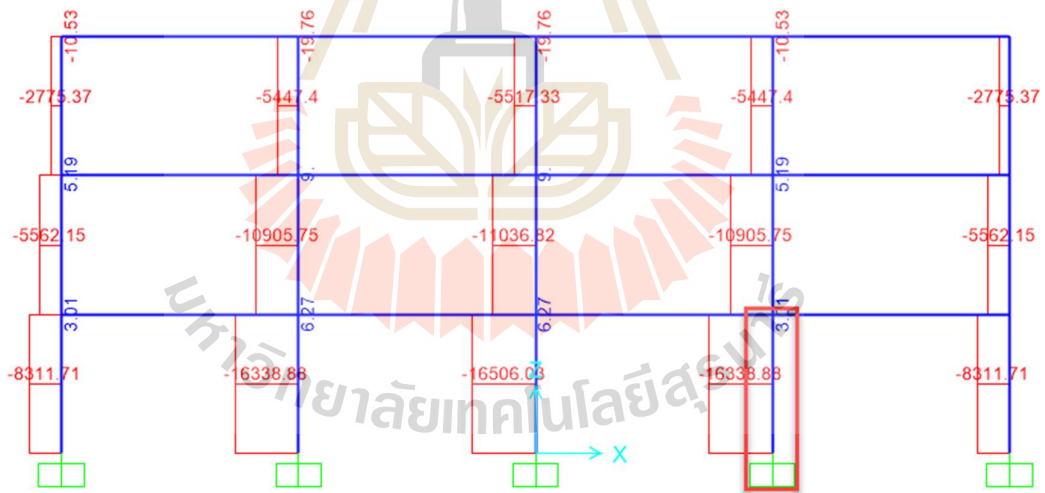


**Figure E.6** Live load case axial force of the column as shown in the rectangular box



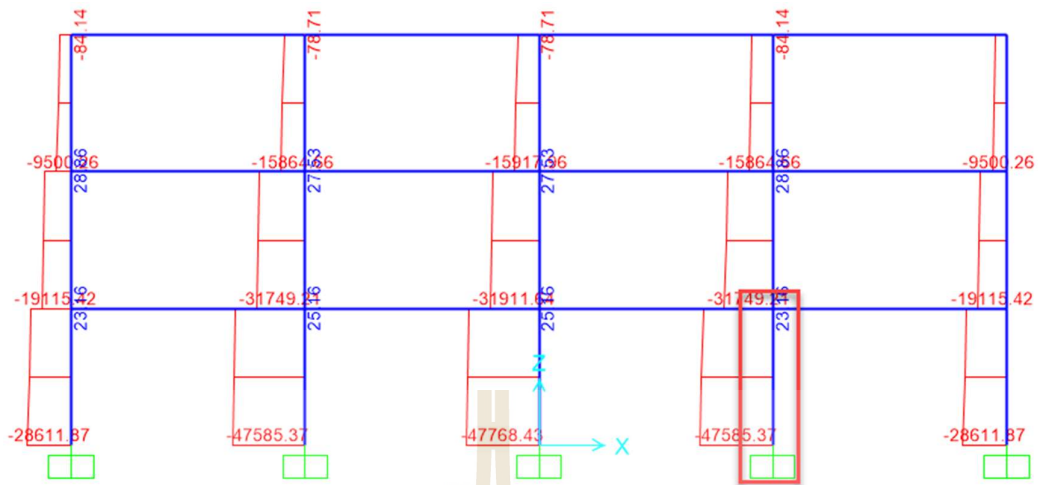


**Figure E.7** Super impose dead load case axial force of the column as shown in the rectangular box

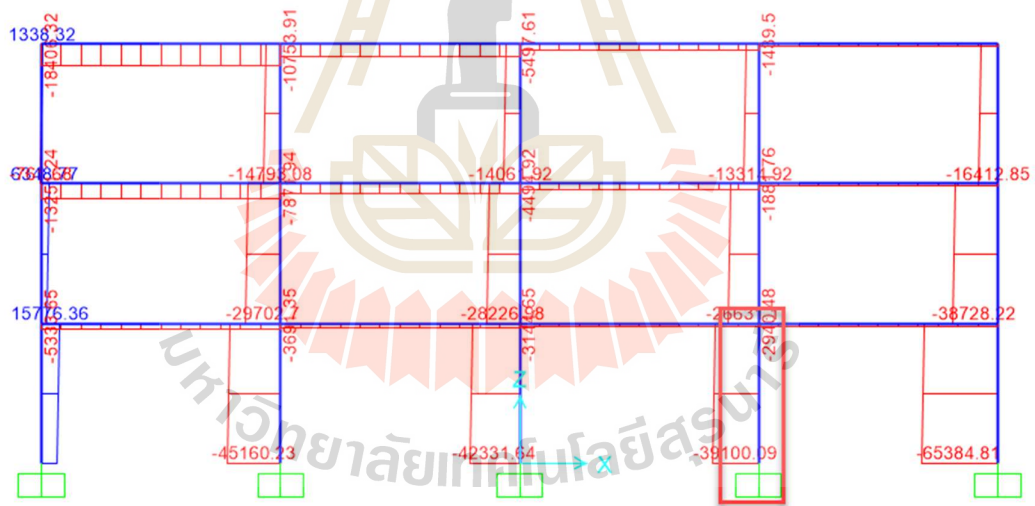


**Figure E.8** Lateral load case axial force of the column as shown in the rectangular box

Moment at grid 5-D

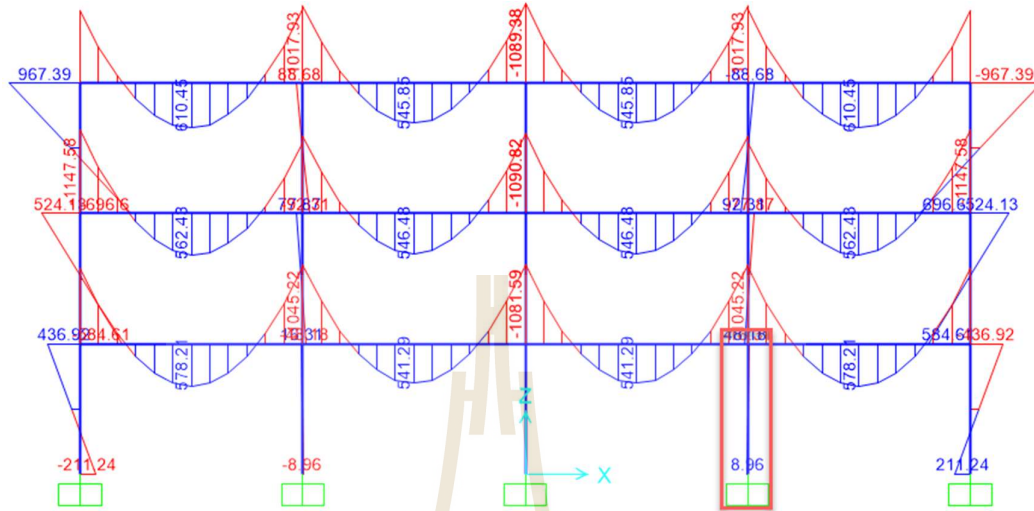


**Figure E.9** Dead load case bending moment of the column as shown in the rectangular box

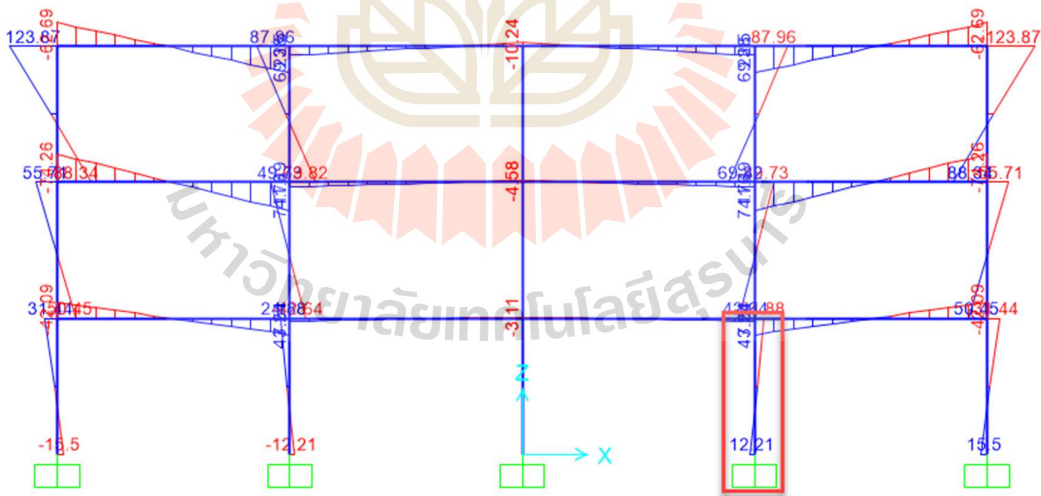


**Figure E.10** Live load case bending moment of the column as shown in the rectangular box

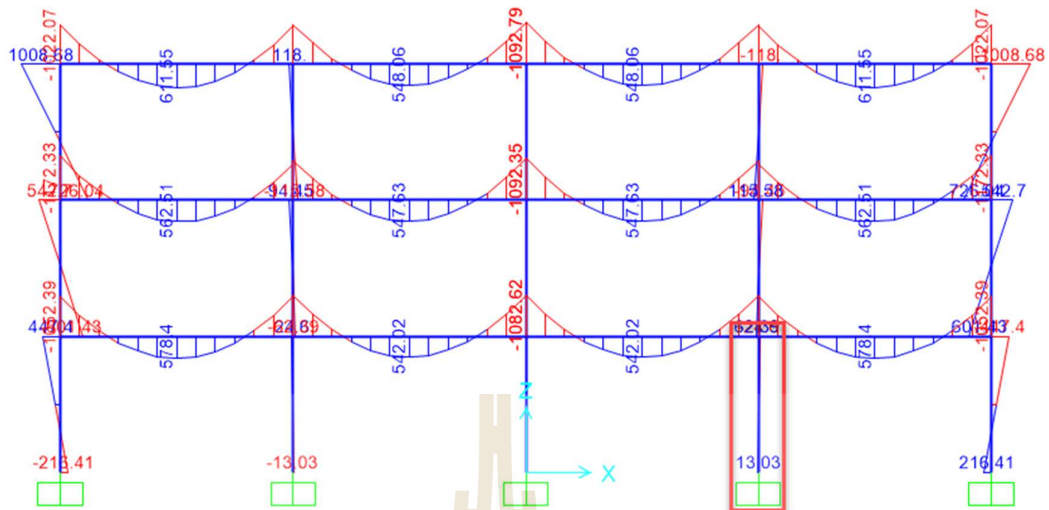


**Figure E.11** Super impose dead load case bending moment of the column as shown in the rectangular box

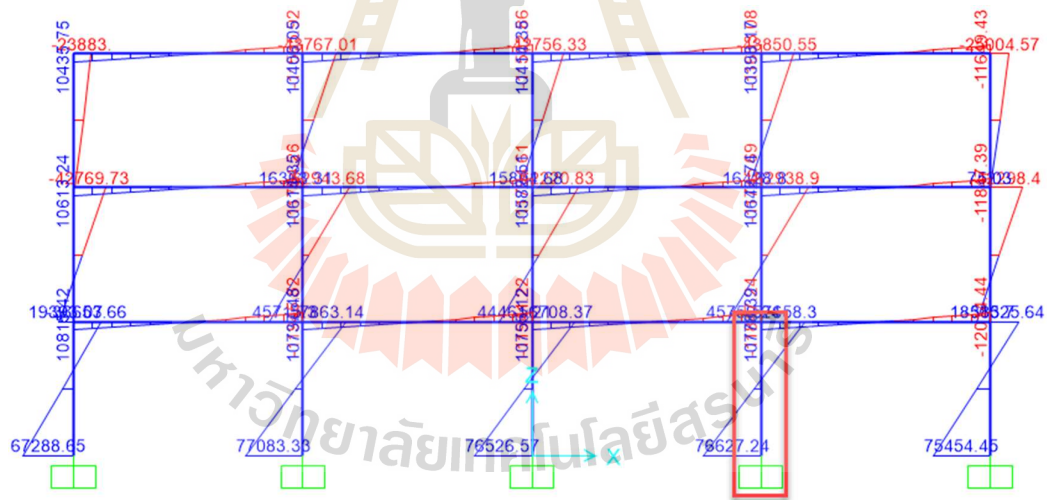


**Figure E.12** Lateral load case bending moment of the column as shown in the rectangular box

## 1. Column

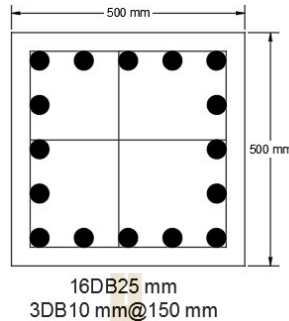


**Figure E.13** Column Section of the first floor

Cover =40 mm

Column length =3500 mm

$f'_c = 22.54 \text{ MPa}$

$f_y = 392.29 \text{ MPa}$

Using first floor to assess the building performance

Determine IO, LS, and CP for flexural capacity (given the axial and shear stress ratios):

Determine Axial Stress Ratio:

$$P_{\text{bot}} = P_{\text{dead}} + P_{\text{SDL}} + 0.25P_{\text{live}} + P_E$$

$$P_{\text{bot}} = 42139.07 + 47585.37 + 0.25 \cdot 16338.88 + 39115.62$$

$$P_{\text{bot}} = 132924.78 \text{ kg}$$

$$P_{\text{top}} = P_{\text{dead}} + P_{\text{SDL}} + 0.25P_{\text{live}} + P_E$$

$$P_{\text{top}} = 40039.07 + 45485.37 + 0.25 \cdot 16338.88 + 37000.09$$

$$P_{\text{top}} = 126609.25 \text{ kg}$$

Axial stress ratio using demands from the load combination

$$\frac{P}{A_g f_c} = \frac{132924.78 * 9.81}{500 * 500 * 23.54} = 0.221$$

Determine shear stress ratio:

Shear reinforcement: DB10@ 10 cm, shear stirrups, with 3 legs resisting shear.

$$V = V_{\text{dead}} + V_{\text{SDL}} + 0.25V_{\text{live}} + V_E$$

$$V = 7.22 + 10.75 + 0.25 * 10.6 + 38397.87$$

$$V = 38418.49 \text{ kgf}$$

Shear stress ratio using demands from the load combination

$$\frac{V}{b_w d \sqrt{f_c}} = \frac{38418.49 * 9.81}{500 * 351.24 \sqrt{23.54}} = 0.442$$

Find shear reinforcing ratio

$$\frac{A_v}{b_w s} = \frac{3 * 0.785}{30 * 15} = 0.005$$

Determine condition using Table 10-11:

In order to determine the condition from Table 10-11, the flexural demands must be computed. According to §10.3.3, flexural loading is a deformation-controlled action. Therefore, demands will be computed using Eq. 7-34. Note that there are significant flexural demands at the base of the column, which is very different from the moment being 0 kg.m if modeled with a pinned base and no grade beams.

To determine  $V_p$  in ASCE 41-13 Table 10-11, run a commercially available P-M interaction analysis program with  $f_c' = 23.54$  MPa,  $f_y = 392.29$  MPa, and  $\phi = 1.0$ . Capacity-based design principles require that the maximum shear demand from seismic loading

cannot be larger than the shear demand when the column has reached its expected flexural capacity ( $V_p$ ). Also by capacity-based design principles, if the column reaches its flexural capacity, then the column will experience the associated shear based on the flexural capacity of the column.

- Bottom flexural capacity of the column

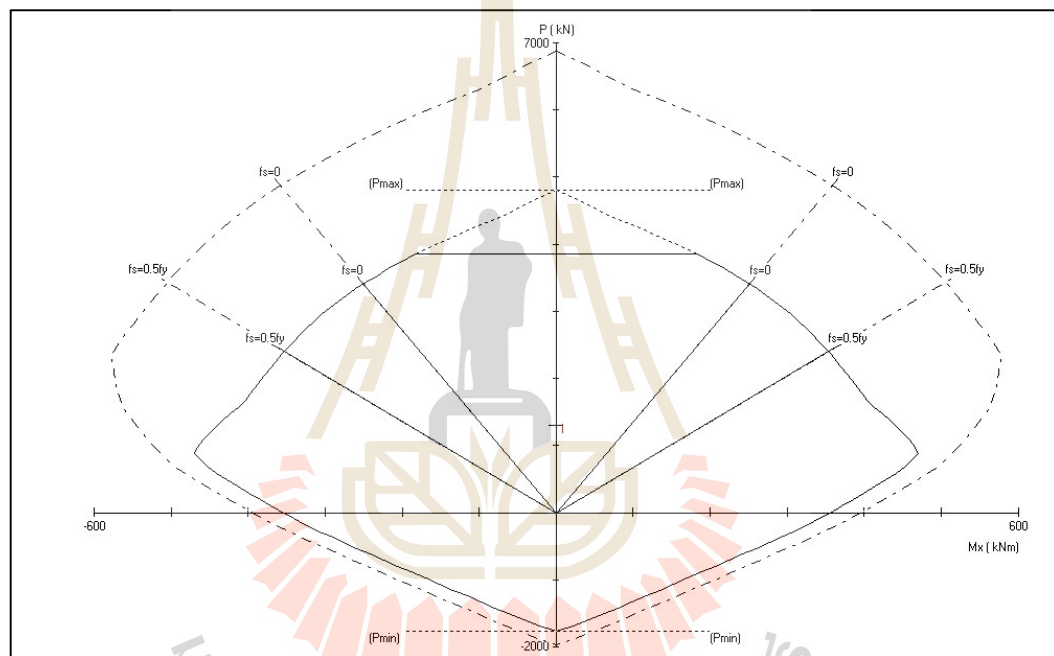


Figure E.14 Bottom flexural capacity of the column

- Top flexural capacity of the column

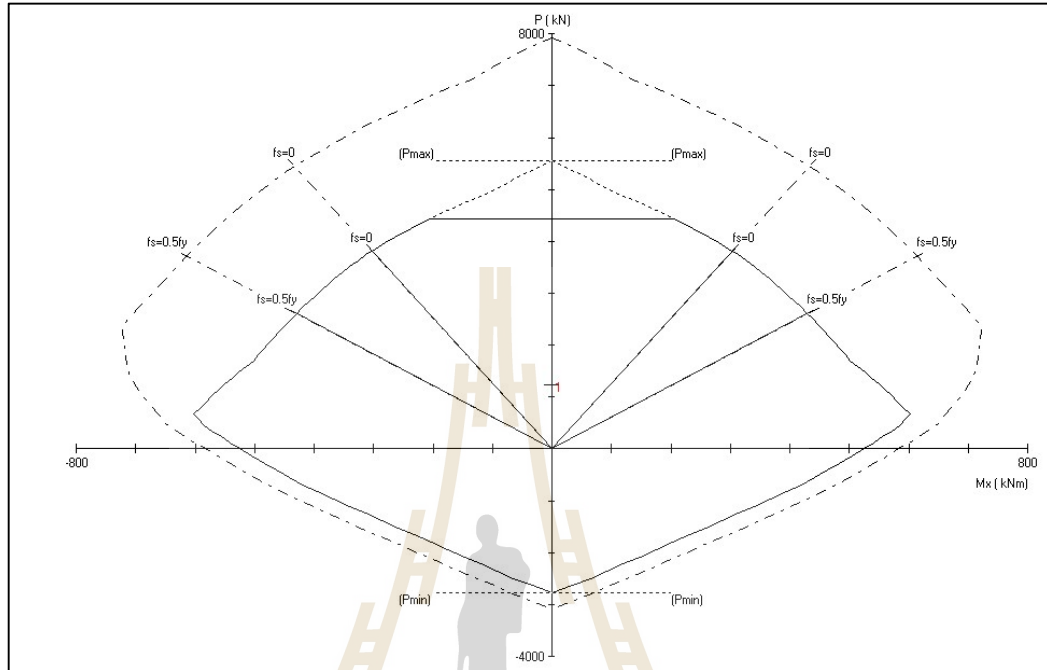
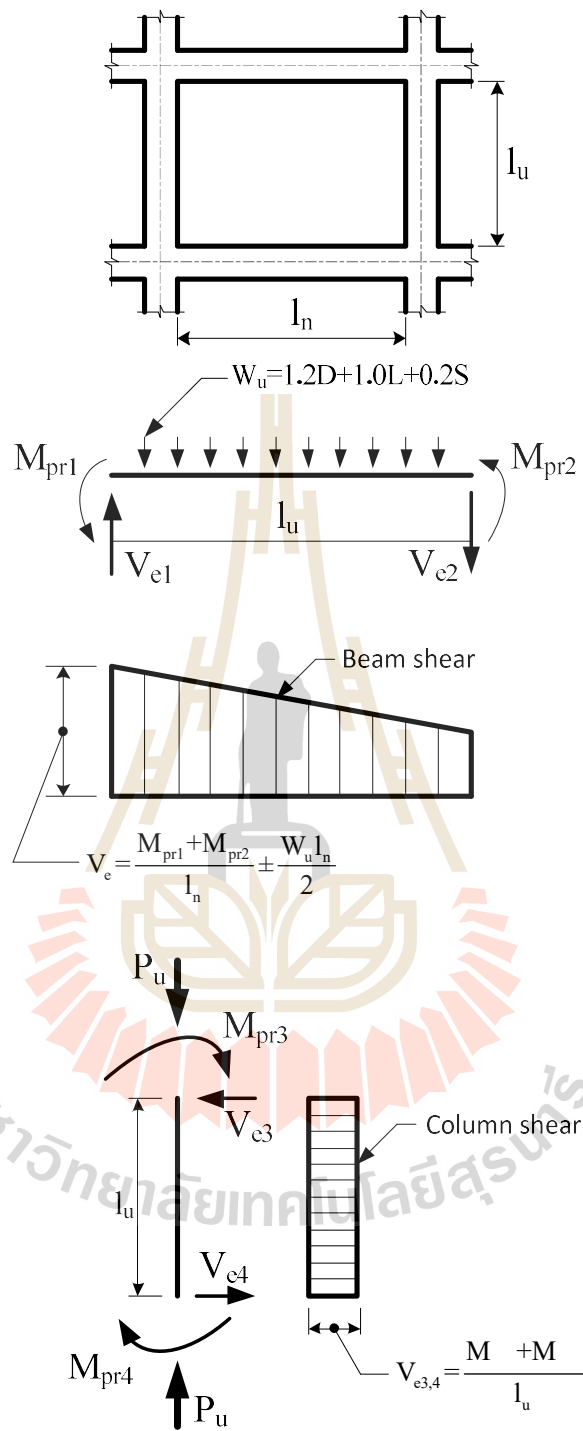


Figure E.15 Top flexural capacity of the column

$$M_{n,bot} = 441 \text{ KN.m}, M_{n,top} = 550 \text{ KN.m}$$

$$V_p = \frac{M_{n,top} + M_{n,bot}}{L} = \frac{441 + 550}{3.5} = 283 \text{ KN}$$

ACI 318 Fig R18.4.2



**Figure E.16** Design shears for beams and columns. (ACI 318-14)



$$V_o = V_s + V_c$$

$$V_o = \frac{A_v f_y d}{s} + \lambda \left( \frac{6\sqrt{f'_c}}{\frac{M}{Vd}} \sqrt{1 + \frac{N_u}{6\sqrt{f'_c} A_g}} \right) 0.8 A_g$$

$$M = 8.96 + 12.21 * 0.25 + 13.03 + 76627.24 = 76651.67 \text{ kg.m}$$

$$\frac{M}{Vd} = \frac{76651.67}{0.351 * 28300} = 7.7 > 4$$

the largest ratio of moment to shear times effective depth under design loadings for the column but shall not be taken greater than 4 or less than 2.

$N_u$  is the axial compression force (set to zero for tension force)

$$N_u = 42139.07 + 47585.37 + 0.25 * 16338.88 = 93809.16 \text{ kg}$$

$$V_o = \frac{3 * 0.785 * 4000 * 35.1}{10} + \left( \frac{6\sqrt{240}}{4} \sqrt{1 + \frac{93809.16}{6\sqrt{240} * 4000}} \right) 0.8 * 2500$$

$$V_o = 88033.34 \text{ kg}$$

$$\frac{V_p}{V_o} = 0.32$$

**Table E.1** Transverse Reinforcement Details: Condition to Be Used for Columns in table E.2

Shear Capacity Ratio	ACI 318 Conforming Seismic Details with 135-Degree Hooks	Closed Hoops With 90-Degree Hooks	Other (Including Lap-Spliced Transverse Reinforcement)
$V_p/V_o \leq 0.6$	i <sup>a</sup>	ii	ii
$1.0 \geq V_p/V_o > 0.6$	ii	ii	iii
$V_p/V_o > 1.0$	iii	iii	iii

<sup>a</sup>To qualify for condition i, a column should have  $A_v/b_w s \geq 0.002$  and  $s/d \leq 0.5$  within flexural plastic hinge region. Otherwise, the column is assigned to condition ii

For  $V_p/V_o \geq 0.6$ , the condition is adjusted from condition i to ii for columns with 90-degree hooks or lap-spliced transverse reinforcement to reflect the observation from experiments that poor transverse reinforcement details can result in decreased deformation capacity. Assume that the transverse reinforcements of the column are closed hoops with 90° hooks. According to ASCE 41-13 Table C.1, the condition to be used in ASCE 41-13 Table C.2 as shown in figure 3.5 is Condition (ii) (flexure-shear failure, where yielding in flexure is expected before shear failure), because of the combination of  $V_p/V_o \geq 0.6$  and the assumed closed hoops with 90-degree hooks.

**Table E.2** Modeling Parameters and Numerical Acceptance Criteria for Nonlinear Procedures-Reinforced Concrete Columns

Conditions			Acceptance Criteria <sup>a</sup>		
			Plastic Rotations Angle (radians)		
			Performance Level		
			IO	LS	CP
Condition ii. <sup>b</sup>					
$\frac{P}{A_g f'_c}$	$\rho = \frac{A_v}{b_w s}$	$\frac{V}{b_w d \sqrt{f'_c}}$ <sup>d</sup>			
≤0.1	≥0.006	≤3 (0.25)	0.005	0.045	0.060
≤0.1	≥0.006	≥6 (0.5)	0.005	0.045	0.060
≥0.6	≥0.006	≤3 (0.25)	0.003	0.009	0.010
≥0.6	≥0.006	≥6 (0.5)	0.003	0.007	0.008
≤0.1	≤0.0005	≤3 (0.25)	0.005	0.010	0.012
≤0.1	≤0.0005	≥6 (0.5)	0.004	0.005	0.006
≥0.6	≤0.0005	≤3 (0.25)	0.002	0.003	0.004
≥0.6	≤0.0005	≥6 (0.5)	0.0	0.0	0.0

NOTE:  $f'_c$  is in lb/in.2 (MPa) units.

<sup>a</sup>Values between those listed in the table should be determined by linear interpolation.

<sup>b</sup>Refer to Section 10.4.2.2.2 for definition of conditions i, ii, and iii. Columns are considered to be controlled by inadequate development or splices where the calculated steel stress at the splice exceeds the steel stress specified by Eq. (10-2). Where more than one of conditions i, ii, iii, and iv occurs for a given component, use the minimum appropriate numerical value from the table.

<sup>c</sup>Where  $P/A_g f'_c > 0.7$ , the plastic rotation angles should be taken as zero for all performance levels unless the column has transverse reinforcement consisting of hoops with 135-degree hooks spaced at  $\leq d/3$  and the strength provided by the hoops ( $V_s$ ) is at least 3/4 of the design shear. Axial load  $P$  should be based on the maximum expected axial loads caused by gravity and earthquake loads.

<sup>d</sup> $V$  is the design shear force from NSP or NDP.

According to table C.2, the conditions have axial stress ratio, shear reinforcing ratio, and shear stress ratio that equal to 0.221, 0.005, and 0.442, respectively. By using these conditions, we can determine the performance level at the condition ii. The performance levels have Immediate Occupancy, Life Safety, and Collapse Prevention that equal to 0.004, 0.018, and 0.0231, respectively. Values between those listed in the table should be determined by linear interpolation. These values used to compare with the plastic hinge rotation, gotten from the SAP2000 that equal 0.0093 radians. The performance level in the first story is Life Safety (LS) performance level.

## 2. BEAM

Shear force at grid 5-D

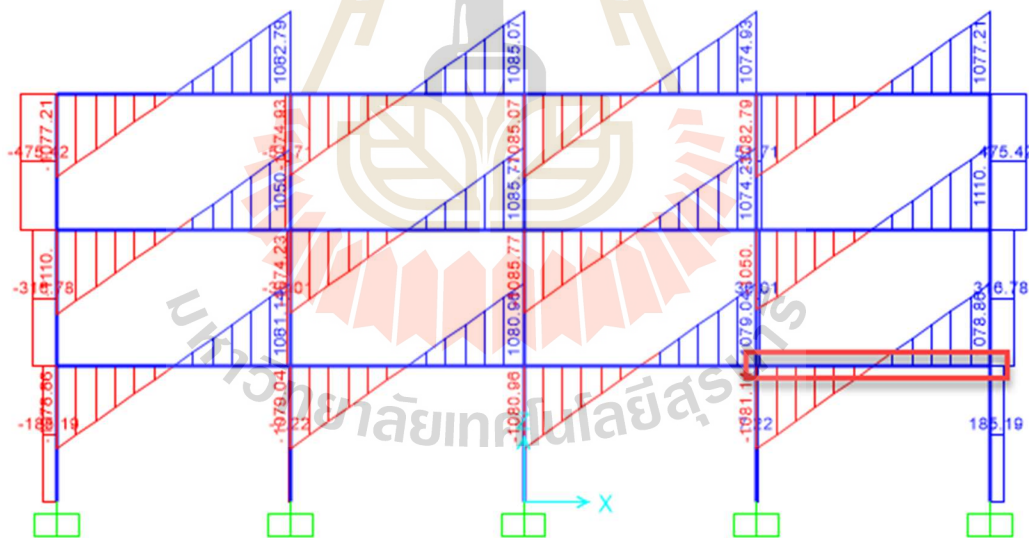


**Figure E.17** Dead load case shear force of the column as shown in the rectangular box

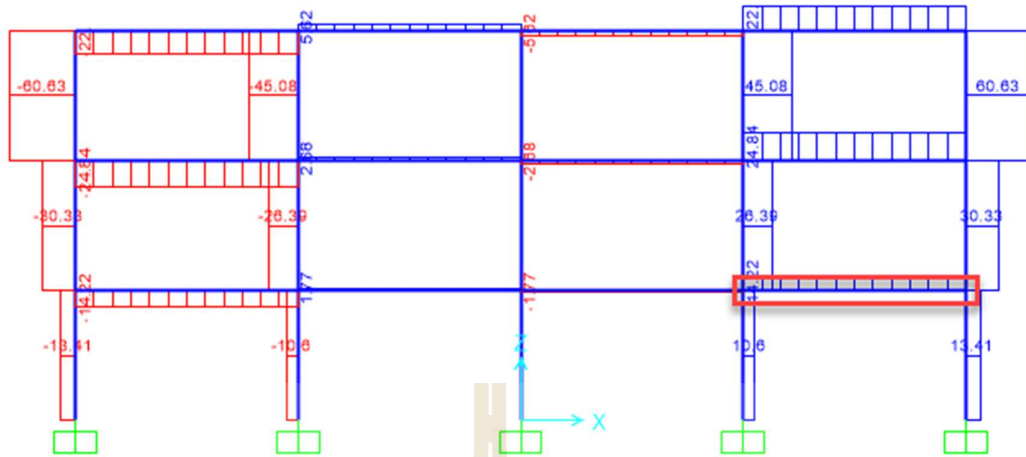


**Figure E.18** Live load case shear force of the column as shown in the rectangular box

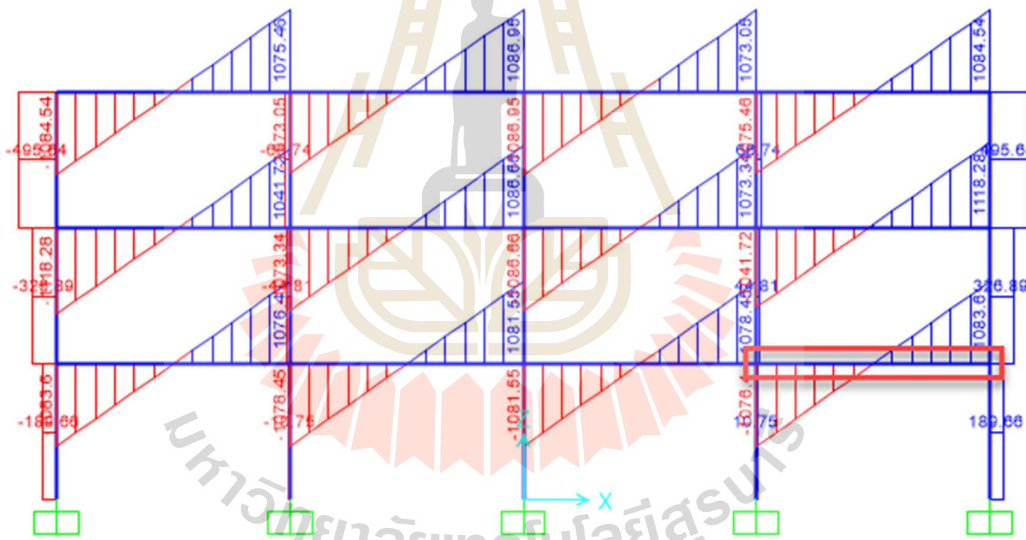


**Figure E.19** Super impose dead load case shear force of the column as shown in the rectangular box

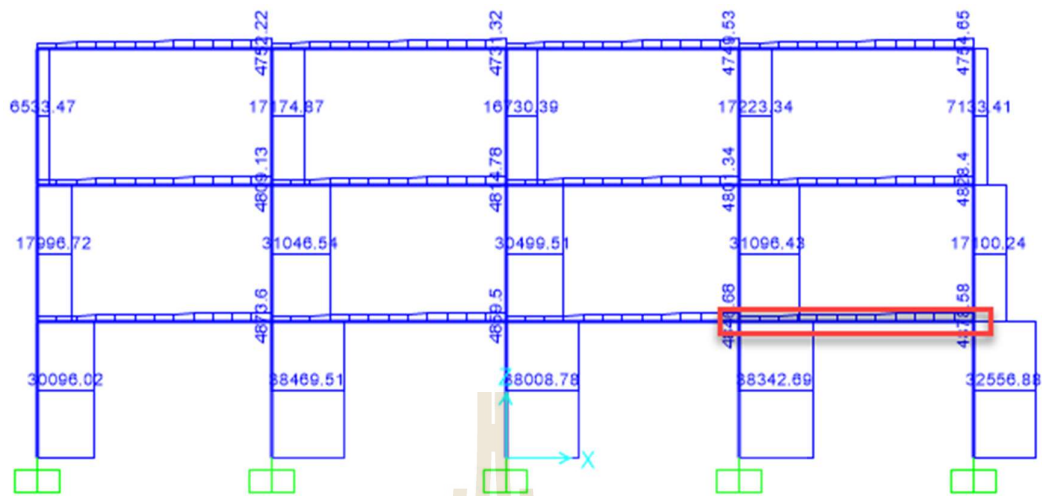


**Figure E.20** Lateral force load case shear force of the column as shown in the rectangular box

Determine if beam is shear controlled

The shear demand at the flexural yielding of the beam is found for both directions of loading and compared to the shear capacity of each side of the beam. The beam may not be shear controlled in one direction of loading and shear controlled in the other if the longitudinal reinforcing is different on the left side of the beam from the right side. Also the shear reinforcing may be different on the different sides of the beam causing one side of the beam to have more shear capacity than the other side. In the example building, the shear reinforcing is the same, but the longitudinal reinforcing is slightly different on each side of the beam.

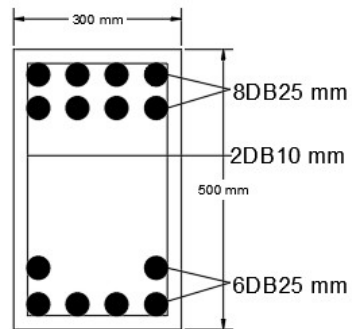


**Figure E.21** Beam section of the first floor

Concrete shear capacity:

$$V_c = 0.53 \sqrt{f'_c} b_w d = 0.53 * \sqrt{240} * 30 * 41.3$$

$$V_c = 10173 \text{ kg}$$

Shear reinforcement capacity:

$$V_s = A_s f_y \frac{d}{s} = \frac{2 * 0.785 * 4000 * 41.3}{12}$$

$$V_s = 21613.67 \text{ kg}$$

Reduction of shear reinforcement effectiveness due to spacing:

$$\text{For } \frac{s}{d} = \frac{12}{13.8} = 0.87 > 0.5, \text{ use } \alpha_{sp} = 2 * (1 - 0.87) = 0.26$$

$$V_n = V_c + \alpha_{sp} V_s = 10173 + 0.26 * 21613.67$$

$$V_n = 15792.55 \text{ kg}$$

$$f'_s = \left( \frac{c-d'}{c} \right) \epsilon_{cu} E_s$$

$$M_n = 0.85 f'_c ab \left( d - \frac{a}{2} \right) + A'_s f'_s (d-d')$$

Determine longitudinal reinforcing ratios:

$$\rho = \frac{A_s}{bd} = \frac{24.55}{30 \times 41.3} = 0.0182$$

$$\rho' = \frac{A'_s}{bd} = \frac{39.28}{30 \times 41.3} = 0.029$$

$$\rho - \rho' = -0.0108$$

$$(\rho - \rho')_{\min} = 0.85 \beta_1 \left( \frac{f'_c}{f_y} \right) \left( \frac{d'}{d} \right) \left( \frac{6120}{6120 - f_y} \right) = 0.026$$

$\rho - \rho' < (\rho - \rho')_{\min}$  the compressive steel may reach the yielding point

$$\rho_{\text{bal}} = \frac{0.85 \beta_1 f'_c}{f_y} \left( \frac{6120}{6120 + f_y} \right) = 0.026$$

Determine ratio of difference in longitudinal reinforcing ratios to balanced reinforcing ratio:

$$\frac{\rho - \rho'}{\rho_{\text{bal}}} = \frac{0.0182 - 0.029}{0.026} = -0.42$$

Shear stress ratio using demands from the load combination

$$V = 1078.86 + 1083.6 + 0.25 \times 14.22 + 4878.88 = 7044.9 \text{ kg} = 69110.42 \text{ N}$$



$$\frac{V}{b_w d \sqrt{f'_c}} = \frac{69110.42}{300 * 413 * \sqrt{23.54}} = 0.115$$

According to footnote C in Table E.3, the transverse reinforcing is conforming if the spacing of the hoops is less than  $d/3$  in the regions where flexural plastic hinges are expected to occur and if (for components with moderate- to high-ductility demand) the strength provided by the hoops is at least 75% of the design shear demand.

$$\frac{d}{3} = \frac{413}{3} = 138 \text{ mm} > s = 120 \text{ mm}$$

At this stage in the analysis, the ductility demand on this component is unknown. However, it can be reasonably assumed that the ductility demand will be at least moderate for this component for the given hazard. If the spacing of the hoops was less than  $d/3$ , the transverse reinforcement capacity must be at least 75% of the design shear in order to be considered conforming for the purposes of determining the value of IO, LS and CP in Table E.3.

**Table E.3** Modeling Parameters and Numerical Acceptance Criteria for Nonlinear Procedures-Reinforced Concrete Beams

Conditions			Acceptance Criteria <sup>a</sup>		
			Plastic Rotations Angle (radians)		
			Performance Level		
			IO	LS	CP
Condition ii. Beams controlled by flexure <sup>b</sup>					
$\frac{\rho - \rho'}{\rho_{bal}}$	Transverse Reinforcement <sup>c</sup>	$\frac{V}{b_w d \sqrt{f'_c}}$ <sup>d</sup>			
$\leq 0.0$	C	$\leq 3$ (0.25)	0.010	0.025	0.050
$\leq 0.0$	C	$\geq 6$ (0.5)	0.005	0.020	0.040
$\geq 0.5$	C	$\leq 3$ (0.25)	0.005	0.020	0.030
$\geq 0.5$	C	$\geq 6$ (0.5)	0.005	0.015	0.020
$\leq 0.0$	NC	$\leq 3$ (0.25)	0.005	0.020	0.030
$\leq 0.0$	NC	$\geq 6$ (0.5)	0.0015	0.010	0.015
$\geq 0.5$	NC	$\leq 3$ (0.25)	0.005	0.010	0.015
$\geq 0.5$	NC	$\geq 6$ (0.5)	0.0015	0.005	0.010

NOTE:  $f'_c$  in lb/in.2 (MPa) units.

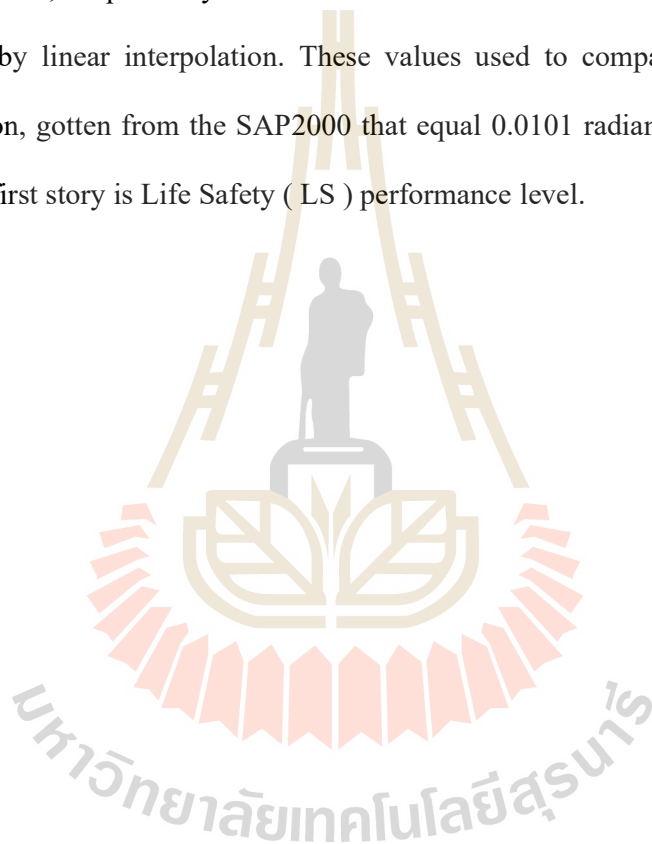
<sup>a</sup>Values between those listed in the table should be determined by linear interpolation.

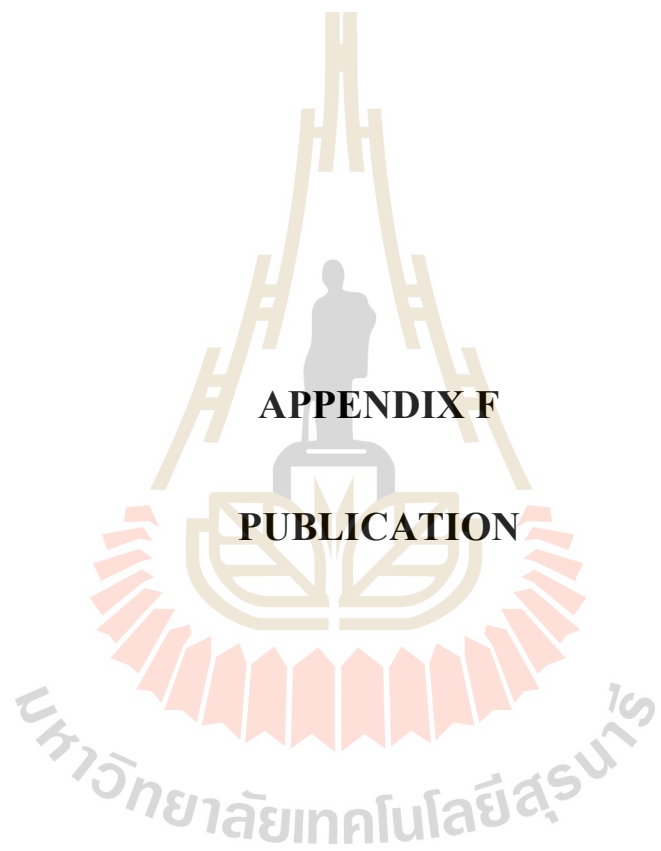
<sup>b</sup>Where more than one of conditions i, ii, iii, and iv occur for a given component, use the minimum appropriate numerical value from the table.

<sup>c</sup>“C” and “NC” are abbreviations for conforming and nonconforming transverse reinforcement, respectively. Transverse reinforcement is conforming if, within the flexural plastic hinge region, hoops are spaced at  $\leq d/3$ , and if, for components of moderate and high ductility demand, the strength provided by the hoops ( $V_s$ ) is at least 3/4 of the design shear. Otherwise, the transverse reinforcement is considered nonconforming.

<sup>d</sup> $V$  is the design shear force from NSP or NDP.

According to table E.3, the conditions have ratio of difference in longitudinal reinforcing ratios to balanced reinforcing ratio, transverse reinforcement, and shear stress ratio that equal to -0.442, C, and 0.115, respectively. By using these conditions, we can determine the performance level at the condition i. The performance levels have Immediate Occupancy, Life Safety, and Collapse Prevention that equal to 0.01, 0.025, and 0.05, respectively. Values between those listed in the table should be determined by linear interpolation. These values used to compare with the plastic hinge rotation, gotten from the SAP2000 that equal 0.0101 radians. The performance level in the first story is Life Safety ( LS ) performance level.





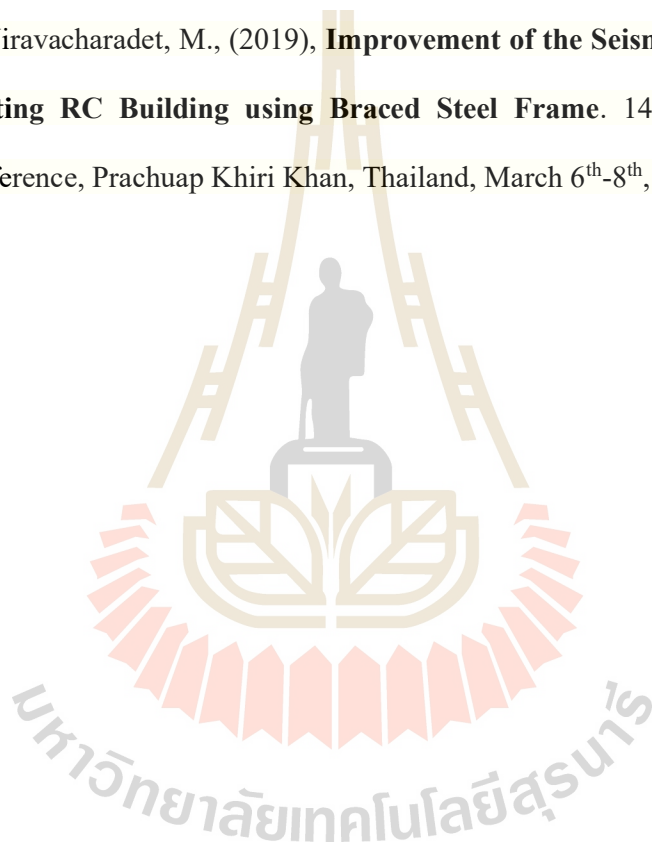
**APPENDIX F**

**PUBLICATION**

## List of Publications

Khoy, R., Jiravacharadet, M., and Hoy, M., (2019). **Seismic Performance Evaluation of Existing RC Building using Braced Steel Frames.** International Journal of Civil Engineering and Technology (IJCIET). January, 2019, Vol. 10, pp. 1758-1771.

Khoy, R., Jiravacharadet, M., (2019), **Improvement of the Seismic Performance of Existing RC Building using Braced Steel Frame.** 14<sup>th</sup> Annual Concrete Conference, Prachuap Khiri Khan, Thailand, March 6<sup>th</sup>-8<sup>th</sup>, 2019, pp. 1-10.



**International Journal of Civil Engineering and Technology (IJCIET)**

Volume 10, Issue 01, January 2019, pp. 1758-1771, Article ID: IJCIET\_10\_01\_163

Available online at <http://www.iaeme.com/ijciyet/issues.asp?JType=IJCIET&VType=10&ITType=01>

ISSN Print: 0976-6308 and ISSN Online: 0976-6316

© IAEME Publication



Scopus Indexed

## **SEISMIC PERFORMANCE EVALUATION OF EXISTING RC BUILDING USING BRACED STEEL FRAMES**

**Rithy Khouy**

Graduate Student, School of Civil Engineering, Suranaree University of Technology  
Nakhon Ratchasima, Thailand.

**Mongkol Jiravacharadet**

Assistant Professor, School of Civil Engineering, Suranaree University of Technology  
Nakhon Ratchasima, Thailand.

**Menglim Hoy**

Lecturer, School of Civil Engineering, Suranaree University of Technology  
Nakhon Ratchasima, Thailand.

### **ABSTRACT**

*Earthquake is a natural disaster that destroyed the large property and two deaths with many injuries during this decade, occurring at the northern of Thailand. By this cause, this paper aims to evaluate the performance level of existing reinforced concrete building by retrofitting with the braced steel frames. Moreover, a three-story building is analysed in SAP2000, used the Nonlinear Static Procedure Method. Therefore, three different methods are chosen to study in this paper. The first of all, Displacement Coefficient Method presented in ASCE/SEI 41-13 and FEMA 440, used to calculate target displacement to point out building performance levels. The second method, Capacity Spectrum Method published in ACT 40, used deformation limits to compare with total roof displacement ratio ( $\Delta_{roof top} / H$ ) at the performance point to classify various performance levels. The last one, The ASCE/SEI 41-13 uses plastic rotation limit criteria to compare with maximum plastic hinge rotation for member evaluation of the RC frames. According to the result before retrofitting, the first and second methods meet Life Safety (LS) and Immediate Occupancy (IO) levels, respectively. The third method of this paper separated into column and beam performance levels which meet performance levels in both Life Safety (LS) levels. From the experiment, It shows that if we use the concentrically braced steel frames to retrofit the structure, it will lie*

*in Immediate Occupancy (IO) level for all of the methods. Furthermore, the construction works of outer steel frames do not stop the function of the buildings.*

**Keywords:** Nonlinear static procedure, Braced steel frame, Retrofitting, Seismic performance evaluation, SAP2000.

**Cite this Article:** Rithy Khouy, Mongkol Jiravacharadet and Menglim Hoy, Seismic Performance Evaluation of Existing Rc Building Using Braced Steel Frames, International Journal of Civil Engineering and Technology, 10(01), 2019, pp. 1758–1771

<http://www.iaeme.com/IJCIET/issues.asp?JType=IJCIET&VType=10&IType=01>

## 1. INTRODUCTION

Many existing reinforced concrete have designed to use conventional code that never considers earthquakes to combine with gravity and another load because they believe that Thailand does not require seismic load for analyzing the building in the past, but everything has changed after the earthquakes have occurred in the north part of Thailand. By the way, many structures have collapsed and damaged that need to redesign and to strengthen for the whole or element of the building. The new standard, DPT.1303-57, is to assess and retrofitting of the building structure in the area of the earthquake zones, This standard referred from ASCE/SEI 41-06 that updated to ASCE/SEI 41-13. Therefore, this paper has selected some standards, ASCE/SEI 41-13, FEMA 440, ATC 40 to assess building performance levels. After that, the nonlinear static analysis is one of the methods that use to evaluate the structural performances. There are plenty of technologies that build up the structure to resist the lateral load such as steel plate shear wall, damping, steel bracing, shear wall and so on. Moreover, braced steel frames were chosen to research the reaction of the building that opposed to the dynamic load. The evidence has seen clearly about the characteristics of the structural behaviors before and after retrofitting braced steel frames that to upgrade the strength, to increase the structural stiffness, to reduce structural deformation, to reduce construction time and to construct outside the building that does not affect building service.

This paper is a case study that utilizes many standards, separating into three different procedures like the Displacement Coefficient Method, the Capacity Spectrum Method, and member-level performance to assess the building performance levels. Additionally, these varied approaches obtained similar results before retrofitting and the same results after retrofitting the building.

## 2. PARAMETERS INFORMATION FOR SEISMIC ASSESSMENT

A three-story building that locates in Chiang Rai city, Chiang Rai province, assume an existing building for studying the structural performance levels, is an ordinary reinforced concrete moment frame. This building is the symmetry configuration, 4x4@6 meters bays in both X and Y directions as shown in figure 1 and 2, a low-rise structure located in the high seismic zone in Thailand. The beam and column dimensions are 30x50 cm and 50x50 cm. The slab thickness and story high are 20 cm and 350 cm. The material properties determined to be 23.54 N/mm<sup>2</sup> for concrete compressive strength and to be 392.27 N/mm<sup>2</sup> for both longitudinal and transversal reinforcement bars. Gravity and earthquake load that to be referred from ASCE/SEI 41-13 used to account for the seismic assessment. The soil class for this building is site class D with many parameters to determine earthquake load such as the reduction factor (R) is 3, the overstrength factor ( $\Omega_0$ ) is 3, the deflection amplification factor ( $C_d$ ) is 2.5, and the importance factor (I) is 1.5. The others required parameters are the spectral response acceleration parameter at short

period is 0.798g, the spectral response acceleration parameter at 1 s period is 0.232g and the fundamental period of the building  $T$  is 0.21 seconds. The site coefficient  $F_a$  and  $F_v$  that got from the spectral response acceleration parameter short and 1 s period on the site class D are 1.181 and 1.936, respectively. From table 1.6-1 and 1.6-2 of DPT 1302-52 (Thai Code), it shows that  $S_{D5} > 0.5$  and  $S_{D1} > 0.2$  used to point out the risk category, meet the high level of seismicity and high level of seismicity that similar to the risk category D of ASCE 7, respectively. All of the parameters used to calculate the base shear coefficient  $C$ , is 0.315g to determine the pseudo seismic force then simulate as the pushover static load.

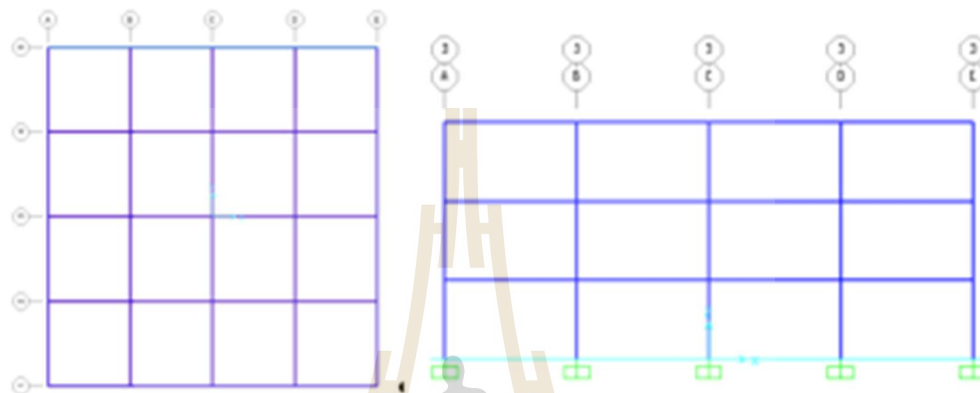


Figure. 1 Plan view

Figure. 2 Elevation view

### 3. PERFORMANCE EVALUATION OF EXISTING BUILDING

#### 3.1. Nonlinear Static (Pushover) Analysis

The nonlinear pushover analysis is carried out the analytical building model that consists of gravity and lateral load pattern. Before running the lateral load, the gravity load that considered as linear static is applied to the analyzed model in a step-by-step following ASCE/SEI 41-13 equation 7.3. At the end of the analytical gravity load, the lateral force continues to apply monotonically increasing in a stepwise till the building reached a target displacement or collapsed condition. The lateral load pattern is performed on the structure with two different types the first mode shape of the analysis in the direction under consideration or the load pattern defined by the user. The moment-curvature analyses are performed base on the section properties and the reinforcement at the plastic hinges in all members. The moment-rotation that to be instead of moment-curvature is used to performance elevation levels all the members. The relationship between base shear and lateral displacement of the control node is plotted to establish for control node displacements multiple by 1.5 of the target displacement. The control node displacement increases monotonically at every step of the analysis to reach the equilibrium between the external and the internal force of the structural deformation at this step. When the analysis reaches the equilibrium, then the analysis starts to the next step. During the proceeded analysis, the analysis will be terminated when the analysis meets the termination condition such as the target displacement, the maximum deformation of element and component. Therefore, deformation -controlled and force-controlled action compared to the corresponding acceptance criteria to determine performance elevations.



### 3.2. Displacement Coefficient Method of the Existing Building

Displacement coefficient method was used to calculate the target displacement of the control node on the roof that presented in both ASCE 41-13 Eq. 7-28 and FEMA 440 Eq. 3-9 (2005). The building that used to evaluate the performance levels is the symmetry configuration, needed only one direction for qualified its performance. The magnitude of the target displacement that shown in table 1 obtained from the maximum value between ASCE 41-13 Eq. 7-28 and FEMA 440 Eq. 3-9 to compare with the data in each step as shown in table 2. The maximum target displacement between two standards equals 0.0517 m, uses to point out in table 2 that meet in step 3 of the 0.092645 m displacements, and performance level of the structure is met in between Immediate Occupancy (IO) to Life Safety (LS) levels.

Table 1 Parameter and target displacement ( $\delta_t$ ) of the existing building

Parameter	FEMA 440	ASCE 41-13	Note
$C_0$	1.233	1.350	ASCE 41-13 Table 7-5. Values for Modification Factor
$C_1$	1.133	1.090	Modification Factor to relate the expected max disp
$C_2$	1.011	1.009	Values for Modification Factor
$C_3$	1.000		Building with post-yield stiffness
$S_a$	0.628	0.628	Spectral response acceleration
$T_p$	0.425	0.472	Effective natural vibration
$\delta_t$	0.040	0.0517	FEMA 440: $\delta_t = C_0 C_1 C_2 C_3 S_a (T_p / 2\pi)^2 g$ ASCE 41-13: $\delta_t = C_0 C_1 C_2 S_a (T_p / 2\pi)^2 g$

Table 2 Pushover steps of the existing building

Step	Displacement m	Base Force kgf	A to B	B to IO	IO to LS	LS to CP	CP to C	C to D	D to E	Beyond E	Total
0	2.61E-06	0.00	390	0	0	0	0	0	0	0	390
1	0.014988	291624.52	388	2	0	0	0	0	0	0	390
2	0.049999	832423.50	290	100	0	0	0	0	0	0	390
3	0.092645	1127561.68	242	114	34	0	0	0	0	0	390
4	0.096581	1142979.45	238	114	38	0	0	0	0	0	390
5	0.101275	1158335.73	234	106	50	0	0	0	0	0	390
6	0.108365	1174948.23	222	114	54	0	0	0	0	0	390
7	0.111575	1179462.12	218	117	55	0	0	0	0	0	390
8	0.112596	1171650.64	218	117	55	0	0	0	0	0	390
9	0.111581	1171688.29	218	117	55	0	0	0	0	0	390
10	0.112132	1174498.65	218	117	55	0	0	0	0	0	390
11	0.114282	1180434.95	216	115	59	0	0	0	0	0	390
12	0.116744	1183094.81	216	109	65	0	0	0	0	0	390
13	0.116749	1137346.28	216	109	65	0	0	0	0	0	390
14	0.121715	1178674.70	214	111	65	0	0	0	0	0	390
15	0.126755	1194282.24	208	114	68	0	0	0	0	0	390
16	0.168523	1243069.84	202	114	49	0	0	25	0	0	390
17	0.207791	1215594.98	202	114	24	0	0	50	0	0	390
18	0.29217	1040064.96	202	114	24	0	0	50	0	0	390
19	0.354992	910430.01	202	114	24	0	0	50	0	0	390
20	0.397037	828796.53	202	114	24	0	0	50	0	0	390
21	0.420003	788401.09	202	114	24	0	0	50	0	0	390

### 3.3. Capacity Spectrum Method of the Existing Building

The nonlinear static analysis procedure has also included the capacity spectrum method (CSM) that uses the intersection of the capacity-demand curve to estimate maximum roof displacement

at the performance point. The performance point that found to check the structural performance levels of the IO, LS or CP depended on deformation limits specified in ATC-40 were 0.01, 0.02 and 0.33( $V_i/P_i$ ) as shown in table 3, respectively. Building design needs to consider the performance level that bases upon the importance and function of the building such as the hospital to be considered Immediate Occupancy (IO) level. A case studying the three-story building used SAP2000, analysed the pushover static analysis, and determined performance point that represents in the Acceleration-Displacement Response Spectra (ADRS) as shown in figure 3. To depend on figure 3, it shows that the magnitude of base shear and tip displacement at the performance point are 6605789 N and 0.04 m, respectively. To determine the building performance levels, it can use the deformation limits to compare with the roof drift ratio at the performance point as follows: Roof drift ratio at the performance point is  $0.04/10.5=0.0038<0.01$ . Referring to this value, it can point out the structural performance level, meets the immediate occupancy (IO) level.

Table 3 Deformation limits

Standard	Interstory drift limit	Structural Performance Levels			
		Collapse Prevention	Life Safety	Damage Control	Immediate Occupancy
ATC 40	Maximum total drift	$0.33 \frac{V_i}{P_i}$	0.02	0.01-0.02	0.01
	Maximum inelastic drift	no limit	no limit	0.005-0.015	0.005

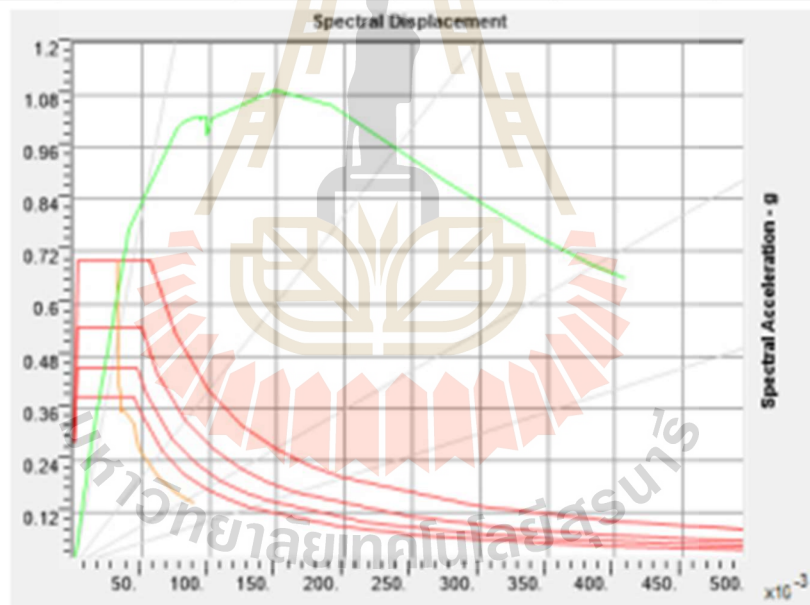


Figure. 3 Capacity spectrum curve of the existing building

### 3.4. Acceptance Criteria of the Existing Building

The acceptability of force and deformation actions shall be evaluated for each component that classified as primary or secondary, and each action shall be classified as deformation-controlled (ductile) action or force-controlled (nonductile) action. The primary elements provide the capacity of the structure to resist collapse under seismic forces induced by ground motion in any direction. The secondary elements do not contribute significantly or reliably in resisting

earthquake effects in any direction because of low lateral stiffness, strength or deformation capacity. Deformation-controlled or force-controlled uses the force-deformation curves to classify all the component actions as shown in figure 4.

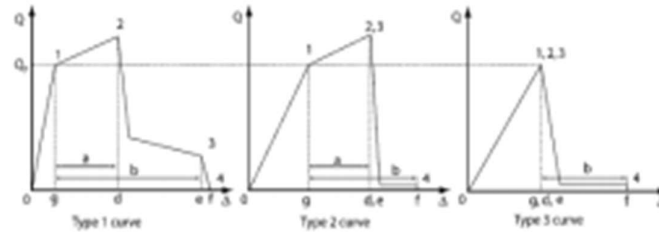


Figure. 4 Component force versus deformation curves

The type 1 curve in figure 4 is a ductile behaviour that there is an elastic behaviour range (point 0-1), followed by plastic behaviour range (1-3 on the curve), and non-negligible residual strength and ability to support gravity loads after 3. The plastic range includes a work hardening or softening range (points 1-2-3). Primary component actions with this behavior that classified as deformation-controlled for the flexural element depended on the plastic range for this value  $d \geq 2g$ . The type-2 curve in figure 4 is the ductile behavior that there is an elastic behavior range (point 0-1) and a plastic behavior range (1-3) followed by loss of strength and ability to support gravity loads beyond at point 2. The components with this behavior can categories as deformation-controlled if the plastic range is such that  $e > 2g$ , otherwise force-controlled. The type 3 curve as shown in figure 4 is a brittle (no ductile) behavior that there is an elastic behavior range (0-1 on the curve) followed by loss capacity of seismic-force resistant and able to support gravity loads beyond at point 1. The components with this behavior can consider as force-controlled. As shown in figure 5, it explains the acceptance criteria for deformation ratio for primary and secondary components that correspond to the target Structural Performance Levels of CP, LS, IO to be called Collapse Prevention, Life Safety, and Immediate Occupancy, respectively.

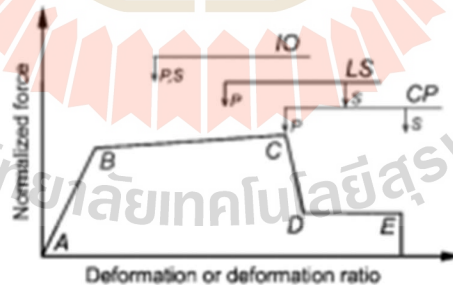


Figure. 5 Generalized component force-deformation relations

### 3.4.1 Performance Evaluation of the Column

According to ASCE 41-13, it shows that the axial compression of the column is classified as a force-controlled action. To know the column is adequate for axial compression, the lower-bound strength of column must be more than the maximum requirement force at the target displacement. Shear of the column has also classified as a force-controlled action. Both the

axial and shear capacity of the column are more than the maximum analysis force at the target displacement. The performance levels of the columns were shown in table 4. The value of the transverse reinforcement details ( $V/P \leq 0.6$ ) that is a condition to be used for the columns to which chooses the closed hoops with 90-degree hooks (ii). Other requirement parameters used to determine performance levels of the column as shown in table 4. The columns of the three stories building were classified in each story level such as the first story, the second story, and the third story met Life Safety (LS) level, Immediate Occupancy (IO) level, and Immediate Occupancy (IO) level, respectively. The 3<sup>rd</sup> step of the pushover analysis with plastic hinge rotation was shown in figure 6.

**Table 4** Numerical acceptance criteria for plastic hinge rotation of the columns of the existing building

Level	Conditions			Acceptance Criteria			Plastic Hinge Rotation (radians)	Performance Level
	$\frac{P}{A_g f_c}$	$\frac{A_v}{b_w s}$	$\frac{V}{b_w d_v f_c}$	Plastic Rotations Angle (radians)				
				IO	LS	CP		
3	0.075	0.005	0.137	0.0050	0.0275	0.036	0.0000	IO
2	0.149	0.005	0.255	0.0041	0.021	0.0272	0.0015	IO
1	0.221	0.005	0.442	0.0040	0.018	0.0231	0.0093	LS

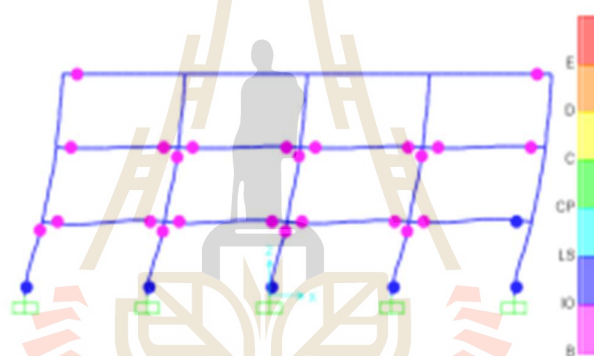


**Figure. 6** Performance levels of the existing building

### 3.4.2 Performance Evaluation of the Beam

The beam shear must be evaluated on three locations of the beam, which are yield zones for two ends of the beam, and the center of the beam known as a non-yield zone. After checking the result, it shows that the lower-bound shear capacity of the beam is more than the shear demand of the beam at the given performance objective. Moreover, the flexural of the beam must be checked at all locations where the loads produce the maximum effects to the beam elements. The beam was classified as positive and negative flexural demand that examined for adequacy at the left, middle, and right of beam segments and the left and right of beam segments, respectively. Before defining the performance levels of the beam, it must be examined for the shear-controlled or flexure-controlled. Base on the result, The beam shear capacity is more than the beam shear requirement, shown that the beam is the flexure-controlled (condition i). The transverse reinforcing was classified as conforming and nonconforming transverse reinforcement that abbreviated as "N" and "NC", respectively. The other required parameters are shown in table 5 that the first story, the second story, and the third story met Life Safety (LS) level, Immediate Occupancy (IO) level, and Immediate Occupancy (IO) level, respectively. The performance levels of the beams were shown in table 5.

**Table 5** Numerical acceptance criteria for plastic hinge rotation of the beams of the existing building

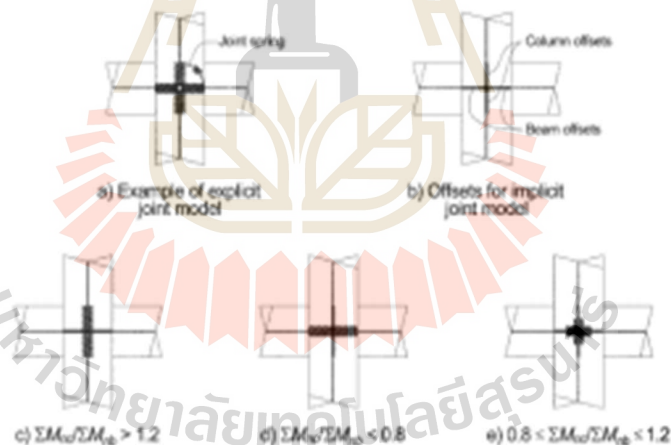
Level	Conditions			Acceptance Criteria			Plastic Hinge Rotation (radians)	Performance Level
	$\rho - \rho'$	Transverse reinforcement	$\frac{V}{d_w d_w \sqrt{f'_c}}$	Plastic Rotations Angle (radians)				
	$\rho_{bat}$			Performance Level				
3	0.00	C	0.111	0.01	0.025	0.05	0.0006	IO
2	-0.28	C	0.115	0.01	0.025	0.05	0.0047	IO
1	-0.42	C	0.115	0.01	0.025	0.05	0.0101	LS

### 3.4.3 Stiffness Calculation Beam-Column Joints

Joint stiffness shall be modelled the joint stiffness implicitly by adjusting the centerline model following by three types as shown in figure 7. Moreover, the interior column was used to calculate the ratio of the column-beam moments as shown in table 6. For example, it shows that the first story of the building has  $\Sigma M_{nc} / \Sigma M_{nb} > 1.2$ . Using beam rigid end length offset is 0.00 and column rigid end length offset is 1.00. The other stories of the building were shown in table 6.

1. For  $\Sigma M_{nc} / \Sigma M_{nb} > 1.2$ , column offsets are rigid and beam offsets are not;
2. For  $\Sigma M_{nc} / \Sigma M_{nb} < 0.8$ , beam offsets are rigid and column offsets are not; and
3. For  $0.8 \leq \Sigma M_{nc} / \Sigma M_{nb} \leq 1.2$ , half of the beam and column offsets are considered rigid.

Where:  $M_{nc}$  is the nominal moment capacities at the column and  $M_{nb}$  is the nominal moment capacities at the beam.

**Figure 7** Beam-Column joint stiffness modeling**Table 6** Joint stiffness of the interior columns

Level	$M_{nc}$ kg.m	$M_{nb}^+$ kg.m	$M_{nb}^-$ kg.m	$\Sigma M_{nc}$ kg.m	$\Sigma M_{nb}$ kg.m	$\frac{\Sigma M_{nc}}{\Sigma M_{nb}}$	Rigid Factor Column	Rigid Factor Beam
3	45500	25961.6	49492.8	45,500	75,454	0.75	0	1
2	94500	25961.6	49492.8	140000	75,454	1.56	1	0
1	99000	25961.6	49492.8	193500	75,454	1.64	1	0

#### 4. PERFORMANCE EVALUATION OF RETROFITTING BUILDING

Steel bracing is the best method for global retrofit of the existing building that sees much lowrise, mid rise, highrise building, using many types of steel bracing to resisting the earthquake load. By the way, the structure with inverted V Bracing gives minimum Storey drift as compared to other X, V. The magnitudes of storey drift for all the stories are found to be within limits, i.e. 0.004 times to storey height according to IS 1893:2002 (Part I) [1]. For the story drift, it is not enough to choose inverted V that should be studied for other cases to qualified as the best steel bracing. The results of the study and analysis of the retrofit model to resist earthquakes from all data. Knee Braced strengthening is inappropriate. The inverted V models provide better engineering results and less budget than others [2]. Inverted V bracing system significantly reduces the bending moment and shear force than V type bracing system [3]. Node displacements and storey drifts are minimum for inverted V braced frame as compared to V braced frame [3]. This paper is used inverted V steel bracing that has yield strength is 245.17 N/mm<sup>2</sup>, ultimate strength is 392.27 N/mm<sup>2</sup>, and modulus of elasticity is 200055.66 N/mm<sup>2</sup>. The outer steel frames have the column dimension of W300X300X94, beam dimension of W350X250X79.7, and bracing dimension of HSS200X200X8.0 as shown in figure 8.

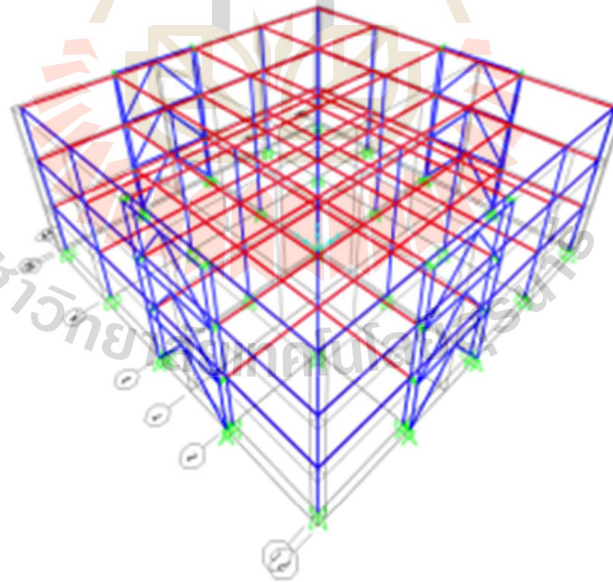


Figure. 8 3D view of the braced steel frame

#### 4.1 Displacement Coefficient Method of the Retrofitted Building

Displacement coefficient method was also used to calculate the target displacement of the retrofitted building at the control node on the roof that similar the procedure as the existing building. The magnitude of the target displacement of the retrofitted building that computed by using the method of ASCE 41-13 and FEMA 440 was shown in table 7. The result from table 7 needed to compare with the data in each step as shown in table 8. The maximum target displacement of ASCE 41-13 equals to 0.0263 m used to point out in table 8 that met in step 2 of the 0.026578 m displacements, and performance level of the structure is met in Immediate Occupancy (IO) level.

Table 7 Parameter and target displacement of the retrofitted building

Parameter	FEMA 440	ASCE 41-13	Note
$C_0$	1.218	1.373	ASCE 41-13 Table 7-5. Values for Modification Factor
$C_1$	1.122	1.101	Modification Factor to relate the expected max disp
$C_2$	1.006	1.005	Values for Modification Factor
$C_3$	1.000		Building with post-yield stiffness
$S_a$	0.628	0.628	Spectral response acceleration
$T_g$	0.304	0.333	Effective natural vibration
$\delta_t$	0.020	0.0263	FEMA 440: $\delta_t = C_0 C_1 C_2 C_3 S_a (T_g / 2\pi)^2 g$ ASCE 41-13: $\delta_t = C_0 C_1 C_2 S_a (T_g / 2\pi)^2 g$

Table 8 Pushover steps of the retrofitted building

Step	Displacement m	Base Force kgf	A to B	B to D	D to L5	L5 to OP	OP to C	C to D	D to E	Roof to E	Total
0	0	0	555	0	0	0	0	0	0	0	555
1	0.00958	5245.891	555	2	0	0	0	0	0	0	555
2	0.026578	9691.527	495	53	0	0	0	0	0	0	555
3	0.044003	11844.042	445	58	0	0	0	6	0	0	555
4	0.061428	12222.058	445	60	0	0	0	0	0	0	555
5	0.078853	12222.26	445	62	0	0	0	0	0	0	555
6	0.096278	12195.284	420	62	0	0	0	0	0	0	555
7	0.113703	12432.368	488	61	28	0	0	0	0	0	555
8	0.131128	12484.550	494	60	56	0	0	0	0	0	555
9	0.148553	12483.022	435	61	51	0	0	0	0	0	555
10	0.165978	12485.525	435	61	51	0	0	0	0	0	555
11	0.183403	12521.954	485	60	52	0	0	0	0	0	555
12	0.200828	12536.239	486	58	52	0	0	0	0	0	555
13	0.218253	12627.988	432	58	54	0	0	0	0	0	555
14	0.235678	12643.543	432	58	55	0	0	0	0	0	555
15	0.253103	12682.555	393	58	55	0	0	0	0	0	555
16	0.270528	12721.257	393	61	61	0	0	0	0	0	555
17	0.287953	12688.291	396	61	61	0	0	0	0	0	555
18	0.305378	12733.874	394	60	61	0	0	0	0	0	555
19	0.322803	12770.286	393	60	63	0	0	0	0	0	555
20	0.340228	12805.205	392	60	63	0	0	0	0	0	555
21	0.357653	12835.543	392	64	63	0	0	0	0	0	555
22	0.375078	12868.491	390	64	63	0	0	0	0	0	555
23	0.392503	12903.965	385	64	64	0	0	0	0	0	555
24	0.409928	12932.008	385	65	64	0	0	0	0	0	555
25	0.427353	12973.586	382	65	64	0	0	0	0	0	555
26	0.444778	12999.067	385	65	64	0	0	0	0	0	555
27	0.462203	13037.158	389	64	64	0	0	0	0	0	555
28	0.479628	13065.054	388	64	64	0	0	0	0	0	555
29	0.497053	13093.022	385	65	62	0	0	0	0	0	555
30	0.514478	13121.022	385	65	62	0	0	0	0	0	555
31	0.531903	13168.73	385	65	61	0	0	0	0	0	555
32	0.549328	13205.669	385	61	62	0	0	0	0	0	555
33	0.566753	13261.993	384	65	64	0	0	0	0	0	555
34	0.584178	13305.321	380	65	67	0	0	0	0	0	555
35	0.601603	13351.258	380	65	67	4	0	0	0	0	555
36	0.619028	13393.829	376	65	62	0	0	0	0	0	555
37	0.636453	13434.504	374	65	65	0	0	0	0	0	555
38	0.653878	13473.202	374	65	64	0	0	0	0	0	555
39	0.671303	13519.333	374	65	64	0	0	0	0	0	555

#### 4.2. Capacity Spectrum Method of the Retrofitted Building

Capacity Spectrum Method (CSM), primarily described in ATC 40, was also used to evaluate the performance levels of the retrofitted building. Capacity Spectrum Method (CSM) was described in section 3.3 that talked about the Capacity Spectrum Method of the existing

building. The structure with inverted V Bracing gives minimum Story drift as compared to other X, V. The magnitudes of story drift for all the stories are found to be within limits, i.e. 0.004 times to story height according to IS 1893:2002 (Part I) [1]. To depend on figure 9, it shows that the magnitude of base shear and tip displacement at the performance point are 7218051 N and 0.019 m, respectively. To determine the building performance levels, it can use the deformation limits in table 3 to compare with the roof drift ratio at the performance point as follows: Roof drift ratio at the performance point is  $0.019/10.5 = 0.0018 < 0.01$ . Referring to this value, it can point out the structural performance level, meets the Immediate Occupancy (IO) level.

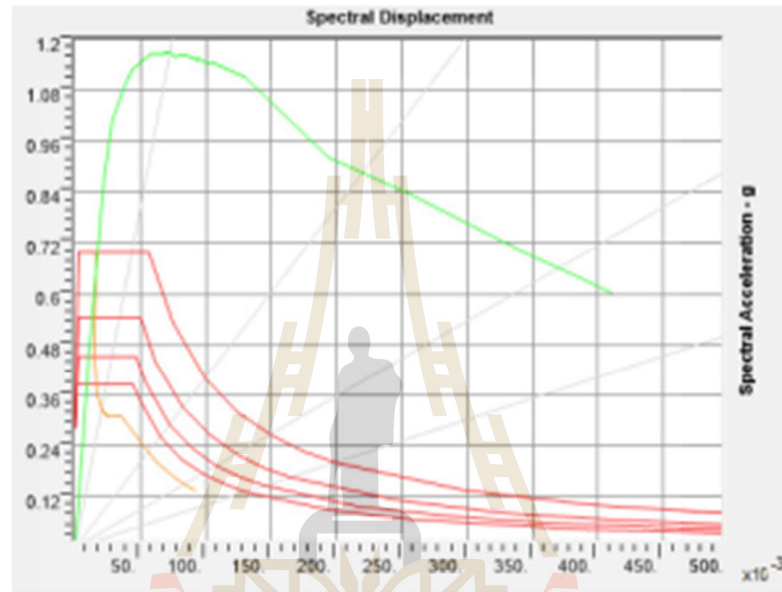


Figure. 9 Capacity spectrum curve of the retrofitted building

### 4.3. Acceptance Criteria of the Retrofitted Building

#### 4.3.1 Performance Evaluation of the Column

All the conditions that used to evaluate the performance levels of the retrofitted building of the column were performed the same as the performance levels of the existing building of the column. The acceptance criteria of the retrofitted building are quite similar to the acceptance criteria of the existing building. The most of the columns do not have the plastic hinge rotation (radian), and a little bit of the column has plastic hinge rotation (radian) in the first story. The acceptance criteria were used to compare with the plastic hinge rotation (radian) of the retrofitted building to classify the performance levels of the retrofitted building. The braced steel frame that used to retrofit the existing building can reduce the performance levels of the column from Life Safety (LS) to Immediate Occupancy (IO) levels. In table 9, it shows that the first story, the second story, and the third story meet Immediate Occupancy (IO) level, Immediate Occupancy (IO) level, and Immediate Occupancy (IO) level, respectively. The 2<sup>nd</sup> step of the pushover analysis of the retrofitted building with plastic hinge was shown in figure 10.

Table 9 Numerical acceptance criteria for plastic hinge rotation of the columns of retrofitted building



Level	Conditions			Acceptance Criteria Plastic Rotations Angle (radians)			Plastic Hinge Rotation (radians)	Performance Level
	$\frac{p}{A_g f'_c}$	$\frac{A_g}{b_w s}$	$\frac{V}{b_w d \sqrt{f'_c}}$	Performance Level				
				IO	LS	CP		
3	0.091	0.005	0.065	0.0050	0.0275	0.0360	0.0000	IO
2	0.181	0.005	0.105	0.0038	0.0196	0.0252	0.0000	IO
1	0.271	0.005	0.228	0.0037	0.0159	0.0200	0.0004	IO

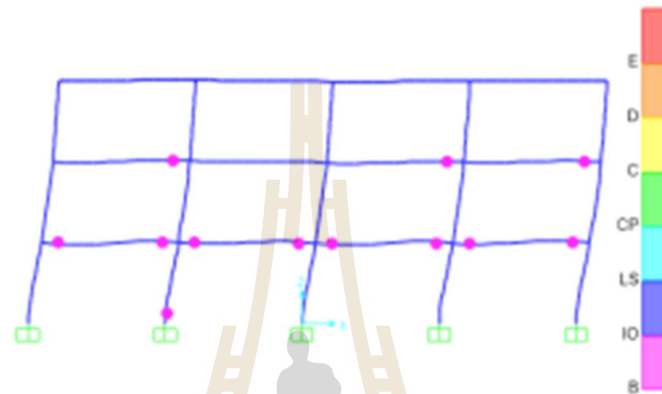


Figure. 10 Performance levels of the retrofitted building

#### 4.3.2 Performance Evaluation of the Beam

All the conditions that used to evaluate the performance levels of the retrofitted building of the beam were performed the same as the performance levels of the existing building of the beam. The acceptance criteria of the retrofitted building are quite similar to the acceptance criteria of the existing building. The most of the beams have a little bit the plastic hinge rotation (radian) in the first and second floor, and the columns do not have the plastic hinge rotation (radian) in the third story. The acceptance criteria were used to compare with the plastic hinge rotation (radian) of the retrofitted building to classify the performance levels of the retrofitted building. Moreover, the steel bracing that used to strengthen the existing building can reduce the performance levels of the beams from Life Safety (LS) to Immediate Occupancy (IO) levels. In table 10, it shows that the first story, the second story, and the third story met Immediate Occupancy (IO) level, Immediate Occupancy (IO) level, and Immediate Occupancy (IO) level, respectively.

Table 10 Numerical acceptance criteria for plastic hinge rotation of the beams of retrofitted building

Level	Conditions			Acceptance Criteria Plastic Rotations Angle (radians)			Plastic Hinge Rotation (radians)	Performance Level
	$\frac{\rho - \rho'}{\rho_{bal}}$	Transverse reinforcement	$\frac{V}{b_w d \sqrt{f'_c}}$	Performance Level				
				IO	LS	CP		
3	0.00	C	0.125	0.01	0.025	0.05	0.0000	IO
2	-0.28	C	0.155	0.01	0.025	0.05	0.0003	IO
1	-0.42	C	0.162	0.01	0.025	0.05	0.0025	IO

## 5. CONCLUSION

This case study evaluated the seismic performance of a three-story R/C existing building located in Thailand considering to use steel bracing to improve the structural performance levels of the existing building. This paper uses many standards such as ASCE/SEI 41-13, ACT 40, FEMA 440, FEMA356, and FEMA 273 that separates into three different methods for the first method is displacement coefficient method, the second method is capacity spectrum method, and the third method is acceptance criteria to determine the performance levels. Depend on the result of these three methods, and it shows that the building meets the Immediate Occupancy (IO) after using the steel bracing to improve the seismic performance in the following.

1. The displacement coefficient method can reduce the target displacement of the R/C building from 0.0517 m to 0.0263 m that equal to 50% of the target displacement. This method also improves the performance levels from Life Safety (LS) - Collapse Prevention (CP) to Immediate Occupancy (IO).

2. The capacity spectrum method can reduce the performance point of the R/C building from 0.0038 m to 0.018 m that equal to 47% of the performance point. This method meets Immediate Occupancy (IO) for both existing and retrofitted building.

3. The performance of the column changes from Life Safety (LS) of the existing building to Immediate Occupancy (IO) of the retrofitted building.

4. The performance of the beam changes from Life Safety (LS) of the existing building to Immediate Occupancy (IO) of the retrofitted building.

5. The braced steel frames could be designed to the desired performance limit states specified in FEMA, ASCE, ATC and Thai earthquake standard, and utilized for seismic retrofitting the existing building in Thailand.

6. The braced steel frames were rigidly connected to the foundations and column of the existing building, but this study did not detail the type of the connection that used to connect between the braced steel frames to the existing structure.

7. The braced steel frames can improve the performance levels of the structure from Life Safety (LS) of the existing building to Immediate Occupancy (IO) of the retrofitted building.

## REFERENCES

- [1] Soundarya N. Gandhi, Y. P. Pawar, Dr. C. P. Pise, S.S. Kadam, C. M. Deshmukh, D. Mohite, Strengthening of reinforced concrete and steel structure by using steel bracing systems, IRJET, 04, 2017, 517-522.
- [2] Channarong Taenseesaeng, Mongkol Jiravacharadet, The Study of the Reinforced Earthquake Resistance Building Structure in Sanklangvittaya School, Chiangrai Thailand, The 21st National Convention on Civil Engineering, Songkhla, Thailand, 2016, 1-8.
- [3] Shachindra Kumar Chadhar, Dr. Abhay Sharma, Seismic behavior of RC building frame with steel bracing system using various arrangements, IRJET, 02, 2015, 479-483.
- [4] Federal Emergency Management Agency (FEMA 440). Improvement of Nonlinear Static Seismic Analysis Procedures, Redwood City, California, 2005.
- [5] Applied Technology Council (ATC-40). Seismic Evaluation and Retrofitting of concrete Buildings. Volume 1 and 2, Seismic Safety Commission, Redwood City, 1-346, 1996.
- [6] American Society of Civil Engineers (ASCE 41-13). Seismic Evaluation and Retrofit of Existing Buildings, Reston, VA, 2013.
- [7] American Concrete Institute (ACI 318). Building Code Requirements for Structural Concrete and Commentary, Farmington Hills, MI. 2011.

- [8] American Concrete Institute (ACI 369). Guide for Seismic Rehabilitation of Existing Concrete Frame Buildings and Commentary, Farmington Hills, MI, 2011.
- [9] Joint ACI-ASCE Committee 352R. Recommendations for Design of Beam - Column Connections in Monolithic Reinforced Concrete Structures, USA, 2003.
- [10] DPT 1302. Standard of earthquake resistant design of building, Department of Public Works and Town & Country Planning, Bangkok, Thailand, 2009.
- [11] Mehmet Inel, Hayri Baytan Ozmen, Huseyin Bilgin. " Re-evaluation of building damage during recent earthquakes in Turkey". Engineering Structures, 30, 2007, 412-427.
- [12] Dhangar Laxmi Balappa and Venu Malagavelli. "Pushover analysis of high rise building with and without bracings". IJCIET, 9, 2008, 759-767.
- [13] Haijuan Duan, Mary Beth D. Hueste. " Seismic performance of a reinforced concrete frame building in China". Engineering Structures, 41, 2012, 77-89.
- [14] Dilip J. Chaudhari, Gopal O. Dhoot, Performance Based Seismic Design of Reinforced Concrete Building, Open Journal of Civil Engineering, 6, 2016, 188-194.
- [15] S. Chandrasekaram1, G. Serino and V. Gupta, Performance evaluation and damage assessment of buildings subjected to seismic loading, WIT Press, 98, 2008, 313-322.
- [16] Waiel MOWRTAGE (Vail KARAKALE), Simple strengthening techniques and new technologies for seismic safety of existing building: recent research and applications in turkey, International Burdur Earthquake and Environment Symposium (IBEES), 2015.
- [17] Mehmet Inel, Hayri Baytan Ozmen, Effects of plastic hinge properties in nonlinear analysis of reinforced concrete buildings, Engineering Structures, 28, 2006, 1494-1502.
- [18] A.Q. Bhatti and H.Varum, Application of Performance Based Nonlinear Seismic Design and Simulation static Pushover Analysis for Seismic Design of RC Buildings, 15th WCEE, LISBOA, 2012.
- [19] B Bharath Reddy, Analytical investigation on seismic strengthening of RC frame using steel cage and viscous damper, IRJET, 9, 2018, 644-653.
- [20] S. Ramasundaram and K. Agilesh, Effect of bracings on tall buildings for seismic loads using pushover analysis, IRJET, 8, 2017, 891-897.
- [21] Chakraphan Wutimuangkwan, Seismic rehabilitation by linear and nonlinear analysis: case study of an RC building in Chiang Mai, Master diss, Chulalongkorn University, Bangkok, Thailand, 2013.
- [22] DPT 1303. Standard of assessment and strengthening of the building structures in areas of the earthquake zone, Department of Public Works and Town & Country Planning, Bangkok, Thailand, 2014.
- [23] Hendramawat A Safarizki , S.A. Kristiawan, and A. Basuki, Evaluation of the Use of Steel Bracing to Improve Seismic Performance of Reinforced Concrete Building, Procedia Engineering, 54, 2013, 447-456.

## **BIOGRAPHY**

Mr. Rithy Khouy was born in 1990 in Takeo province, Cambodia. He went to study at Kirivong high school and graduated in 2008. After high school, he went to Phnom Penh city to study his bachelor degree at Norton University in 2008. Two years later, he got the scholarship to study the bachelor degree in civil engineering at National University of Laos, Vientiane, Laos PDR. He graduated his bachelor degree and worked at Engineering Design and Consultants Ltd, Vientiane, Laos PDR in 2015. He got the scholarship to pursue his Master of Engineering in Structural Engineering in School of Civil Engineering, Institute of Engineering, Suranaree University of Technology under the financial support provided by Office of the Higher Education Commission (OHEC) and Suranaree University of Technology, Thailand.

